

Comparative functional analysis of factors  
controlling glial differentiation in  
*Drosophila* and mouse

Dissertation

Zur Erlangung des Grades  
Doktor der Naturwissenschaften

Am Fachbereich Biologie  
Der Johannes Gutenberg-Universität Mainz

von Álvaro Enrique Bustos Bustos  
geb. am 24.04.1984  
in Concepción, Chile

Mainz, 2015

Dekan:

1. Berichterstatter:

2. Berichterstatter:

Tag der mündlichen Prüfung: 18.02.2015

**Chapter Index**

|   |    |
|---|----|
| Chapter Index .....   | i  |
| 1 Introduction.....   | 1  |
| 1.1 Factors involved in myelination.....  | 3  |
| 1.2 NG2+ cells in vertebrates, not only progenitors of myelinating oligodendrocytes .....                 | 5  |
| 1.3 The NG2 proteoglycan; properties, pathways and function .....   | 6  |
| 1.4 Role of Src kinases and hnRNPs in <i>Drosophila</i> embryogenesis and nervous system development..... | 8  |
| 1.5 Kon-tiki/Perdido, the <i>Drosophila</i> homologue of NG2 .....  | 9  |
| 1.6 Tripartite signaling at the <i>Drosophila</i> neuromuscular junction .....                            | 10 |
| 1.7 Questions and aims.....   | 14 |
| 2 Materials and methods .....   | 15 |
| 2.1 Animal care, genotypes and crosses.....   | 15 |
| 2.1.1 Animal care.....  | 15 |
| 2.1.2 Fly strains.....  | 15 |
| 2.1.3 GAL4/UAS System in <i>Drosophila</i> .....  | 17 |
| 2.1.4 GAL4/GAL80 and GAL80 <sup>ts</sup> system.....  | 18 |
| 2.2 Immunohistochemistry and <i>in situ</i> hybridization.....  | 18 |
| 2.2.1 Antibodies used .....   | 18 |
| 2.2.2 $\alpha$ -Kon <sup>ecto</sup> antibody generation.....  | 19 |

---

|       |   |    |
|-------|---|----|
| 2.2.3 | Embryos fixation and antibody staining .....  | 21 |
| 2.2.4 | Whole larvae and larvae NMJ antibody staining.....                                  | 21 |
| 2.2.5 | Staining with fluorescent secondary antibodies .....                                | 22 |
| 2.2.6 | Anti- <i>kon</i> DIG labeled probe generation for <i>in situ</i> hybridization..... | 22 |
| 2.2.7 | <i>In situ</i> hybridization .....  | 23 |
| 2.3   | Imaging and microscopy .....  | 24 |
| 2.3.1 | Sample preparation for microscopy.....  | 24 |
| 2.3.2 | Imaging and image processing .....  | 24 |
| 2.3.3 | VNC length measurements.....  | 24 |
| 2.3.4 | 4D recordings.....  | 25 |
| 2.3.5 | Antibody staining intensity measurements .....                                      | 25 |
| 2.4   | NMJ phenotype score and statistics.....   | 26 |
| 2.4.1 | NMJ phenotypes.....   | 26 |
| 2.4.2 | Statistics.....   | 26 |
| 2.5   | Western blot .....  | 27 |
| 2.5.1 | Tissue preparation.....   | 27 |
| 2.5.2 | SDS-PAGE and western blot .....   | 27 |
| 2.6   | Solutions and chemicals.....  | 28 |
| 3     | Results .....   | 30 |
| 3.1   | <i>Drosophila</i> Src kinases .....   | 31 |

---

|       |   |    |
|-------|---|----|
| 3.1.1 | Src42A expression pattern throughout embryogenesis .....  | 31 |
| 3.1.2 | Src64B expression pattern during embryonic development .....  | 33 |
| 3.1.3 | Src42A is involved in the proper formation of longitudinal axons in the VNC ...                               | 34 |
| 3.1.4 | Neuronal microtubule pattern is not affected in Src42A mutant .....   | 35 |
| 3.1.5 | Src42A is not involved ePG migration in the PNS.....  | 37 |
| 3.2   | The <i>Drosophila</i> hnRNP F/H homologue, Glorund.....   | 39 |
| 3.2.1 | Glorund is ubiquitously expressed during embryonic and larva development in <i>Drosophila</i> .....           | 39 |
| 3.2.2 | Glorund mutant analysis in embryo and larva .....   | 41 |
| 3.3   | Kon-tiki, the <i>Drosophila</i> NG2/CSPG4 homologue.....  | 43 |
| 3.3.1 | Kon embryonic and larval expression .....   | 43 |
| 3.3.2 | Kon is not involved in embryonic glial development in the nervous system.....                                 | 45 |
| 3.3.3 | Glia derived Kon accumulates at the NMJ and contributes to the NMJ .....                                      | 46 |
| 3.3.4 | Identifying the PNS glial layer(s) involved in Kon dependent NMJ phenotype ..                                 | 49 |
| 3.3.5 | Effect of glial <i>kon</i> knockdown in pre-and postsynapse .....   | 52 |
| 3.3.6 | <i>kon</i> knockdown leads to impaired axonal transport and glia proliferation.....                           | 55 |
| 3.3.7 | Muscle derived Kon also participates in NMJ formation .....   | 57 |
| 3.3.8 | The rescue of <i>kon</i> in muscle rescues muscle-tendon network impairment but induces an aberrant NMJ ..... | 59 |
| 3.3.9 | Kon overexpression in glia also leads to a NMJ phenotype .....  | 61 |

---

|        |   |    |
|--------|---|----|
| 3.3.10 | Kon overexpression in glia results in an extremely elongated VNC.....   | 62 |
| 3.3.11 | Suppressor screen to identify Kon PDZ-BD interacting partners in glia.....  | 65 |
| 3.3.12 | Kon is also processed in <i>Drosophila</i> glial cells.....   | 68 |
| 3.3.13 | DGrip and Kuzbanian are involved in glial Kon processing and NMJ dynamics..   | 70 |
| 4      | Discussion.....   | 73 |
| 4.1    | Src kinases and Glorund are not involved in glial differentiation and neuron-glia cross-talk in <i>Drosophila</i> ..... | 73 |
| 4.2    | Kon-tiki is also expressed in glia during embryonic development .....   | 74 |
| 4.3    | Glia derived Kon may interact with Laminins and Integrins at the NMJ .....  | 74 |
| 4.4    | Peri-and Subperineurial glia layers contribute distinctively to Kon dependent NMJ phenotype.....                        | 75 |
| 4.5    | Pre-and postsynaptic changes upon <i>kon</i> knockdown in glia result in NMJ degeneration.....                          | 76 |
| 4.6    | <i>kon</i> knockdown in glia affects neuronal transport along the NER .....   | 78 |
| 4.7    | <i>kon</i> knockdown results in less glia along the NER.....  | 79 |
| 4.8    | Postsynaptic Kon allows sprout consolidation .....  | 80 |
| 4.9    | Kon rescue in muscle and aberrant NMJ branches .....  | 82 |
| 4.10   | Kon overexpression in glial promotes NMJ branches formation .....   | 82 |
| 4.11   | Kon also interacts with DGrip in glial cells.....   | 83 |
| 4.12   | Kon processing in <i>Drosophila</i> .....   | 83 |
| 4.13   | DGrip and Kuzbanian pave the road for glial Kon to reach muscles and the NMJ.....                                       | 84 |

---

|      |  |     |
|------|--|-----|
| 4.14 | Kon, a pleiotropic factor in glial development .....                                     | 86  |
| 5    | Summary .....  | 88  |
| 6    | References.....  | 89  |
| 7    | Appendix .....   | 100 |
|      | $\alpha$ -Kon <sup>ecto</sup> antibody generation, nucleotide and peptide sequence ..... | 100 |
|      | Abbreviation index.....  | 102 |
|      | Figures index .....  | 104 |
|      | Tables index .....   | 106 |
|      | Curriculum vitae.....  | 107 |
|      | Eidesstattliche Erklärung .....  | 108 |
|      | Acknowledgements.....  | 109 |

## 1 Introduction

Comparative studies of development and function of the nervous system in *Drosophila* and mammals revealed many similarities. They are both divided in central (CNS) and a peripheral nervous system (PNS), and they are integrally built by neurons and glial cells. More in detail, on a cell-cell interaction level, several glia-neuron and glia-neuron-muscle interaction pathways in mouse are also found in *Drosophila*. For instance, the Blood-Brain-Barrier (BBB) in mouse and in *Drosophila*, made up by glial cells, which tightly insulate neurons and avoid a direct neuronal contact with the blood or hemolymph, respectively (Stork et al., 2008). An example of conserved interaction between glia, neuron and muscles is the glia derived TGF- $\beta$  signaling pathway that modulates the growth of the neuromuscular junction (NMJ) in both organisms (Feng and Ko, 2008) (Fuentes-Medel et al., 2012). Even some of the common vertebrate glia subtype classification features can also be identified in *Drosophila* glial cells; this includes cell markers, shape and function (Doherty et al., 2009).

Although there are many similarities, there are also profound differences. A key difference between both animals is the presence of compact myelin in mammals, whereas *Drosophila* is a non-myelinated organism. The main components of the myelin sheath are Myelin Basic Protein (MBP) and Proteolipid protein (PLP), together with its splicing variant (DM20). The presence of myelin in vertebrates allows the saltatory conduction of the action potential, making it exponentially faster than in non-myelinated insects. This accounts for the fact that vertebrates need to cover longer distances than insects. Myelination deficits and myelin sheath loss is associated with several pathologies in humans, including Multiple sclerosis (MS) and other demyelinating neurodegenerative diseases. Myelin is produced by oligodendrocytes (CNS) and myelinating Schwann cells (PNS). Both glial cell types derive from progenitor cells that share a common marker, the proteoglycan NG2 (Richardson et al., 2011). The process by which MBP is deposited at the neuron-glia contact site is regulated by the neuronal dependent activation of the glial Src kinase Fyn, a key step during myelination. The other main component of the myelin sheath, PLP/DM20, has its ratio regulated by members of the superfamily of heterogeneous nuclear ribonucleoproteins (hnRNPs), which



have also been described to be involved in MBP mRNA silenced transport. In PLP/DM20 ratio regulation, the hnRNP F/H family plays a crucial role. The aim of this research is to comparatively study in *Drosophila* three proteins involved in glial differentiation and glia-neuron interaction in the mouse nervous system.

## 1.1 Factors involved in myelination

The myelin sheath is a multilayered glial process that serves as electrical insulation for axons to allow the saltatory conduction of the action potential, from node to node. At first, oligodendrocytes extend protrusions which will then wrap around axons concentrically, using the inner tongue as growth zone, together with simultaneous lateral extension of the glial sheath towards the nodes (Figure 1.1).

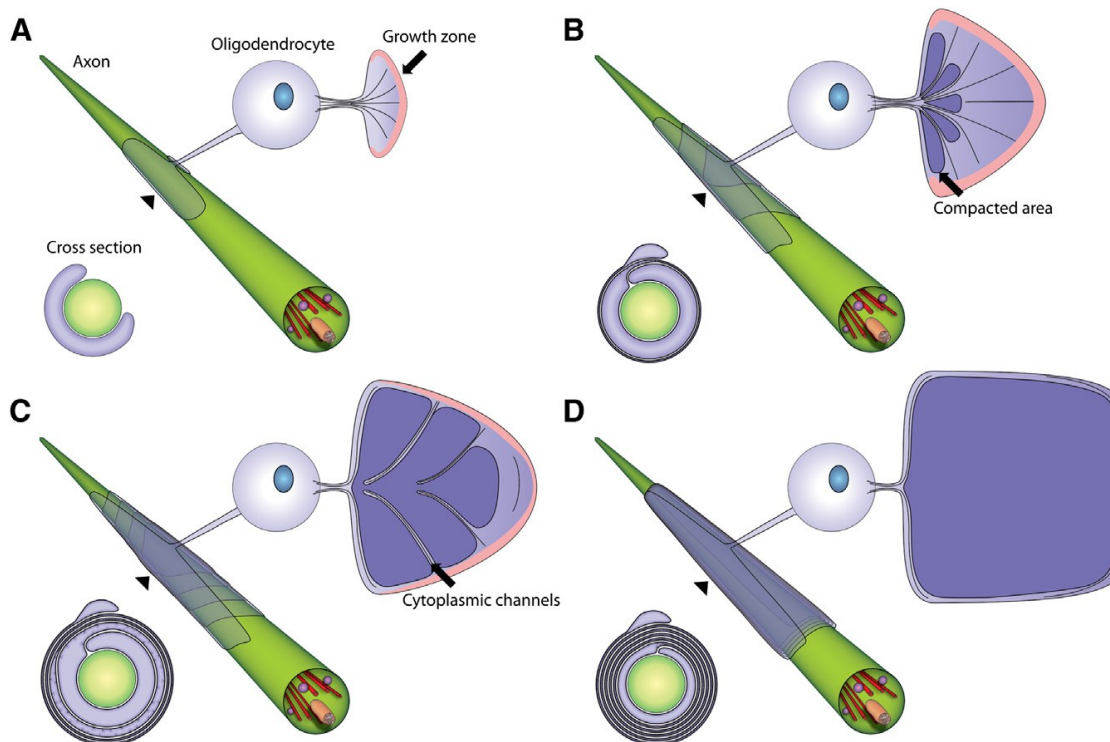


**Figure 1.1 Model of the myelin sheath wrapping in vertebrates nervous system**

(A) After the initial contact, oligodendroglial protrusions start rolling around the axon using the growth zone as leading edge. (B) The leading edge enters the inner face, between axon and oligodendroglial sheath, and extends forming layers concentrically. (C) Compact myelin area starts extending from the portion closest to the oligodendrocyte body towards the leading edge/growth zone. (D) Myelin sheath starts uniformly growing towards the nodes together with a consolidation of the myelin compaction throughout the whole myelin sheath. Figure copied from (Snaidero et al., 2014)

One of the main myelin components is MBP, whose translation is a tightly regulated process, only allowed at the sites where it is required. MBP mRNA is transported in granules in a silenced state to the glia-neuron contact site (Figure 1.2). This silenced state is produced by MBP mRNA interaction with hnRNP A2 through the cis acting A2 response element. Additionally, other hnRNPs also participate in MBP mRNA silenced transport, for instance hnRNP E1. Once those granules reach the neuron-glia contact site, neuronal dependent activation of Fyn Src kinase in oligodendrocytes will phosphorylate hnRNP A2, releasing MBP mRNA and allowing its translation. The local activation of Fyn occurs through the neuronal L1-glia F3 activation pathway (Figure 1.2) (White et al., 2008).

The most abundant myelin protein is PLP (Jahn et al., 2009). hnRNP F/H has been shown to play a role in PLP expression, especially in regulating the ratio between PLP and its splicing variant DM20. A developmentally regulated decrease in the expression of hnRNP F/H, due to oligodendrocyte maturation, results in a modification in the PLP/DM20 ratio from 1,5:1 to 3:1 in mature oligodendrocytes (Wang et al., 2007).

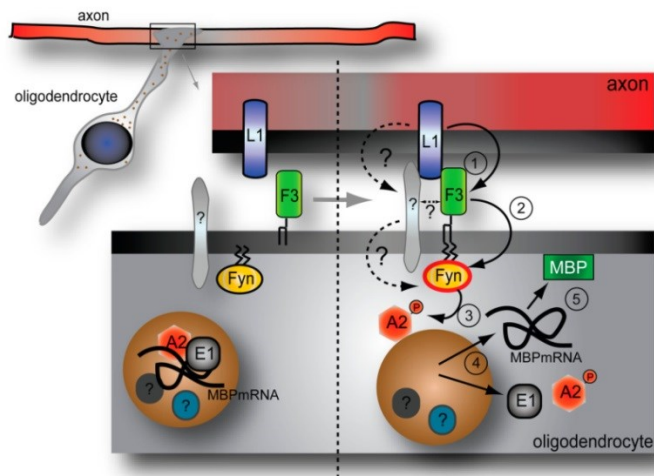


**Figure 1.2 Illustration of MBP mRNA silenced transport and site specific translation**

In the left side illustrated the granules that transport in silenced state MBP mRNA along oligodendroglial processes that contact neurons. Granules are composed by hnRNP A2, E1 and other hnRNPs. When neuronal L1 contacts glial F3, it leads to the activation of Fyn, and ultimately the release of silenced MBP mRNA for translation. Image copied from (White et al., 2008).

## **1.2 NG2+ cells in vertebrates, not only progenitors of myelinating oligodendrocytes**

NG2+ cells in the mammalian nervous system represent about 5-10% of all glia and are thus considered the fourth major glial cell type together with oligodendrocytes, astrocytes and microglia (Nishiyama et al., 2009). They are distributed in both gray and white matter, and remain mitotically active until adulthood. NG2+ cells have been shown to be progenitors for myelinating oligodendrocytes and Schwann cells and also to give rise to astrocytes (Schneider et al., 2001 372) (Trotter et al., 2010). In developmental stages, NG2+ cells are highly proliferative during myelination, and then turn into a resting state that can be reverted either by injury and demyelinating episodes or disease (Zuo and Nishiyama, 2013). It has been a matter of debate whether NG2+ cells have the ability to give rise to neurons. In a recent publication it was shown that adult born neurons in the mouse hypothalamus were progeny of NG2+ cells from the same brain region (Robins et al., 2013). Furthermore, NG2+ cells are the only non-neuronal cell type in the CNS to receive synaptic signaling from neurons (Lin and Bergles, 2002), although it has been recently shown that NG2 protein itself plays a minor or no role in the formation of this type of synapse (Passlick et al., 2014). Besides the above described NG2+ cells, the NG2 proteoglycan is also expressed in pericytes and in malignant brain tumors (Chekenya et al., 2002; Birbrair et al., 2014).

Outside the vertebrate's nervous system, NG2 can be also found in melanomas, developing digits, developing heart and vasculature forming tissue (Stallcup, 2002). It has been also shown that NG2 is expressed in humans at the sarcolemma and in postnatal skeletal muscle, specifically at the neuromuscular junction, and its accumulation reduces gradually with age. Altered amounts of NG2 proteoglycan in the sarcolemma and NMJ were observed in patients with various types of myopathies (Petrini et al., 2003; Petrini et al., 2005).

### 1.3 The NG2 proteoglycan; properties, pathways and function

The rat NG2 is a 2325 amino acids long single-pass transmembrane protein. It has a short intracellular tail of 76 amino acids, containing a C-terminal PDZ binding domain (PDZ-BD). The extracellular portion, 2224 amino acids long, contains an  $\alpha$ -helix structure that receives N-linked oligosaccharides, followed by a single chondroitin sulfate chain at ser-999. At the posterior end of the extracellular domain there are 2 Laminin G-type motifs (LamG), intermingled by two disulfide bonds (Figure 1.3) (Stallcup and Huang, 2008).

NG2 has been described to play a role in various pathways, most of them related to cell migration, cell adhesion, angiogenesis, tumorous vascularization, cytoskeleton rearrangement and extracellular matrix modifications. In all those pathways, NG2 has been shown to interact with several proteins, for instance Integrins, Collagen IV and V and PDGF-AA through its extracellular portion, and with GRIP, Mupp1 and Syntenin-1, through the PDZ-BD (Karram et al., 2005; Stallcup and Huang, 2008).

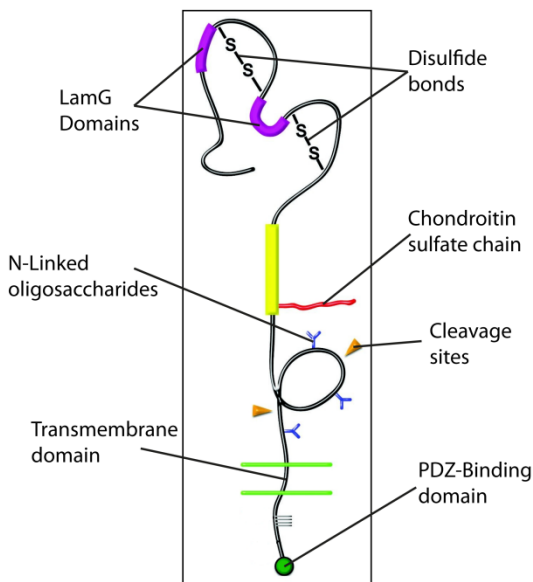


**Figure 1.3. NG2 structure and domains.**

Illustration modified from (Stallcup and Huang, 2008).

As part of the functions and processing of NG2, it has been described a metalloproteinases dependent shedding of the ectodomain, or soluble NG2 (sNG2), as a functional entity. Among others, sNG2 has been shown to play a role in the cross-talk between pericytes and endothelial cells (EC), where sNG2 interacts with both Galectin-3 and  $\alpha 3\beta 1$  Integrin, to form a complex and thus together promote EC morphogenesis and migration during angiogenesis (Fukushi et al., 2004). An example for noxious levels of sNG2 availability is seen in Alzheimer's disease (AD) related histological changes. The accumulation of oligomeric depositions of A $\beta$  1-42 directly raises the activity of matrix metalloproteinase (MMP)-9, increasing the release of sNG2 and promoting EC morphogenesis. This causes the detachment of pericytes from EC, BBB permeabilization, vascular integrity impairment and cognitive status deterioration, at last AD progression (Schultz et al., 2014). There is also a neuronal network modulatory function attributed to sNG2 release. It was recently demonstrated that activity dependent NG2 ectodomain shedding, mediated by ADAM-10, is a necessary step in normal glutamate dependent long term potentiation (LTP) in mice. Besides LTP impairment in NG2 knockout mice (NG2<sup>-/-</sup>), it was also reported impaired or reduced behavioral response to environmental stimulus, such as odors or noises with different intensities, symptoms often related with impaired integration of sensory information and diseases such as Huntington's disease. These results suggest a physiological function for NG2 beyond their role in NG2+ cells, mediated by the synaptic activation of NG2+ cells, triggering the cleavage of the proteoglycan. This will then in turn directly affect glutamate dependent neuronal communication (Sakry et al., 2014).

#### 1.4 Role of Src kinases and hnRNPs in *Drosophila* embryogenesis and nervous system development

In *Drosophila*, there are two Src kinases, Src42A and Src64B (the name indicates their location in the genome). In general, Src kinases are related to signal transduction and membrane remodeling pathways. In *Drosophila* embryonic development, Src kinases have been addressed as important players in cell-cell cross-talk, interacting with E-Cadherin for instance in the remodeling and consolidation of adherence junctions ((Takahashi et al., 2005) (Shindo et al., 2008)). They are further involved in neuronal pathfinding and commissures formation ((Wouda et al., 2008)). Glial phagocytosis of severed axons in the adult fly nervous system has been shown to be mediated by Src42A, in a pathway that also includes Draper, *Drosophila* homologue of CED-1, and the non-receptor tyrosine kinase Shark ((Ziegenfuss et al., 2008)).

In *Drosophila*, hnRNPs A/B and F/H have been both related to mRNA translation control during oogenesis. Hrp48, *Drosophila* homologue of hnRNP A/B, binds and represses the translation of premature or mislocalized *oskar* mRNA (Yano et al., 2004). Glorund (Glo) on the other hand, hnRNP F/H *Drosophila* homologue, represses the translation of mislocalized *nanos* mRNA. It also acts in a complex with Hrp48 and the splicing factor Half-pint to regulate *gurken* and *oskar* mRNA translation. All three proteins; Oskar, Nanos and Gurken, are master regulators of anterior-posterior and dorsal-ventral axis formation during *Drosophila* oogenesis. The translation of those three factors requires a tight spatio-temporal regulation. Another example of spatio-temporal regulation of mRNA translation is the role of Glo in regulating *nanos* translation in neurons to control dendritic arborization during larval development (Brechbiel and Gavis, 2008). Hence hnRNPs have shown to control site-specific mRNA translation in mouse and *Drosophila*, in a variety of tissues, but still remains to be studied the role they have in glia-neuron interaction during *Drosophila* nervous system development.

## 1.5 Kon-tiki/Perdido, the *Drosophila* homologue of NG2

Kon-tiki (Kon), also known as Perdido (Perd), is the *Drosophila* NG2 homologue, and was reported in 2007 by two independent groups to play a key role in muscle-tendon network formation during embryogenesis (Estrada et al., 2007; Schnorrer et al., 2007). In Kon, almost all major protein domains present in NG2 are conserved, starting with the 2 Extracellular LamG domains and 15 glycosylation domain repeats, except for the Ser-999 modification for the attachment of the chondroitin sulfate chain present in vertebrates (Schnorrer et al., 2007). There is 21% - 25% identity and 39% - 46% similarity between the extracellular domain of Kon and CSPG4/NG2. The single-pass transmembrane domain is conserved, as well as the C-terminal PDZ-DB. Intracellular domains are less well conserved, except for the PDZ-BD, which is identical in *Drosophila*, mouse, rat and humans (Schnorrer et al., 2007).

Kon mRNA is first detected in embryonic stage 10, being expressed in precursor of longitudinal visceral muscles and later, in stage 14, in body wall muscles from which the ventral-longitudinal group shows the highest expression. Antibody staining against Kon shows protein localization at the plasma membrane of extending myoblasts that will form the ventro-lateral muscles 1 to 4. This staining can be observed from stage 14 until stage 16, when the muscle-tendon attachment is completed and consolidated. Kon mutations result in aberrant muscle-tendon network formation, characterized by round myoblasts failing to migrate and attach to tendon cells. The most affected group of muscles is the ventro-lateral group (Estrada et al., 2007; Schnorrer et al., 2007).

In order to mediate the muscle-tendon attachment, Kon expressed in myoblast interacts in trans and binds to Integrins expressed in tendon cells. In myoblasts, Kon binds to DGrip, more specifically with the 7<sup>th</sup> PDZ domain of DGrip (Estrada et al., 2007; Schnorrer et al., 2007). Kon also establishes a synergistic interaction with LamininB2 in forming a proper embryonic muscle-tendon network (Wolfstetter and Holz, 2012). Overexpression of Kon in muscle results in aberrant filopodia formation, associated with the ability of Kon to modulate cytoskeleton rearrangements (Schnorrer et al., 2007). Later in development, Kon interacts



with Integrins in the assembly of myofibrils and connection to Z-bands during pupal and adult development (Perez-Moreno et al., 2014).

Unlike NG2, Kon has been poorly studied regarding nervous system development and progenitor cells in the CNS and PNS. The only publication that associates Kon with Neuroblasts (NB), Ganglion Mother Cells (GMC) and their lineage is a genome-wide RNAi screen performed in Juergen Knoblich's lab. They observed that the knockdown of *kon* in larvae using *inscutable*-GAL4 (pan-NB-driver) resulted in a reduction in NB derived GMC lineage. They also observed that the shape of NBs and GMCs were affected (Neumuller et al., 2011).

### **1.6 Tripartite signaling at the *Drosophila* neuromuscular junction**

The expression of NG2 at the sarcolemma and NMJ in humans motivated a deeper study of the homologous structures in the fly. In *Drosophila*, the initial contact between motoneurons and muscles takes place in stage 15, although active synaptic communication does not occur until mid-stage 16. NMJ structures, similar to those of mature NMJ, can be first seen during stage 17, since they require a massive accumulation of proteins that will form the pre- and postsynapse, at the neuron-muscle contact site (Broadie and Bate, 1993). During *Drosophila* embryonic stages, little is known about the role of glial cells in NMJ formation, but during larval stages, many studies give evidence about the influence and the role of glial cells at the NMJ (Brink et al., 2012). In adult flies, glial cells expressing the *Drosophila* excitatory amino acid transporter 1 (dEAAT1) are responsible for glutamate clearance at the synaptic cleft in flight muscles. Interestingly, during larval stages no dEAAT1 can be observed at the NMJ in body wall muscles, thus dEAAT1 accumulation at the NMJ is either restricted to flight muscles or a process that requires NMJ maturation and specification (Rival et al., 2006).

Two *Drosophila* labs (from Vanessa Auld and Vivian Budnik) developed imaging protocols to visualize fluorescently labeled PNS glia at the NMJ in living *Drosophila* larvae, thus allowing a comprehensive analysis of the contribution of glial cells to the modulation and maintenance of the NMJ (Brink et al., 2009) (Fuentes-Medel et al., 2009). Glial cells in the PNS are regularly distributed and cover entirely each neuronal tract. They form around axons three distinct

concentric layers, individually addressable. Every glial layer is formed by predetermined embryonic peripheral glia (ePG), some of which have been shown to survive even until adult stages (von Hilchen et al., 2013; von Hilchen and Altenhein, 2014). During larval stages, every glial layer reaches and contributes differentially to NMJ dynamics. The inner most layer, formed by wrapping glia, has been shown to play a minor or no role at all at the NMJ. The intermediate glial layer, also called subperineurial glia, enters in intimate contact with the NMJ and also mediates synaptic bouton stability, NMJ maintenance and growth. The subperineurial glia layer also forms the BBB. The outer most layer, or perineurial glia layer, extends protrusions that reach entire NMJ branches, participating actively in NMJ remodeling. Nevertheless, perineurial glia forms an irregular sheath that in some regions only partially cover the PNS. There are also other variables that influence glia-NMJ dynamics, such as temperature, developmental stage of the animal, mutations in specific genes, misexpression of mutated proteins, etc. Their effects can be reflected in parameters, such as the number of boutons or branches in the NMJ, the area covered by glia and glia/neuron surface coverage, among others (Brink et al., 2012).

To promote the extension of the NMJ, it is necessary to remove all unwanted not-consolidated boutons and debris. This work is performed by muscle and glia, in which both synergistically and coordinately clear synapse and allow the formation of new boutons, and hence the growth of the NMJ (Figure 1.4) (Fuentes-Medel et al., 2009). Mutations or glial knockdown affecting genes known to be part of the phagocytic pathway, for instance *Draper*, lead to an accumulation of ghost or detached boutons and debris near the synapse, and in consequence a reduction in the number of boutons found at the NMJ in late larval stages (Fuentes-Medel et al., 2009).

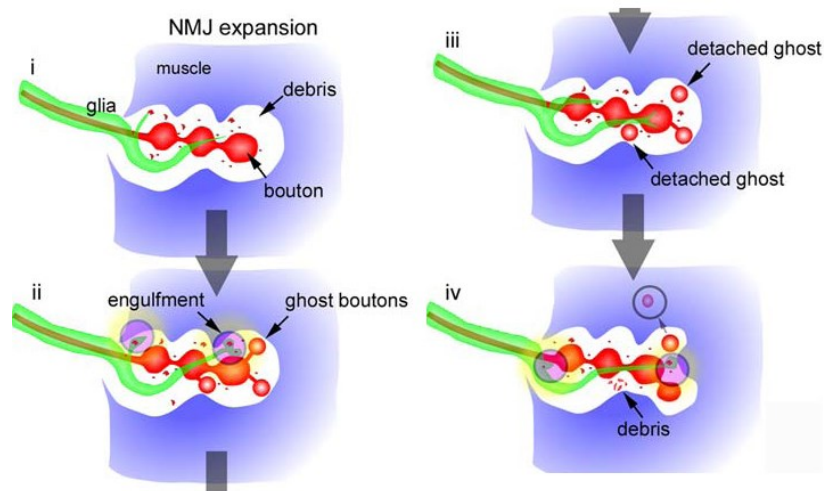


**Figure 1.4 Debris and ghost boutons clearance carried out by glia and muscle at the NMJ**

In the illustration glia membrane is in green, neurons in red and muscle in blue. i) Shows active gliopodia entering the NMJ. ii) Gliopodia detects and reaches debris at the NMJ. iii) Non-consolidated boutons are detached from the main NMJ branch. iv) Muscles and glia engulf detached ghost boutons and debris. Modified from (Fuentes-Medel et al., 2009)

The active clearance of debris and ghost boutons is not the only mechanism employed by glial cells to contribute to the maintenance, growth and plasticity of the NMJ. Glial secreted signaling molecules also contribute to the NMJ in the same process. In glia-neuron signaling, glial expressed Eiger (TNF- $\alpha$ ) directly commands NMJ branch retraction through its interaction with Wengen (TNF- $\alpha$  receptor), expressed in motoneurons, which mediates modifications in the spectrin/ankyrin skeleton. This pro-degenerative pathway was tested in ankyrin mutant larvae, which resembles Amyotrophic Lateral Sclerosis (ALS) like NMJ lesions in *Drosophila*. In this disease model, knockdown of either *eiger* or *wengen* results in a reduction in the severity of the NMJ phenotype (Keller et al., 2011). Glial cells also release signaling molecules that act in muscles to mediate NMJ physiology. In a recent publication it was shown that Repo regulates glial Wingless (Wg) deposition at the NMJ and muscle. In muscles, glial Wg was shown to modulate the correct assembly of glutamate receptor (GluRIIA) clusters at the postsynapse. Either *repo* or *wg* mutants, or their knockdown in glia, resulted in compromised synaptic communication, as shown by a reduction in excitatory

junction potential amplitude in electrophysiological experiments (Kerr et al., 2014). A more complex tripartite communication pathway (glia, muscle and neuron) is the one in which glial secreted TGF- $\beta$  ligand Maverick (Mav) induces muscle release of Glass Bottom boat (Gbb), which will then in turn activate motoneurons to promote presynaptic expansion (Figure 1.5). This whole pathway, from glia-to-muscle-to-neuron, represents how intrinsically related each component of the NMJ is with one another, and highlights the role of glia in the modulation of the NMJ (Fuentes-Medel et al., 2012).

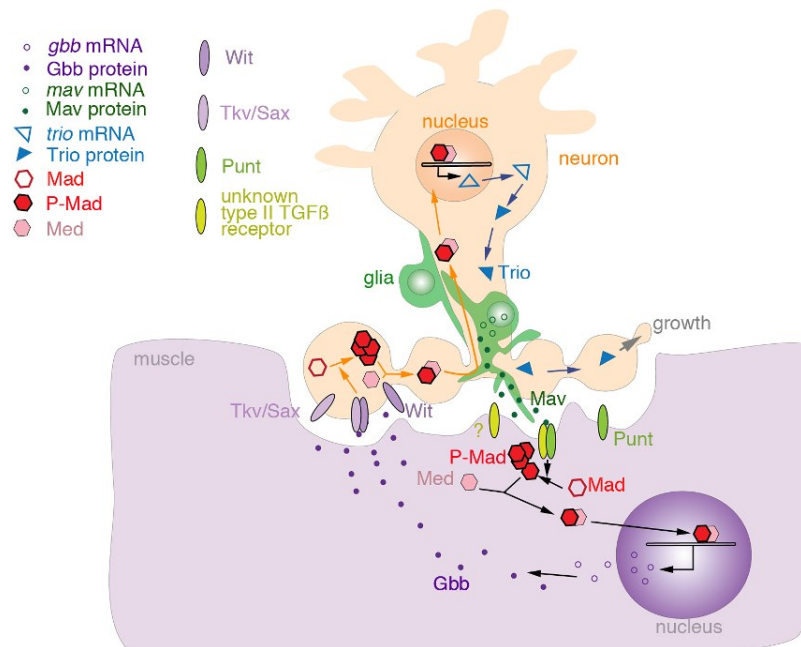


**Figure 1.5 Illustration of glia-muscle-neuron signaling cascade to promote NMJ growth**

Glia secreted Mav protein is deposited at the postsynapse and activates through Punt/unknown type II TGF- $\beta$  receptor the cytoplasmic phosphorylation of Mad, which will then translocate, together with Med, to the nucleus and promote the expression of *gbb*. Muscle expressed Gbb is secreted and activates in motoneurons Wishful thinking (Wit) together with either Thick veins (Tkv) or Saxophone (Sax). The activation of the last TGF- $\beta$  receptors leads to the phosphorylation of Mad in motoneurons, which will then associate with Med and translocate to the nucleus, promoting the expression of Trio, which will at last shuttle to the presynapse where it promotes the expansion of the NMJ. Illustration copied from (Fuentes-Medel et al., 2012).

## 1.7 Questions and aims

The main goal of this research was to comparatively study in the genetically accessible model system *Drosophila*, factors involved in glia differentiation and neuron-glia interaction in vertebrates. Starting with an exploratory phase, in which the expression of each of the candidate genes was studied in the *Drosophila* embryonic and larval nervous system, followed by a focused analysis of the one candidate gene that showed the most significant role on nervous system development. The main questions to answer were; to what extent can one comparatively analyze the role of Src kinases, hnRNP F/H and NG2/Kon in the development of mouse and *Drosophila*, and which homologous role, or roles, can be identified.

On the light of the results during the exploratory phase, my attention was oriented towards the study of Kon/NG2 and its function in larval stages, especially focusing on the role of Kon at the larval NMJ. In humans, this tripartite structure has been already shown to express and accumulate NG2 and where alterations of NG2 levels are associated with muscle dystrophy. Here I will use the *Drosophila* larval NMJ, a well-studied model, to answer whether glial Kon contributes to the maintenance and dynamics of the NMJ, and hopefully open the field for further studies in vertebrates, addressing the role that glial NG2 has in the PNS and especially at the NMJ during development and disease.

## 2 Materials and methods

### 2.1 Animal care, genotypes and crosses

#### 2.1.1 Animal care

All fly stocks used in this research were kept at all times under controlled temperature, in plastic cylindrical vials containing about 1/5 its volume fly food (internal recipe). Depending on the experiment they were being used and condition of the flies, they were kept either at 18 or 25 °C.

For egg collection of desired genotypes, flies were kept in cylindrical plastic vial containing apple juice agar (28 gr agar in 1 L of commercially available apple juice). Embryos collected were aged and kept in controlled conditions, prior fixation and thereafter antibody staining.

#### 2.1.2 Fly strains

Following, the complete list of fly stocks genotypes used during this research, and the source they were obtained from (Table 2.1).

**Table 2.1 Fly strains used during the course of this investigation**

| Notation                                       | Genotype  | Origin                              |
|--|---|-------------------------------------|
| <b>Control and mutant flies</b>                |   |                                     |
| Wildtype                                       | OregonR   | General stock Institute of Genetics |
| <i>Src42A</i> <sup>26-1</sup>                  | <i>;Src42A</i> <sup>26-1</sup> / <i>CyO,wg-lacZ</i>                                   | (Takahashi et al., 2005)            |
| <i>Src64B</i> <sup>KO</sup>                    | <i>;;Src64B</i> <sup>KO</sup> / <i>TM6b, Ant</i> <sup>Hu</sup> , <i>e,abdA-lacZ</i>   | (O'Reilly et al., 2006)             |
| <i>glo</i> <sup>162x</sup>                     | <i>;;glo</i> <sup>162x</sup> , <i>e/ TM6b, Ant</i> <sup>Hu</sup> , <i>e,abdA-lacZ</i> | (Kalifa et al., 2006)               |
| <i>kon</i> <sup>c0025</sup>                    | <i>;kon</i> <sup>c0025</sup> / <i>CyO,wg-lacZ</i>                                     | (Schnorrer et al., 2007)            |
| <i>kon</i> <sup>c452</sup>                     | <i>;kon</i> <sup>c452</sup> / <i>CyO,wg-lacZ</i>                                      | (Schnorrer et al., 2007)            |
| <i>kon</i> <sup>A04</sup>                      | <i>;kon</i> <sup>A04</sup> / <i>CyO,wg-lacZ</i>                                       | (Schnorrer et al., 2007)            |
| <i>kon</i> <sup>c0025</sup> , <i>mef2-GAL4</i> | <i>;kon</i> <sup>c0025</sup> , <i>mef2-GAL4/ CyO,twi-GAL4,UAS-GFP</i>                 | (Schnorrer et al., 2007)            |

|  |   |                              |
|--|---|------------------------------|
| <i>kon</i> <sup>c1139</sup> ,UAS- <i>kon</i> ::HA    | ; <i>kon</i> <sup>c1139</sup> ,UAS- <i>kon</i> ::HA / <i>CyO,twi-GAL4,UAS-GFP</i> | (Schnorrer et al., 2007)     |
| Kon Df(2L)2364                                       | Df(2L)M36F-2/SM5  | *BSC #2364                   |
| <b>GAL4 lines</b>                                    |   |                              |
| <i>repo</i> >CD4::GFP                                | ;; <i>repo-GAL4,UAS-CD4</i> ::GFP   | C. von Hilchen               |
| <i>dicer</i> ; <i>repo-GAL4</i>                      | ;UAS- <i>dicer2</i> ; <i>repo-GAL4</i>  | B. Altenhein                 |
| <i>nrv2-GAL4</i>                                     | ; <i>nrv2-GAL4</i>  | (Sun et al., 1999)           |
| <i>Gli-GAL4</i>                                      | ; <i>Gli-GAL4</i>   | (Sepp and Auld, 1999)        |
| <i>46F-GAL4</i>                                      | ; <i>46F-GAL4</i>   | (Xie and Auld, 2011)         |
| <i>elav-GAL4</i>                                     | P{w[+mW.hs]=GawB}elav[C155]   | *BSC #458                    |
| <i>mef2-GAL4</i>                                     | P{w[+mC]=UAS- <i>Dcr-2.D</i> }1, w[1118];<br>P{w[+mC]= <i>GAL4-Mef2.R</i> }R1     | *BSC #25756                  |
| <i>repo-GAL4,tub</i> >GAL80 <sup>ts</sup>            | <i>repo4.3</i> >CD8::GFP; <i>repo-GAL4,tub</i> >GAL80 <sup>ts</sup>               | C. Klämbt                    |
| UAS- <i>kon</i> ; <i>repo-GAL4</i> suppressor screen | ;UAS- <i>kon</i> ::HA; <i>repo-GAL4,UAS-GAP</i> ::GFP/TM6, <i>tub</i> >GAL80      | AG Technau                   |
| <b>UAS Lines</b>                                     |   |                              |
| UAS- <i>kon</i> ::HA                                 | UAS- <i>kon</i> ::HA/ <i>CyO,twi-GAL4,UAS-GFP</i>                                 | (Schnorrer et al., 2007)     |
| UAS- <i>kon</i> <sup>VG</sup> ::HA                   | UAS- <i>kon</i> <sup>VG</sup> ::HA/ <i>CyO,twi-GAL4,UAS-GFP</i>                   | (Schnorrer et al., 2007)     |
| UAS- <i>kon</i> <sup>Delta-LamG</sup>                | ; UAS- <i>kon</i> <sup>Delta-LamG</sup> ::HA/ <i>CyO,twi-GAL4,UAS-GFP</i>         | F. Schnorrer (Not Published) |
| UAS- <i>kon</i> <sup>Delta-CSPG</sup>                | ; UAS- <i>kon</i> <sup>Delta-CSPG</sup> ::HA/ <i>CyO,twi-GAL4,UAS-GFP</i>         | F. Schnorrer (Not Published) |
| UAS- <i>kuz</i>                                      | w* ; P{UAS- <i>kuz.F</i> }DF1   | *DGRC #108440                |
| <b>RNAi lines</b>                                    |   |                              |
| Src42ARNAi   | w <sup>1118</sup> ; P{GD10610}v26019/ <i>CyO, wg-lacZ</i>                         | *VDRC #26019                 |
| <i>kon</i> RNAiKK                                    | P{KK102101}VIE-260B/ <i>CyO,twi-GAL4,UAS-GFP</i>                                  | *VDRC #106680                |
| <i>kon</i> RNAiGD                                    | w <sup>1118</sup> ; P{GD2633}v37283/ <i>CyO,twi-GAL4,UAS-GFP</i>                  | *VDRC #37283                 |
| <i>kon</i> RNAiC2                                    | ; P{GD2633}/ <i>CyO,twi-GAL4,UAS-GFP</i>  | F. Schnorrer (Not Published) |

|                   |                                  |               |
|-------------------|----------------------------------|---------------|
| <i>dgrip</i> RNAi | $y^1 v^1$ ; P{TRiP.JF02969}attP2 | *BSC #28334   |
| <i>kuz</i> RNAi   | P{KK103555}VIE-260B              | *VDRC #107036 |

(\*) BSC (Bloomington Drosophila Stock Center), VDRC (Vienna Drosophila Resource Center)

### 2.1.3 GAL4/UAS System in *Drosophila*

The GAL4/UAS system was used in a series of experiments during this work for either ectopically express proteins (GFP, Kon, Kuz, etc), or for a targeted knockdown of genes of interest (*kon*, *kuz*, *dgrip*, etc). GAL4 is a transcription factor that binds to an Upstream Activating Sequence (UAS) in order to promote the transcription of a desired DNA sequence. This system, identified in *Saccharomyces cerevisiae*, belongs to the wide genetic toolbox available in *Drosophila* and is a standardized technique. Both, GAL4 and UAS are inserted into the *Drosophila* genome in targeted or random sites and generally brought together by mating parental lines containing either of them (Figure 2.1) (Duffy, 2002).

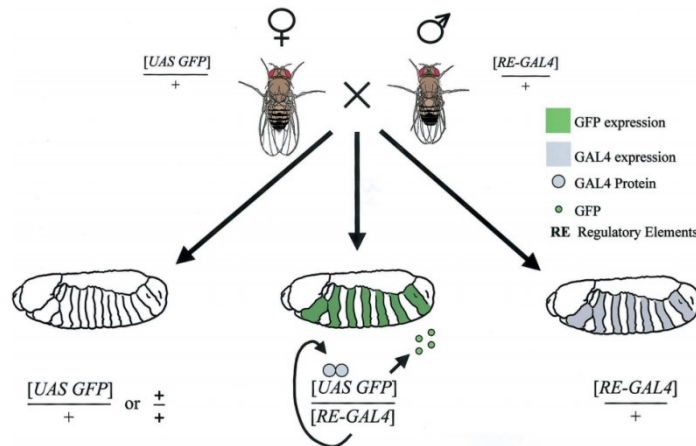


**Figure 2.1 GAL4/UAS system in *Drosophila***

Illustration copied from (Duffy, 2002), showing the crossing of a female parental line carrying the UAS-GFP sequence and the male parental line carrying a GAL4 under a Regulatory Element (RE) control. From this crossing, 4 different genotypes in the progeny can be found: wildtype (+/+), UAS only (UAS GFP/+), GFP ectopic expression (UAS GFP/RE-GAL4) and GAL4 only expression (RE-GAL4/+). GFP is shown in green and GAL4 protein in grey.



### 2.1.4 GAL4/GAL80 and GAL80<sup>ts</sup> system

The GAL80 protein also derives from *S. cerevisiae*. It binds to GAL4 and also to GAL4-UAS-sequence complex, and inhibits the transcription (Lue et al., 1987). The GAL80 protein was used in a balancer chromosome that helped overcome the lethality caused by the overexpression of Kon in glial cells (*repo-GAL4* and *UAS-kon* together in one stock), and allowed to cross these flies to UAS-RNAi stocks in the suppressor screen.

The GAL80<sup>ts</sup> protein is a temperature sensitive version of the original GAL80 protein, with the advantage that it allows to control not only spatially, but also temporally the GAL4 dependent transcription, therefore allowing a tightly regulated analysis of the role of genes of interest (McGuire et al., 2003). At low temperatures, the GAL4-GAL80<sup>ts</sup> interaction takes place and blocks transcription, whereas at higher temperatures, from 30 °C upwards, GAL80<sup>ts</sup> is inactive and therefore UAS-sequence transcription is allowed. The GAL80<sup>ts</sup> construct was used to control Kon ectopic expression and thus elucidate the timing required to trigger the elongated VNC phenotype observed in Kon overexpression in glia.

## 2.2 Immunohistochemistry and *in situ* hybridization

### 2.2.1 Antibodies used

Following, the complete list of primary antibodies used in this work.

**Table 2.2. List of antibodies**

| Antigen | Host       | Dilution | Source                   |
|---------|------------|----------|--------------------------|
| Repo    | Guinea pig | 1:1000   | B. Altenhein             |
| Repo    | Rabbit     | 1:1000   | B. Altenhein             |
| Repo    | Mouse      | 1:10     | DSHB                     |
| Src42A  | Rabbit     | 1:200    | (Takahashi et al., 2005) |
| Src64B  | Rabbit     | 1:500    | (O'Reilly et al., 2006)  |
| BP102   | Mouse      | 1:20     | DSHB                     |

|                     |            |       |                        |
|---------------------|------------|-------|------------------------|
| Fas2                | Mouse      | 1:10  | DSHB                   |
| Futsch              | Mouse      | 1:10  | DSHB                   |
| Glorund             | Mouse      | 1:50  | DSHB                   |
| Discs large         | Mouse      | 1:10  | DSHB                   |
| GluRIIA             | Mouse      | 1:5   | DSHB                   |
| Bruchpilot          | Mouse      | 1:5   | DSHB                   |
| DIG-POD             | Rabbitt    | 1:500 | Roche                  |
| HA                  | Rat        | 1:50  | Roche                  |
| HRP-TRITC           | Goat       | 1:50  | Jackson Immunoresearch |
| GFP                 | Rabbit     | 1:200 | Torrey Pines Biolab    |
| Kon <sup>ecto</sup> | Guinea pig | 1:100 | Á. E. Bustos           |

### 2.2.2 $\alpha$ -Kon<sup>ecto</sup> antibody generation

The region between LamG domains and the CSPG repeats in Kon was chosen as epitope for the generation of an  $\alpha$ -Kon<sup>ecto</sup> antibody (Figure 2.2). The desired peptide lies within the transcription product of exon 6 and exon 7. Genomic larval DNA was used as template in a Polymerase chain reaction (PCR) to amplify both respective fragments.

#### Thermocycler program:

|                  |       |        |       |
|------------------|-------|--------|-------|
| Denaturation     | 94 °C | 2 min  | } 40x |
| Denaturation     | 94 °C | 30 sec |       |
| Annealing        | 58 °C | 30 sec |       |
| Elongation       | 72 °C | 30 sec |       |
| Final elongation | 72 °C | 2 min  |       |

Forward and reverse primers were designed to incorporate restriction sites in the amplified fragments and thus allow their integration into the pQE vector. Primers used were as follow

in Table 2.3 (incorporated restriction sites are in bold letters and nucleotides modifications are highlighted in red):

**Table 2.3. List of primers used for the generation of  $\alpha$ -Kon<sup>ecto</sup>**

| Name                           | Sequence                              |
|--------------------------------|---------------------------------------|
| Kon Exon 6 US ( <b>Bam</b> HI) | CG <b>GGATCC</b> TGGTCAACGATCTTCC     |
| Kon Exon 6 DS ( <b>Sac</b> I)  | ACA <b>GAGCTC</b> AAAAGGTCCCTGAAAATCG |
| Kon Exon 7 US ( <b>Sac</b> I)  | CA <b>GAGCTC</b> TTTCACAGAAACCAGTCC   |
| Kon Exon 7 DS ( <b>Pst</b> I)  | GCGA <b>CTGCAG</b> TCTTAATTGCGGTGG    |

The resulting PCR fragments were incorporated sequentially into pQE-32 vector, to conserve the reading frame, and also to add a 6xHis tail at the N-terminus. Thereafter, the vector containing both exon fragments was transfected to *E. coli* (SG13009, Qiagen). The peptide expressed by bacteria in liquid culture was then purified using the NiNTA kit (Qiagen) and sent for immunization of guinea pigs by Pineda Antikörper-Service (Berlin). After 150 days of immunization, the animals were sacrificed and the serum was collected. The specificity of the serum was tested on western blots and by immunohistochemistry. Prior to antibody staining in fixed *Drosophila* embryos or larvae, the serum was pre-adsorbed using young embryos to remove unwanted antibodies.



**Figure 2.2. Epitope for  $\alpha$ -Kon<sup>ecto</sup> generation**

Illustration showing in color codes all Kon domains and with a bracket indicated the peptide used for the generation of the  $\alpha$ -Kon<sup>ecto</sup> antibody.

### **2.2.3 Embryos fixation and antibody staining**

First, the embryos laid in apple-juice-agar vials were collected and chemically dechorionated in 6% sodium hypochlorite for 3 minutes, then thoroughly washed using tap water. Dechorionated embryos were then placed in a two phase solution containing 450µl PEMS buffer, 70 µl formaldehyde solution (37% formaldehyde) and 600µl heptane, and then shaken for 23 minutes at high speed in a rotation table at room temperature, after which the lower phase was removed and replaced by adding methanol, followed by a vigorous vortexing step. The lower phase was removed and methanol (70%) added again. This procedure was repeated twice, which allowed the removal of the vitelline membrane. Embryos without vitelline membrane sunk in methanol, whereas the ones still containing the vitelline membrane were found floating, this allowed to remove all floating embryos and keep the ones ready to enter the antibody staining process. At last, the embryos rinsed three times with methanol (100%).

The antibody staining starts by rehydrating the embryos in three consecutive steps of rinsing and twice washing for 10 min with PBT, after which the embryos were incubated overnight at 4 °C in 100-500 µl PBT plus primary antibody using the dilutions listed in Table 2.2.

### **2.2.4 Whole larvae and larvae NMJ antibody staining**

Most of the experiments performed in this work consisted in antibody staining of L3 larvae and specially the staining of the NMJ from L3 larvae. Animals selected for dissection were L3 wandering larvae. Prior dissection, animals were rinsed with PBS and placed on silicon dishes in a drop of sterilized M3 medium. Using forceps, larvae were properly oriented and pinned to the silicon dish using fine needles (Minucie N° 10, Ento Sphinx, Czech Republic). One needle was placed in the anterior and other in the posterior most part of the larvae, being careful not to damage the brain, nor to stretch too much and cause the larva to break apart. Carefully, and with help of a fine scissor (FST N° 15005-08), a dorsal longitudinal cut along the animal was performed and allowed the fine dissection of the gut and fat body of the animal, to expose the nervous system and NMJs to the fixative. With the help of 4 fine needles, two anterior and two posterior, the whole animal was stretched and pinned to the dish. Within

less than 30 min, fine dissection procedure was completed and animals were rinsed and washed with PBT 0,5% and then incubated with fixative (900  $\mu$ l PBT 0,5% and 100  $\mu$ l formaldehyde 37%). For NMJ imaging animals were incubated with fixative for 10 min, and for whole larva the incubation time was 45 min. After fixation, animals were rinsed and washed with PBT 0,5%, and then incubated overnight with PBT 0,5% containing primary antibodies in the dilutions listed in Table 2.2, at 4 °C.

### **2.2.5 Staining with fluorescent secondary antibodies**

The procedure to develop and visualize embryos or larvae stained with primary antibodies was the same in all experiments. Primary antibodies solution was removed and animals were rinsed and washed three times with PBT at room temperature, followed by 2 hours incubation with secondary antibodies coupled with fluorescent dyes, diluted according to the manufacturer. The incubation with secondary antibodies was performed at room temperature and under gentle shaking. After the incubation with the secondary antibodies, animals were rinsed and washed three times with PBT, and then washed three times with PBS. After this step, animals were ready to proceed with imaging protocols.

### **2.2.6 Anti-*kon* DIG labeled probe generation for *in situ* hybridization**

The anti-*kon* Dig labeled probe was generated using the cDNA clone LD31354 linearized using the restriction enzyme ClaI (Bsu15I, Fermentas). DNA precipitation was carried out by adding 0,1 volumes of NaCl 2M and 2,5 volumes of ethanol 100% and incubating overnight at -20 °C, thereafter the DNA was pelleted by centrifuging at high speed (15.000 g) for one hour. The pellet was then washed with 50  $\mu$ l ethanol (70% ethanol and 30% DEPC-water) and centrifuged for other 5 min. Ethanol was then removed and the pellet was allowed to dry covered with parafilm. After all the ethanol was evaporated and the pellet was dry, it was re-diluted in 15  $\mu$ l of DEPC-water.

The mix for *in vitro* transcription contained 13,5  $\mu$ l linearized plasmid DNA, 2  $\mu$ l 10x DIG-labeling kit (Boehringer), 2  $\mu$ l 10x DIG-labeling buffer, 0,5  $\mu$ l RNase inhibitor and 2  $\mu$ l SP6 RNA polymerase. The mix was incubated for 2 hours at room temperature, then 0,1 volumes of

LiCl and 2,5 volumes of pure ethanol were added and then incubated overnight at  $-20^{\circ}\text{C}$ . A high speed centrifugation step for one hour pelleted the resulting *in vitro* transcribed probe, which was re-suspended in 50  $\mu\text{l}$  DEPC-water after washing and centrifuging the pellet twice.

The specificity of the probe was tested in wildtype and homozygous *kon* deficient embryos (BSC #2364), yielding best results at 1:300 dilution.

### **2.2.7 *In situ* hybridization**

Embryo fixation was performed as described in section 2.2.3, varying slightly the concentration of the fixation solution (350  $\mu\text{l}$  PEMS, 500  $\mu\text{l}$  heptane and 150  $\mu\text{l}$  formaldehyde 37%). To reduce auto fluorescence, embryos were incubated 10 min in  $\text{H}_2\text{O}_2$  and 10 min in sodium borohydrid (1mg/ml). After rehydration of the embryos, while performing the *in situ* hybridization protocol, all solutions contained DEPC.

Embryos were then washed 4 times with PBTw, once with PBTw/hybridization solution (1:1) and once with hybridization solution, each time 10 minutes, before incubating the embryos for 2 hours at  $55^{\circ}\text{C}$  with pre-hybridization solution (5 min at  $100^{\circ}\text{C}$  pre-heated hybridization solution containing 0,1% 10 mg/ml sonicated salmon sperm DNA [ssDNA]), after which the embryos were hybridized overnight at  $55^{\circ}\text{C}$  with prehybridization solution containing anti-*kon* probe DIG-labeled (1:300). The probe was then removed and the embryos thoroughly washed with hybridization solution and hybridization solution/PBTw (1:1), each step 30 min at  $65^{\circ}\text{C}$ , followed by 4 times 20 min wash at  $65^{\circ}\text{C}$  with PBTw and once at room temperature for 10 minutes.

To detect the signal from the *kon* probe, embryos were then incubated for 2 hours in TNB blocking buffer containing anti-DIG-POD antibody, and then washed 3 times with TNT buffer and incubated for 10 minutes in 50 $\mu\text{l}$  Tyramide-Cy3 (Perkin-Elmer TSA Kit). The reaction was stopped by washing Tyramide-Cy3 solution with TNT buffer, three times for 10 minutes at room temperature. At last standard incubation with primary and secondary antibodies was perform to add other markers to the staining, following the protocols described in sections 2.2.3 and 2.2.5.

## **2.3 Imaging and microscopy**

### **2.3.1 Sample preparation for microscopy**

After antibody staining, samples were prepared for microscopy. For imaging embryos, they were first fine dissected on a microscope slide to remove the gut and digestive tract, leaving the muscle network and nervous system intact in flat preparations. Embryos were then immersed in vectashield/glycerol (1:1), to avoid fluorescence bleaching, and then covered with a coverslip.

For larvae brain, the tissue was dissected and the VNC and brain removed from the animal after antibody staining. The VNC and brain were then placed on a microscope slide in the right orientation, immersed in vectashield/glycerol (1:1) and covered with a coverslip.

For whole larvae and larval NMJ, the fine dissection was performed prior antibody staining, thus after the final washing step in the antibody staining protocol the larvae were rinsed with PBS and then carefully placed in the right orientation on a microscope slide, immersed in vectashield/glycerol (1:1) and covered with a coverslip containing small amounts of plasticine in each corner as spacers.

All preparations were at last, prior imaging, sealed with nail polish.

### **2.3.2 Imaging and image processing**

Confocal images of embryos, larval VNC and brain, whole larva and larval NMJ were acquired using Leica TCS SP11 and SP5. Image processing was performed using Leica LCS lite, LAS AF lite, Photoshop and Illustrator

### **2.3.3 VNC length measurements**

Whole larvae were fixed by cold shock (5 min in -80 °C) and then placed in a microscope slide, immersed in glycerol and covered with a coverslip. Images were acquired using Zeiss AxioCam MRm mounted on a Leica binocular. Length measurements were performed using the ruler tool available in Photoshop.

### **2.3.4 4D recordings**

Embryos were selected according to markers and balancers, and manually dechorionated in a two-sided sticky tape. Two stage 13 embryos were selected, one as control and one overexpressing Kon in glia, and carefully glued to a coverslip covered on heptane surrounded by a Plexiglas. Embryos were then embedded in Voltalef oil and the microscope slide was sealed with a transparent tape. Both embryos were imaged together using a Leica SP5 microscope using the following settings. 20x objective plus 1,48x zoom, scanning a region of 95  $\mu\text{m}$  in depth at 1  $\mu\text{m}$  each stack-step for a total scanning and embryo development time of 6 hours. This time comprises the development from late embryonic stage 13 until early stage 17. Images were then processed using LAS AF lite and movie maker to create a video showing the VNC retraction during embryonic development.

### **2.3.5 Antibody staining intensity measurements**

Both imaging software, LCS lite and LAS AF lite, contain tools that allow the measurement of the intensity of the signal obtained for each scanned channel. LCS lite works with scans obtained using the Leica SP11 confocal microscope, and LAS AF lite with the scans from the Leica SP5.

Both software work in a very similar way, a region of interest (ROI) is selected in one stack and the program gives the dimensional properties of the region and, among other statistical parameters, the corresponding mean intensity for each channel, which will be then used to compare either the intensity of Glorund staining in the nucleus of two different glial cell populations throughout development or the loss of Kon at the NMJ after *kon* knockdown in glia compared to control animals.



## **2.4 NMJ phenotype score and statistics**

### **2.4.1 NMJ phenotypes**

For scoring NMJ phenotypes, and to make all data sets comparable to one another, it was always scored either left or right muscle 6/7 (m6/7) NMJ from the abdominal hemisegment A4. In all m6/7 NMJ sets scanned, identical laser and confocal settings were used.

All features of the NMJ were scored manually using the LAS AF lite software. The NMJ features scored were bouton number, single bouton number, branch number, satellite bouton and ghost bouton number.

Bouton was defined as a spherical HRP positive structure surrounded by Dlg staining. Branch was defined as two or more boutons arranged in a row, and when a branch bifurcates in 2 branches, forming a Y, it was overall counted as three. Single bouton was defined as a spherical HRP structure surrounded by Dlg, branching from the main tree, and not having any other bouton around. Satellite boutons are defined as little emerging boutons from a core bigger bouton. Usually, a core bouton bears more than one satellite bouton. Ghost boutons are defined as spherical HRP structures, detached from the NMJ tree, and lacking Dlg staining.

### **2.4.2 Statistics**

Statistical analysis was performed using the software SigmaPlot 11.0. Groups were tested pairwise using Students *t*-test to evaluate statistical differences. Statistical significance was set at p-values below 0,05. Higher degrees of significance were assigned to p-values below 0,01 and 0,001 respectively. Prior Students *t*-test, a Shapiro-Wilk test was performed in order to evaluate a normal distribution of the data sets. In case that one of groups tested had no normal distribution or that the groups displayed unequal variances, a Mann-Whitney Rank Sum Test was performed.

## **2.5 Western blot**

### **2.5.1 Tissue preparation**

For the western blot, a tissue fractionation separating soluble proteins from membrane bound proteins was performed. First, larvae were collected and rinsed with distilled water to remove all traces of food. Larvae were then re-suspended in 10  $\mu$ l TBS+PI (Protein inhibitor Pierce #88666) per larvae and potted, 20 strokes, using glass potter. The lysate was then centrifuged for 10 min at 15.000x g. The resulting supernatant was stored (S1 fraction) and the pellet was re-suspended in the same initial volume with TBS+PI, potted with 10 strokes and centrifuged again for 10 min at 15.000x g. After centrifugation, the supernatant (S2) was stored and the pellet followed the same previous procedure. After the centrifugation, the supernatant was stored (S3) and the supernatant was re-suspended in half the original volume with TBX+PI, potted with 10 strokes and centrifuged for 10 min at 15.000x g. The supernatants was collected (T1) and used as membrane bound not soluble fraction. Prior SDS-PAGE, S1 and T1 fractions were denatured in Laemmli buffer at 95 °C for 5 min.

### **2.5.2 SDS-PAGE and western blot**

SDS-PAGE was carried out by Dr Dominik Sakry using standard SDS-PAGE protocol followed by western-blot. The blot was developed using antibodies against HA and HRP as control, and detection was carried out through chemiluminescence.

## 2.6 Solutions and chemicals

Here a complete list with all the buffers used during this research and their recipes:

### PEMS buffer

- 0,1M Pipes
- 1 mM  $\text{MgSO}_4$
- 1 mM EGTA
- 1,2 M Sorbitol

### 20x PBS (pH 7,4) in 1 liter

- 151,94 g NaCl
- 19,88 g  $\text{Na}_2\text{HPO}_4$
- 8,28 g  $\text{NaH}_2\text{PO}_4 \cdot \text{H}_2\text{O}$

### PBT

- PBS in 0,1; 0,3 or 0,5% Triton X-100

### PBTw

- PBS in 0,1% Tween-20

### Hybridization buffer

- 20 ml Formamide
- 50  $\mu\text{l}$  Tween-20
- 17,5 ml DEPC- $\text{H}_2\text{O}$
- 12,5 ml 20x saline sodium citrate (SSC) buffer

TNB buffer

- 0,1 M Tris-HCl (pH 7,5)
- 0,15 M NaCl
- 0,05% Blocking reagent

TNT buffer

- 0,1 M Tris-HCl (pH 7,5)
- 0,15 M NaCl
- 0,5% Tween-20

TBS

- 0,1 M Tris-HCl (pH 7,5)
- 0,15 M NaCl

TBS+PI

- TBS plus protein inhibitor (Pierce #88666), diluted according to manufacturer

TBX

- TBS in 0,5% Triton X-100

### 3 Results

This chapter summarizes the results obtained in the course of the functional analysis in *Drosophila* of factors controlling glia differentiation in mouse. This chapter is divided in two main blocks: site-specific protein translation (hnRNPs and Src kinases) comprising parts 3.1 and 3.2, and NG2+ cells and the role of Kon during development, described in part 3.3.

Site-specific protein translation is a complex and tightly regulated process. In vertebrates, an example of site-specific protein translation control is mediated by hnRNPA2 and Fyn Src kinase in oligodendrocytes, directing Myelin Basic Protein (MBP) translation exclusively to the glia-neuron contact site during myelination. *Drosophila*, a non-myelinating organism, also uses site-specific protein translation during axis patterning in oogenesis and nervous system development, although to date no pathway has been described relating Src kinases and hnRNPs in protein site-specific translation in glia. The first part of the results will focus on answering whether Src kinases and hnRNPs are also involved in nervous system development in *Drosophila* embryos, starting with antibody staining for each candidate in combination with general markers to visualize protein distribution followed by the analysis of mutants for all candidate genes.

Progenitors of myelinating cells in vertebrates share a common cellular membrane marker, NG2. Those progenitor cells display a number of important properties that classify them as the fourth major glial cell population in vertebrates (together with oligodendrocytes, astrocytes and microglia). Kon, the *Drosophila* homologue of NG2, will be the subject of interest for the second part of this work and the results concerning Kon function during *Drosophila* nervous system development are given in part 3.3. The first set of exploratory experiments, regarding the function of Kon, lead the focus of research towards the larval neuromuscular junction (NMJ) and proteins located at the NMJ either in the pre or postsynapse. At last, I focused on the function and cleavage of Kon, as well as in proteins involved in Kon processing.

### 3.1 *Drosophila* Src kinases

The first part of the results aims to describe the expression pattern of both of the *Drosophila* Src kinases (Src42A and Src64B) during embryonic development, especially in glia and the nervous system. Fluorescent antibody staining and confocal images were acquired of embryos co-labeled with the pan glial marker Repo and each of the Src kinases. The images revealed ubiquitous expression throughout all developmental stages for Src42A, whereas Src64B expression is restricted to the tracheal pit during early developmental stages and commissural and longitudinal axons in later stages.

#### 3.1.1 Src42A expression pattern throughout embryogenesis

Previous publications have already shown Src42A expression during *Drosophila* embryonic development (Takahashi et al., 2005), although they lack a detailed description of Src42A glial expression. Confocal images of *Drosophila* embryos were acquired and analyzed, showing ubiquitous membrane localization and expression in all embryonic developmental stages. Commissural and longitudinal axons show the most prominent staining in the VNC, whereas in the PNS, the Intersegmental nerve (ISN) shows strong immunoreactivity.

In stage 11, all Repo positive glial cells express Src42A (dashed line Figure 3.1 A and A'), with no detectable Src42A enrichment on any specific region or tissue in the embryo. During stage 13, as axons in the VNC start forming bundles and extending longitudinal and commissural projections, they are accompanied by an increase in Src42A accumulation in this region, whereas in neighboring glia Src42A at the membrane remains unaltered (Figure 3.1 B and B'). In stage 15, there is a high Src42A accumulation in longitudinal and commissural axons as well as in the ISN and segmental nerve (SN) in the VNC (Figure 3.1 C and C'). Whole animal maximum projection of a stage 16 embryo (Figure 3.1 D and D') shows how all major axonal tracts have higher Src42A immunoreactivity. In a higher magnification, the Src42A antibody staining pattern along the VNC (Figure 3.1 E and E') resembles the VNC axon marker BP102, labeling all longitudinal and commissural axonal tracts. In the PNS from stage 16 embryo, Src42A is strongly expressed along the ISN (Figure 3.1 F and F').

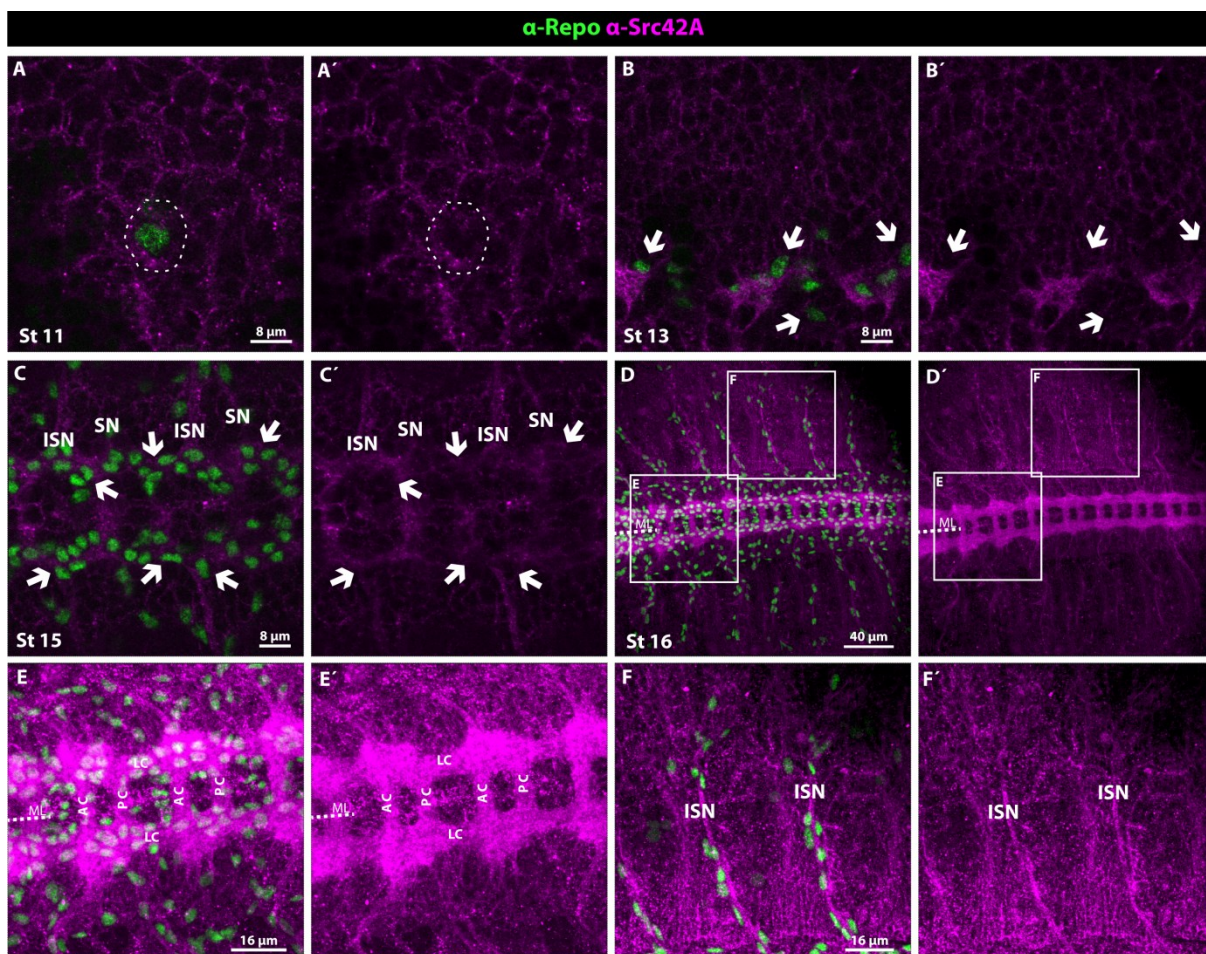


**Figure 3.1. Src42A is ubiquitously expressed during Drosophila embryonic development.**

(A – E) and F  $\alpha$ -Repo and  $\alpha$ -Src42A. (A' - F')  $\alpha$ -Src42A only. **(A - A')** Single focal plane of a stage 11 embryo, showing a ventrally located glia (dashed lined). **(B –B')** Single focal plane of the VNC of a stage 13 embryo. Glial cells locate along the forming axonal commissure (arrows). **(C – C')** Single focal plane of the VNC of a stage 15 embryo. Glial cells arranged along the formed axonal commissures (Arrows). Intersegmental and segmental nerve (ISN and SN) are Src42A positive. **(D – D')** Maximum projection of a stage 16 embryo. Src42A is ubiquitously distributed in the embryo, together with a prominent staining found in the axonal commissures. Higher magnifications shown in E-F' accordingly marked. **(E – E')** Higher magnification of the VNC region marked in D. Anterior, posterior and lateral commissure (AC, PC and LC) are labeled. **(F – F')** Higher magnification of the PNS region marked in D. ISN accumulating high Src42A expression is labeled.

### 3.1.2 Src64B expression pattern during embryonic development

Src64B expression in the *Drosophila* embryo is more restricted than Src42A. In stage 11, only the tracheal pits express the Src64B (Figure 3.2 A and A'), whereas no glia has detectable Src64B expression. *Drosophila* embryos in stage 13 concentrate Src64B expression at the developing longitudinal and commissural axons in the VNC (Figure 3.2 B and B'). In stage 16, Src64B expression is most prominent at the VNC, especially in longitudinal and commissural axons and is also weakly expressed along the ISN (Figure 3.2 C and C').

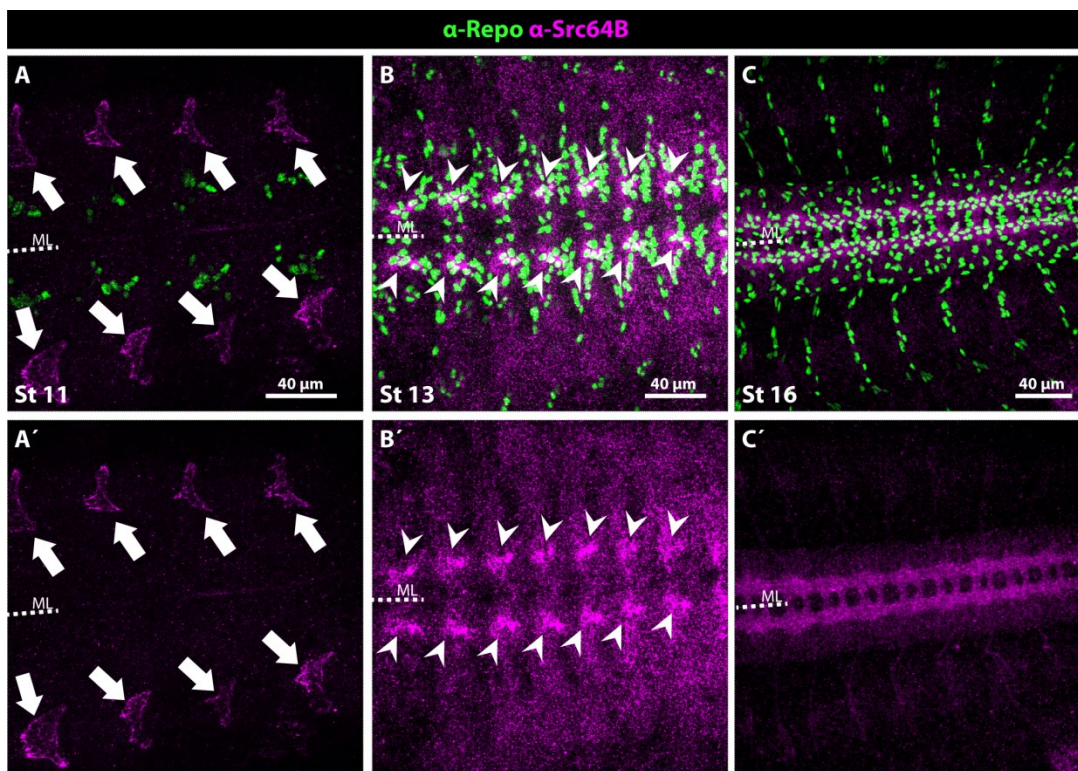


**Figure 3.2. Src64B is expressed in the tracheal pits and longitudinal and commissural axons in the *Drosophila* embryo.**

A, B and C showing  $\alpha$ -Repo and  $\alpha$ -Src64B staining. A', B' and C' showing  $\alpha$ -Src64B staining only. (A - A') Maximum projection of stage 11 wildtype embryo. Tracheal pits prominently stained with  $\alpha$ -Src64B (Arrows). Midline (ML) marked by dashed line. (B - B') Maximum projection of a stage 13 embryo. Forming longitudinal and commissural axons are prominently stained with  $\alpha$ -Src64B (Arrowheads). (C - C') Maximum projection of a stage 16 embryo.  $\alpha$ -Src64B staining concentrates along longitudinal and commissural axons and the ISN in the PNS.



### 3.1.3 Src42A is involved in the proper formation of longitudinal axons in the VNC

Antibody staining against each of the Src kinases showed high immunoreactivity in longitudinal and commissural axons during late embryonic stages (Figure 3.1 E and Figure 3.2 C).  $\alpha$ -BP102 is a widely used marker for longitudinal and commissural axons, and hence a suitable marker to study the proper formation of those axons along the VNC in Src42A or Src64B mutant embryos. In a wildtype embryo,  $\alpha$ -BP102 antibody staining has a stereotypical “ladder like” pattern (Figure 3.3 A), with regular intervals and thickness along it. In *Src42A*<sup>26-1</sup> homozygous mutant embryo, there is a reduction in the width of longitudinal axons (arrows in Figure 3.3 B), whereas commissural axons remain unaffected. On the other hand, *Src64B*<sup>KO</sup> homozygous mutant embryos do not show any alteration in BP102 pattern as compared to wildtype animals (Figure 3.3 C).

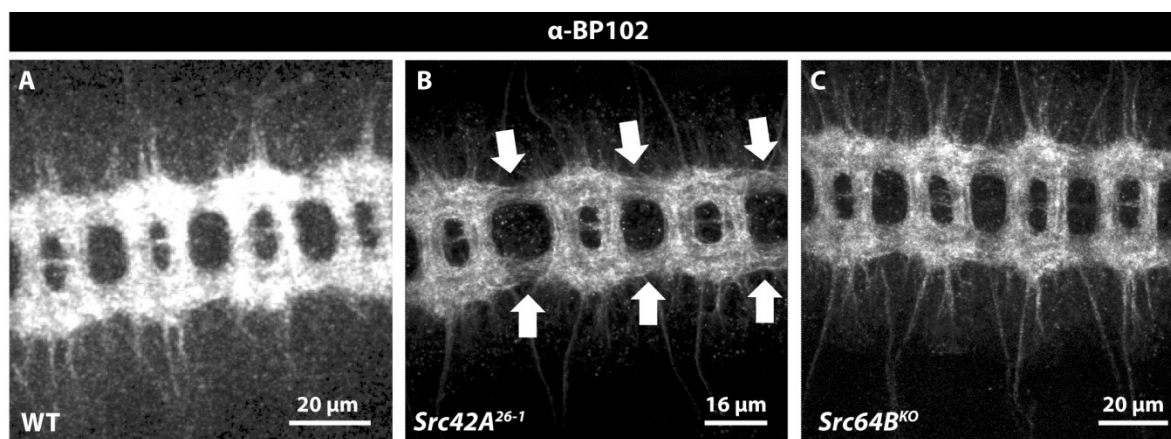


**Figure 3.3. BP102 staining in wildtype and Src kinase mutant embryos.**

A, B and C VNC of a stage 16 Embryo stained with  $\alpha$ -BP102. **(A)** Stereotypical ladder-like pattern observed from the staining of longitudinal and commissural axons in wildtype. **(B)** Homozygous Src42A mutant embryo (*Src42A*<sup>26-1</sup>). Longitudinal axons appear thinner than wildtype (arrows), while commissural axons display relatively normal shape. **(C)** Homozygous Src64B mutant embryo (*Src64B*<sup>KO</sup>). No difference observed in longitudinal or commissural axons as compared to wildtype.

### 3.1.4 Neuronal microtubule pattern is not affected in Src42A mutant

As previously shown, Src42A is expressed in a broader pattern than Src64B, and Src42A mutants display a phenotype in longitudinal axons pattern in the VNC as observed with the  $\alpha$ -BP102 antibody staining. This raised the question whether Src42A mutations would also have other effects in glia-neuron interaction and thus produce other phenotypes.

Hetero- and homozygous Src42A mutant embryos (*Src42A*<sup>26-1</sup>) were stained with the antibodies  $\alpha$ -Repo and  $\alpha$ -Futsch, a neuronal microtubule marker, to study the neuronal wiring in late embryos. Heterozygous (*Src42A*<sup>26-1</sup>/*Cyo*) whole animal confocal images (Figure 3.4 A – B) show wildtype like  $\alpha$ -Futsch and  $\alpha$ -Repo patterns in the VNC and PNS. A higher magnification of the VNC (Figure 3.4 C) shows ventral unpaired median (VUM) neuron projections, and the staining corresponding to ISN and SN leaving the VNC, and projecting towards the PNS. In the PNS, cell body of sensory neurons and axons are also labeled by  $\alpha$ -Futsch (Figure 3.3 D). The pattern shown by  $\alpha$ -Futsch antibody in these heterozygous animals resembles the pattern observed in wildtype (Data not shown). In Src42A homozygous mutant animals (*Src42A*<sup>26-1</sup>/*Src42A*<sup>26-1</sup>), there are no differences in  $\alpha$ -Futsch or  $\alpha$ -Repo antibody staining pattern as compared to Src42A heterozygous mutant embryos (Figure 3.4 E – F), even when comparing higher magnifications of the VNC and PNS, homozygous and heterozygous Src42A mutants show no major differences (Figure 3.4 G and H respectively). Cell body of sensory neurons and axons are not affected.

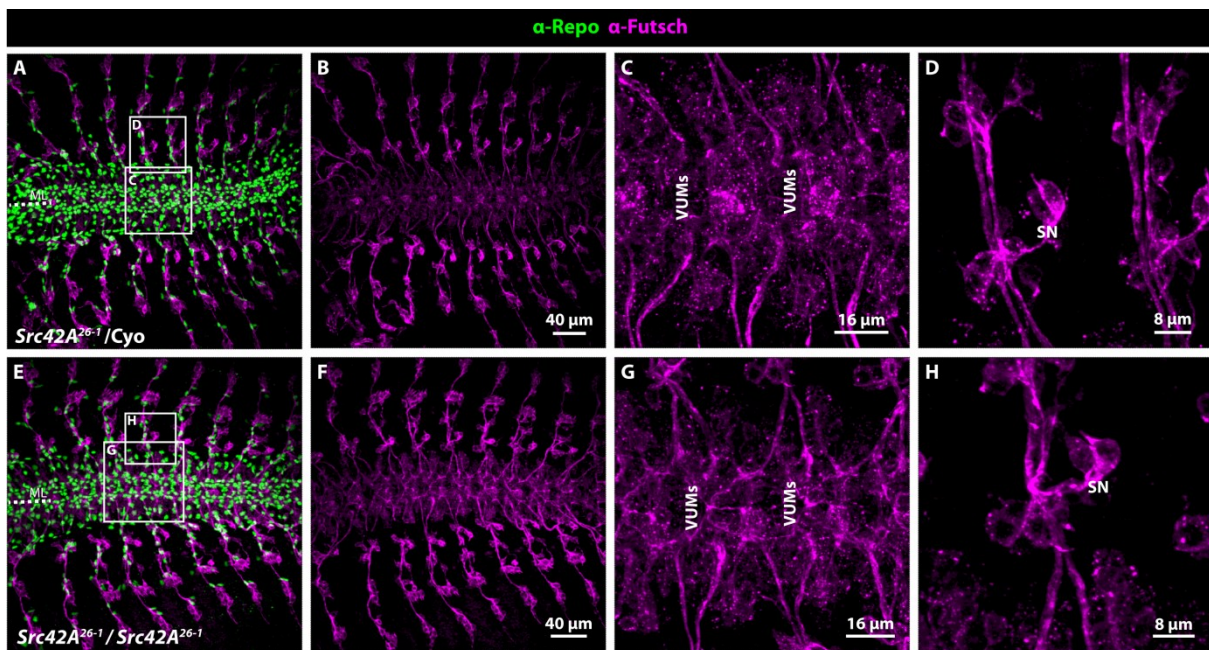


**Figure 3.4. Src42A homozygous and heterozygous mutant embryos stained against the microtubule marker Futsch.**

A and E  $\alpha$ -Futsch and  $\alpha$ -Repo staining. B – D and F – H  $\alpha$ -Futsch only staining. Anterior is to the left in all images. **(A - B)** Stage 16 Src42A transheterozygous mutant embryo (*Src42A<sup>26-1</sup>/Cyo*). **(C)** Enlargement of the VNC region in (A). VUM neuron are marked. **(D)** Enlargement of the PNS region in (A) showing the cell body of sensory neurons (SN). **(E)** Stage 16 Src42A mutant embryo (*Src42A<sup>26-1</sup>/Src42A<sup>26-1</sup>*). **(G)** Higher magnification of the VNC region highlighted in (E). VUM neuron projections are labeled. **(H)** Higher magnification of the PNS region highlighted in (E) showing PNS sensory neurons.

### 3.1.5 Src42A is not involved ePG migration in the PNS

In *Drosophila*, the migration of embryonic peripheral glia (ePG) along the ISN and SN serves as a model to study glia-glia and glia-neuron crosstalk during embryonic nervous system development. Netrins, Frazzled and Uncoordinated 5, all proteins involved in cell-cell communication, have been shown to mediate glia migration from and towards the VNC, where the relative position of ePGs at the end of embryogenesis are means of normal or impaired migration (von Hilchen et al., 2010).

Src kinases have been also involved in cell-cell communication, migration and adherence, thus making Src42A an interesting candidate to study ePG migration in the PNS during embryonic development. To visualize ePG migration, stage 16 embryos with different genetic backgrounds were stained with  $\alpha$ -Fas2 and  $\alpha$ -Repo antibodies, labeling the axonal fascicles in the PNS and glia nuclei, respectively. In Src42A heterozygous mutant embryos (*Src42A<sup>26-1</sup>/Cyo*), same as in Src42A homozygous mutant (*Src42A<sup>26-1</sup>/Src42A<sup>26-1</sup>*), the relative position of all ePG in stage 16 is comparable to wildtype embryos (data not shown), thus meaning that Src42A mutations do not result in migration impairment (Figure 3.5 A – B'). Knockdown of Src42A in glia experiments yield identical results, where control (*UAS-dicer2/Cyo;repo-GAL4/+*) and Src42A knockdown embryos (*UAS-dicer2/Src42ARNai;repo-GAL4/+*) display similar ePG arrangement in the PNS to those found in wildtype (Figure 3.5 C – D').

These results, and the results shown in sections 3.1.3 and 3.1.4, indicate that although Src kinases are widely expressed in the CNS and PNS, their contribution to glia-neuron interaction regulation and nervous system development in *Drosophila* is limited, and no major or key processes depend on their regulation.

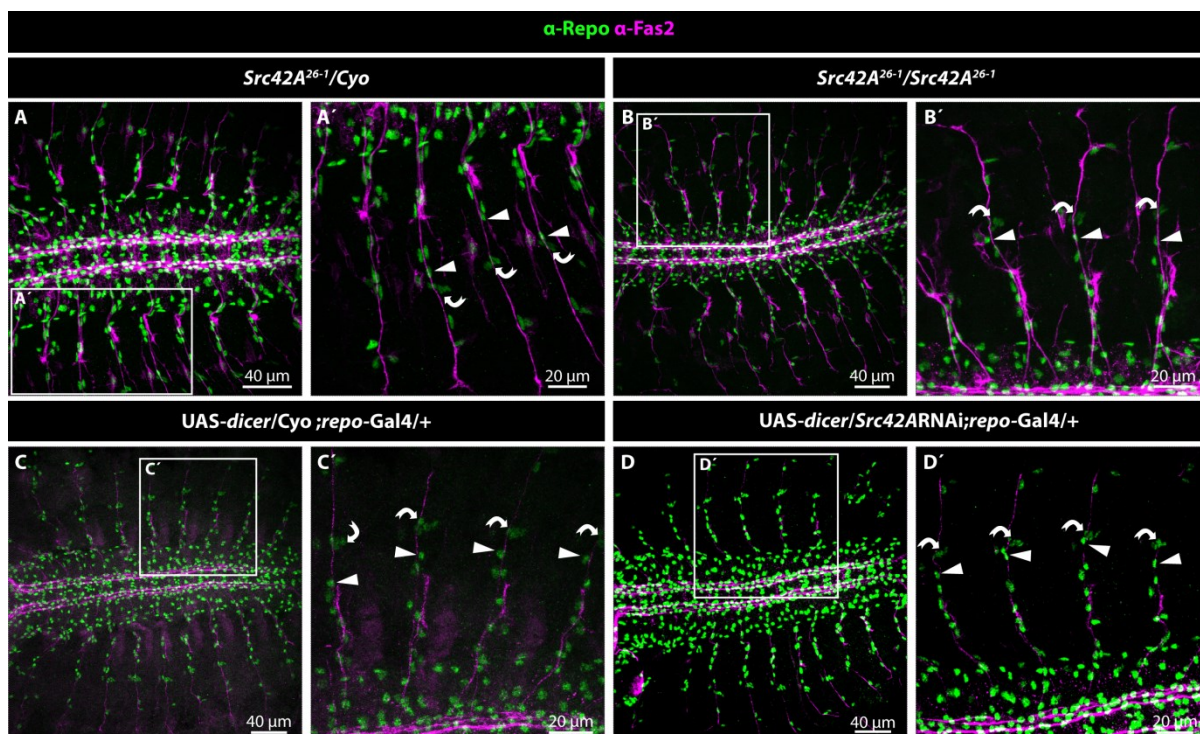


**Figure 3.5. *Src42A* mutant and *Src42A* glial knockdown do not affect ePG migration**

Anterior is to the left. Stage 16 embryos stained with  $\alpha$ -Repo and  $\alpha$ -Fas2. In all higher magnifications (A', B', C' and D') ePG9 (arrowhead) and the lateral chordotonal organ (bend arrow) have been labeled as landmarks. **(A)** *Src42A* transheterozygous mutant embryo (*Src42A*<sup>26-1</sup>/*Cyo*). **(A')** Enlargement of the region highlighted in (A) showing the PNS. **(B)** *Src42A* homozygous mutant embryo (*Src42A*<sup>26-1</sup>/*Src42A*<sup>26-1</sup>). **(B')** Enlargement of the PNS region highlighted in (B). **(C)** Control animal for the knockdown of *Src42A* in glia (*UAS-dicer2/Cyo;repo-GAL4/+*) **(C')** Enlargement of the PNS region highlighted in (C). **(D)** *Src42A* knockdown in glia embryo (*UAS-dicer/Src42ARNai;repo-GAL4/+*). **(D')** Enlargement of the PNS region highlighted region in (D).

### 3.2 The *Drosophila* hnRNP F/H homologue, Glorund

Glorund (Glo) was first described to be involved in the process of anterior-posterior and dorsal-ventral egg axis patterning during early *Drosophila* development (Kalifa et al., 2006; Kalifa et al., 2009). It was shown that Glo acts repressing the translation of mislocalized *nanos*, *oskar* and *gurken* mRNAs, through an orchestrated interaction with Hrp48, the *Drosophila* homologue of hnRNP A/B, and Half-pint, a known splicing factor.

#### 3.2.1 Glorund is ubiquitously expressed during embryonic and larva development in *Drosophila*

*Drosophila* embryos stained with  $\alpha$ -Glorund show ubiquitous nuclear expression that in glial cells varies in intensity according to the glial cell subpopulations and developmental stage. In stage 12 embryos,  $\alpha$ -Glo staining intensity in the nucleus of longitudinal glia (LG) precursors is slightly lower than in the nucleus of subperineurial glia (SPG) (Figure 3.6 A-B'). By stage 14 and later stage 16, the antibody staining intensity difference between LG and SPG is steadily increased (Figure 3.6 C-D' and E-F', stage 14 and 16 respectively). During larval stages, the difference in intensity between LG and SPG is reduced and no longer observed in confocal images (Figure 3.6 G,G'). In vertebrates, hnRNP F/H downregulation in maturing oligodendrocytes has been described as a key step in favoring PLP expression over its splice variant DM20, a developmentally required change during myelination (Wang et al., 2007; Wang and Cambi, 2009).

To quantify Glo expression in LG and SPG during embryonic development, I performed pixel intensity quantification in confocal images obtained in the Leica SP11. The results were then plotted and statistically analyzed. Three animals per developmental stage and from those three LG and three SPG from abdominal hemisegments were taken for pixel intensity measurements, using  $\alpha$ -Repo to normalize  $\alpha$ -Glo intensity in each cell. There is a steady loss in  $\alpha$ -Glo intensity in LG as compared to SPG, starting in stage 13 with 1,5:2 (LG:SPG) and reaching in stage 16 a 1:2 ratio. In all stages,  $\alpha$ -Glo intensity in LG is statistically significant lower than in SPG, obtained by *t-test* (Figure 3.6 H).

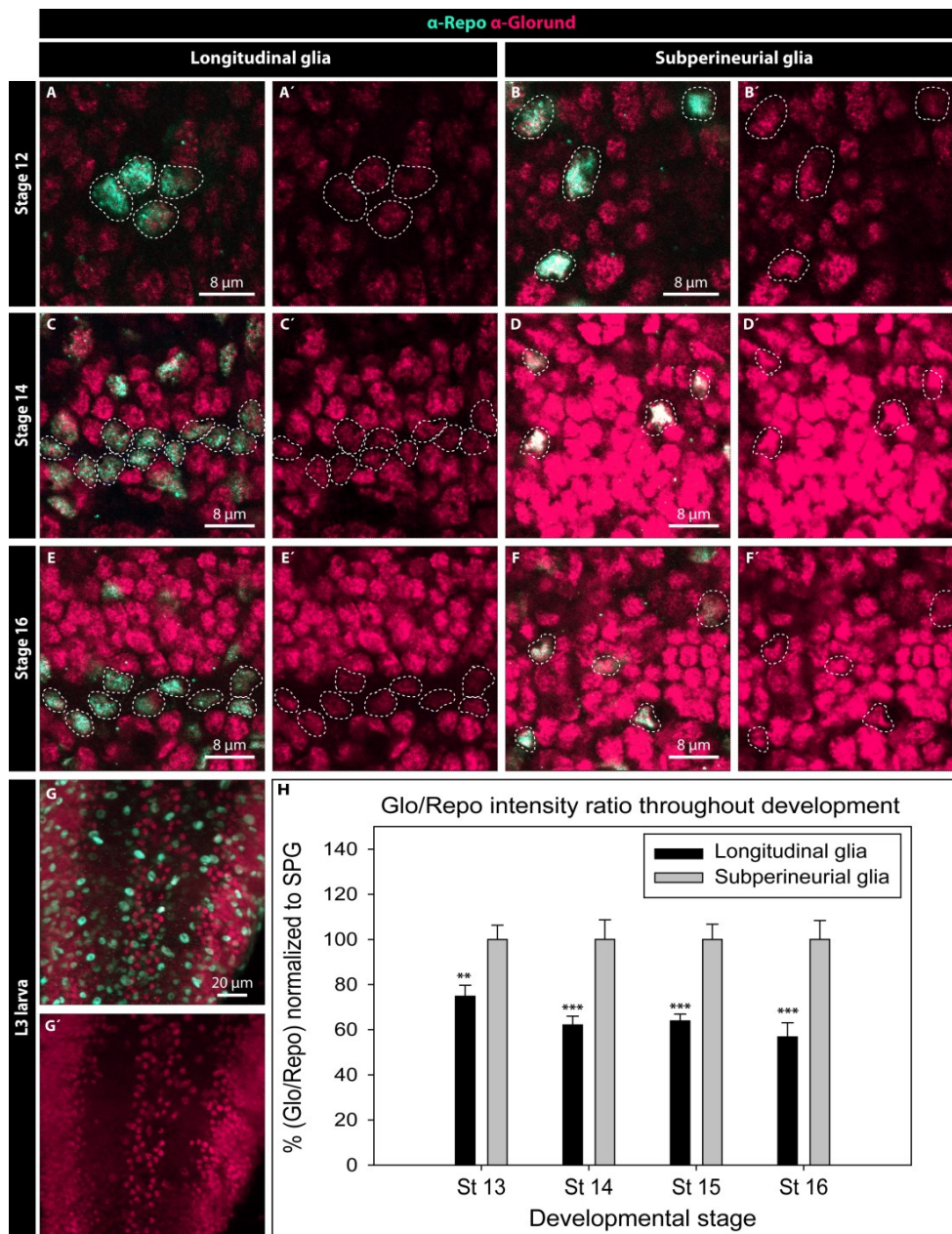


**Figure 3.6. Glo is downregulated in LG during embryonic development**

Wildtype stage 12 (A – B'), stage 14 (C – D'), stage 16 embryo (E – F') and L3 larva (G – G') stained with  $\alpha$ -Repo and  $\alpha$ -Glo. Single focal planes of longitudinal glia (A, A', C, C', E and E') and subperineurial glia (B, B', D, D', F and F') shown in separate panels. (G – G') Maximum projection showing the VNC of L3 larva. (H) Graphic comparing  $\alpha$ -Glo/ $\alpha$ -Repo pixel intensity ratio in LG as compared to SPG. For every embryonic stage, values have been normalized to Glo/Repo ratio in SPG. Statistical analysis reveals significant differences in all developmental stages tested between LG and SPG. *t*-test (\*\*)  $p < 0,01$  and (\*\*\*)  $p < 0,001$ . A - F' anterior is left and G, G' is up.

### 3.2.2 Glorund mutant analysis in embryo and larva

As shown previously, Glo expression starts very early in development, and also includes a strong maternal contribution that helps controlling the site specific translation of the egg axis patterning mRNAs *oskar*, *nanos* and *gurken* (Kalifa et al., 2009). Glo mutant embryos, coming from the cross of two heterozygous parental lines, are thus developing normally in early stages due to the maternal contribution of Glo, leading the focus towards late embryo and larva when analyzing the role of Glorund during nervous system development in *Drosophila*.

Confocal images of stage 16 homozygous Glo mutant (loss of function allele *glo*<sup>162x</sup>) stained with  $\alpha$ -Fas2 and  $\alpha$ -Repo, shows overall normal development (Figure 3.7 A,A'). In the PNS, migration and positioning of glial cells is not affected and the same occurs along the VNC (Figure 3.7 B and C respectively). In the VNC and PNS fascicles also develop normally (Figure 3.7 B' and C' respectively). In wildtype L3 larva, the VNC displays a stereotypical  $\alpha$ -Fas2 pattern showing the arrangement of medial (MF), intermediate (IF) and lateral fascicles (LF) (Figure 3.7 D-D'). In *glo*<sup>162x</sup> homozygous L3 larva, the stereotypical organization of fascicles (MF, IF and LF) along the VNC is impaired (Figure 3.7 E-E'). Unfortunately, with these results is not possible to answer whether the fascicle disorganization observed is due to impaired Glo mediated glia-neuron or neuron-neuron communication, for that further experiments would be needed.

Same as with Src kinases, the results obtained in the Glorund chapter are not conclusive for a key role during *Drosophila* nervous system development, that could be studied in depth in the frame of glia-neuron interaction. Those results allow me to focus my research in the role of the *Drosophila* homologue of mouse NG2.



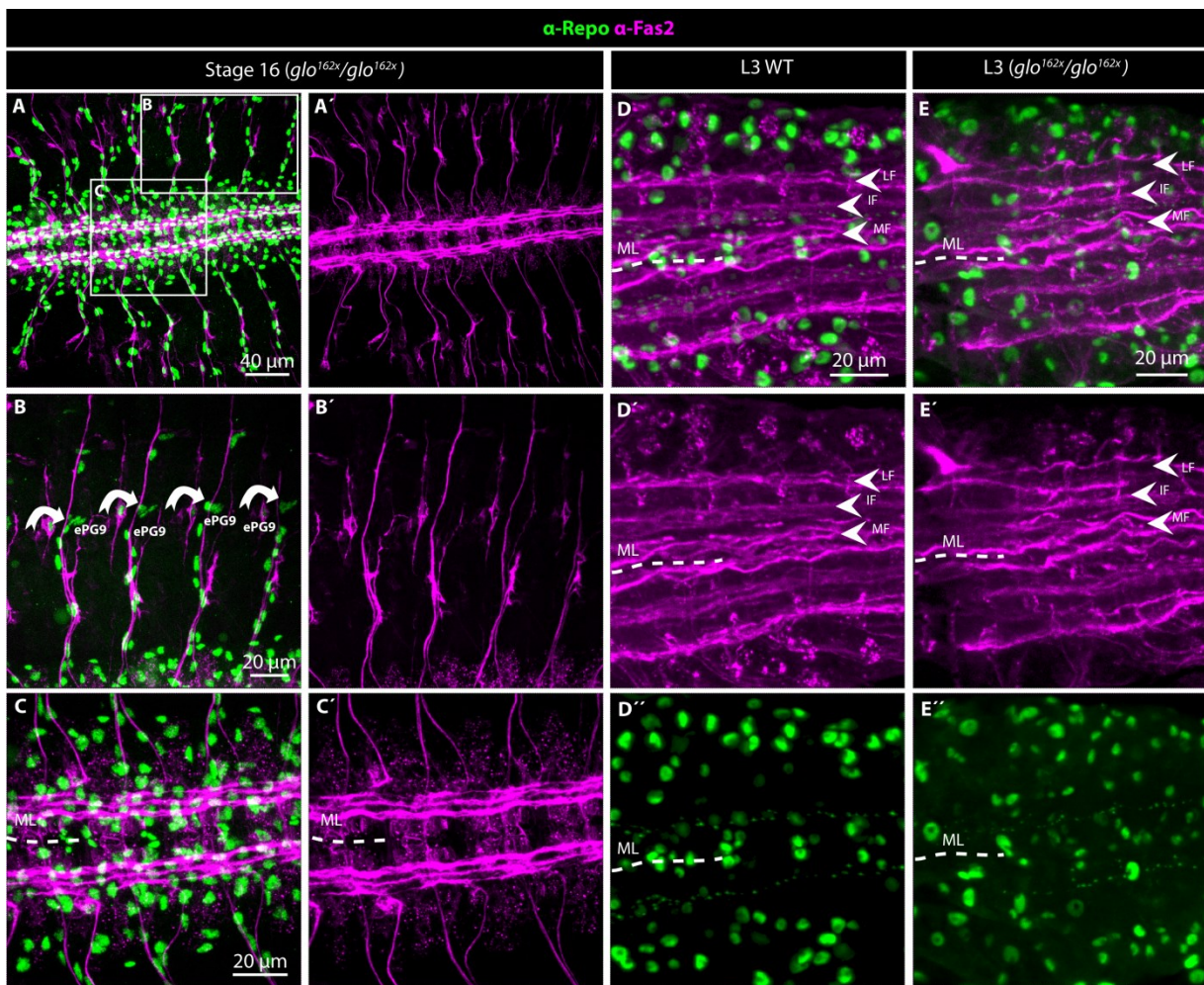


**Figure 3.7. Nervous system development in Glo mutant background**

(A – C') Stage 16 and (E – E'') L3 Glo homozygous mutants (*glo*<sup>162x</sup>/*glo*<sup>162x</sup>), and (D – D'') L3 wildtype stained with  $\alpha$ -Fas2 and  $\alpha$ -Repo. **(A - A')** Maximum projection of whole embryo. **(B -B')** Higher magnification of the PNS region shown in (A). Lateral chordotonal organ (bend arrow) and ePG9 are labeled for glial migration orientation. **(C -C')** Higher magnification of the VNC region shown in (A). **(D)** Maximum projection of a region of the VNC in L3. **(D')**  $\alpha$ -Fas2+ fascicles in wildtype L3 VNC. **(D'')**  $\alpha$ -Repo+ glia in the wildtype L3 VNC. **(E)** Maximum projection of Glo homozygous mutant L3 VNC. In display a similar region as shown in (D). **(E')** Fascicles and **(E'')** glia (E). Fascicle bundles have been labeled in D and E (Lateral – LF, intermediate – IF and medial fascicules – MF). Mid line (ML) is marked with a dashed line.

### 3.3 Kon-tiki, the *Drosophila* NG2/CSPG4 homologue

Kon-tiki (Kon) is a proteoglycan well conserved throughout evolution. It has been ubiquitously found in several organisms, from *C. elegans* to humans. In *Drosophila*, Kon is expressed in myoblasts during embryogenesis and mediates ventral-longitudinal muscle attachment to the corresponding tendon cell, thus allowing the proper muscle-tendon network formation. Kon has been shown to interact with the *Drosophila* Glutamate receptor interacting protein (DGrip) and Integrins, when mediating the proper formation of the muscle-tendon network (Schnorrer et al., 2007) (Estrada et al., 2007). Both Kon interactions, with Grip and Integrins, have been also found to take place in vertebrates, raising the questions whether more conserved pathways and interacting partners can be found.

#### 3.3.1 Kon embryonic and larval expression

Kon is localized at the tip of extending myoblasts during the formation of the muscle-tendon attachment, although the *kon* mRNA pattern, by *in-situ* hybridization, shows a broader expression pattern. In stage 13 embryos, *kon* mRNA was found to be expressed not only in myoblast (Figure 3.8 A,A'), but also in PNS glia, as shown by single focal images (Figure 3.8 B,B'). In the developing brain, several glial cells showed strong *kon* mRNA staining (Figure 3.8 C,C'). From those, two glia per hemisphere, one located ventral and one dorsal, showed strong nuclear *kon* mRNA staining (Figure 3.8 D,D').

Antibody staining against Kon ectodomain ( $\alpha$ -Kon<sup>ecto</sup>) in L3 larvae shows high immunoreactivity along the nerve extension region (NER) as speckles (Figure 3.8 E,E'). These speckles showed to be ubiquitously located along the outer glial cell layer (Figure 3.8 F,F'). Similar  $\alpha$ -Kon<sup>ecto</sup> speckles were also observed in muscles, close to the NMJ. The NMJ itself also shows  $\alpha$ -Kon<sup>ecto</sup> immunoreactivity (Figure 3.8 G,G'). Higher magnification shows presynaptic  $\alpha$ -HRP surrounded by  $\alpha$ -Kon<sup>ecto</sup> staining, although the origin of  $\alpha$ -Kon<sup>ecto</sup> signal is not clear. It could be muscle, neuron or glia derived, or a combination of them (Figure 3.8 H-H').

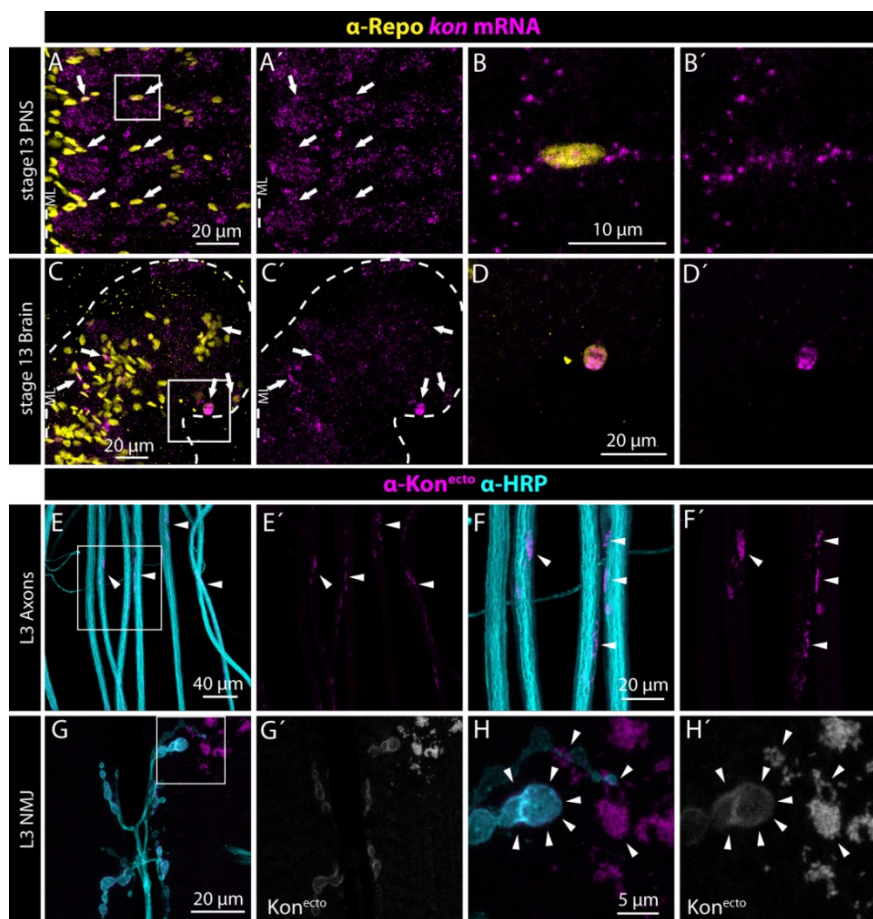


**Figure 3.8. Kon and *kon* expression in embryo and larva.**

(A – D') Stage 13 embryo stained with  $\alpha$ -Repo and *kon* mRNA. (E – H') L3 larva stained with  $\alpha$ -Kon<sup>ecto</sup> and  $\alpha$ -Repo. (A - A') Maximum projection showing the PNS and VNC. Arrows indicate  $\alpha$ -Repo and *kon* positive glia in the PNS. (B - B') Single focal plane of the region highlighted in (A), showing a glia expressing *kon* mRNA expressing glia. (C - C') Maximum projection of the right brain hemisphere. Dashed line marks the contour of the brain hemisphere. Arrows indicate *kon* mRNA expressing glia. (D -D') Single focal plane of the region marked in (C) showing *kon* mRNA nuclear localization in glia. (E - E') Along the axons connecting the CNS and PNS in wildtype L3 larva (NER) stained with  $\alpha$ -HRP and  $\alpha$ -Kon<sup>ecto</sup>. Arrowheads indicate  $\alpha$ -Kon<sup>ecto</sup> speckles. (F - F') Higher magnification of the region highlighted in (E). (G - G') NMJ from muscles 6 and 7 in wildtype L3 larva. (H - H') Higher magnification of the region highlighted in (G), showing the last boutons from a NMJ branch stained with  $\alpha$ -HRP and  $\alpha$ -Kon<sup>ecto</sup>, at the synapse and as speckles, indicated with arrowheads.

### 3.3.2 Kon is not involved in embryonic glial development in the nervous system

In order to investigate Kon's function during embryonic nervous system development, I analyzed  $\alpha$ -Repo and  $\alpha$ -Futsch pattern in Kon mutant and *kon* knockdown in glia in late embryos. Antibody staining in Kon transheterozygous (*konDf(2L)2364/kon<sup>c0025</sup>*) shows overall wildtype glia arrangement and Futsch pattern (Figure 3.9 A). Migration and glia positioning along the PNS and VNC are not affected (Figure 3.9 B,C). These results were also confirmed by glia specific *kon* knockdown, where no migration, proliferation nor position of glial cells was affected (Figure 3.9 D-F). Although by *in-situ* hybridization it was possible to observe *kon* mRNA expression in brain glia, it was not possible to address phenotypes occurring during embryonic brain development.

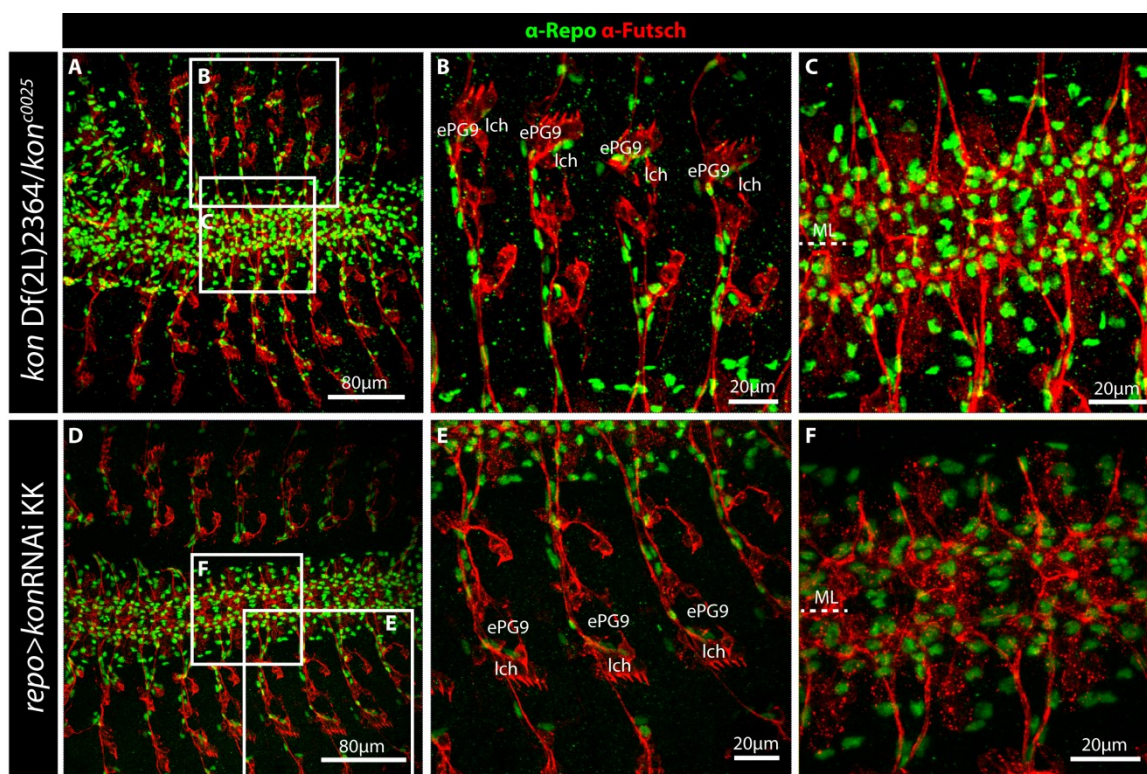


**Figure 3.9.  $\alpha$ -Repo and  $\alpha$ -Futsch staining in Kon mutant and *kon* knockdown in glia.**

Stage 16 (A – C) Kon transheterozygous (*konDf(2L)2364/kon<sup>c0025</sup>*) and (D – F) *kon* knockdown in glia, stained against Repo and Futsch. (A and D) Whole embryo maximum projection. (B) PNS region highlighted in (A). (C) VNC region highlighted in (A). (E) PNS region highlighted in (D). (F) VNC region highlighted in (D). ePG9 and lch are labeled for orientation. Midline (ML) is marked with a dashed line.

### 3.3.3 Glia derived Kon accumulates at the NMJ and contributes to the NMJ

Taking into account that Kon mutations lead to a strong muscle-tendon network phenotype, I decided to use *kon* knockdown in glia instead and avoid the side effects of a malformed muscle-tendon network in other developmental processes. We used three different dsRNA stocks to knockdown *kon* in glia during development. The *repo*-GAL4 stock used was combined with UAS-*dicer2* to increase the efficiency of the knockdown. Control and *kon* glia knockdown larvae were stained with  $\alpha$ -HRP and  $\alpha$ -Dlg to visualize NMJ morphology in late larvae. As control group I used *dicer2;repo*-GAL4 crossed to wildtype. The knockdown of *kon* in glia leads to a NMJ phenotype, which was scored in L3 larvae in muscle 6 and 7 NMJ (m6/7 NMJ) and it was reproducible with all three dsRNA stocks used (Figure 3.10 A - D). In *kon* knockdown in glia, NMJ bouton number counts show a statistically significant increase of 50% on average (Figure 3.10 E). The number of single boutons in *kon* glia knockdown was also increased in two out of the three dsRNA used (Figure 3.10 F), C2 and GD, with significant and highly significant statistical differences. No statistically significant differences were observed in branch number, although glial *kon* knockdown displayed on average at least one branch more than control (Figure 3.10 G). All three *kon* dsRNA stocks were controlled in order to neglect any NMJ phenotypes caused by the insertion of the RNAi construct. Each stock was crossed to wildtype and the main scored NMJ phenotypes were statistically analyzed. No significant differences were observed, except for an increase in branch number in *konRNAiGD* (Figure 3.10 H)

As shown in Figure 3.8 G-H',  $\alpha$ -Kon<sup>ecto</sup> antibody staining labels Kon localized at the synapse in L3 larva, and Figure 3.10 A-G shows that *kon* knockdown in glia results in larval NMJ phenotypes. Combining both results, it suggests that glial derived Kon, or at least the ectodomain, is deposited and accumulates at the synapse. To test this, I measured the  $\alpha$ -Kon<sup>ecto</sup> signal intensity at the synapse in control and *kon* knockdown in glia (*konRNAiGD*) larvae, and statistically compared both. Before comparing directly  $\alpha$ -Kon<sup>ecto</sup> signal intensity, I first controlled for antibody staining intensity dispersion between both groups by comparing the  $\alpha$ -HRP and  $\alpha$ -Dlg quotient ( $\alpha$ -HRP/ $\alpha$ -Dlg) via *t*-test, resulting in no statistical significant difference (Figure 3.10 I). The  $\alpha$ -HRP/ $\alpha$ -Dlg quotient was also used as factor to correct for

dispersion in  $\alpha$ -Kon<sup>ecto</sup> signal, thus resulting the following formula:  $([I]\alpha\text{-Kon}^{\text{ecto}}) * ([I]\alpha\text{-HRP}/[I]\alpha\text{-Dlg})$ , where [I] is mean pixel intensity in the region of interest (ROI) selected. There was a statistically significant decrease ( $p < 0,001$ ) of  $\alpha$ -Kon<sup>ecto</sup> intensity at the NMJ in glial *kon* knockdown as compared to control animals (Figure 3.10 J), although not a complete loss of  $\alpha$ -Kon<sup>ecto</sup> signal. Further experiments will show that muscle derived Kon also accumulates at the NMJ.

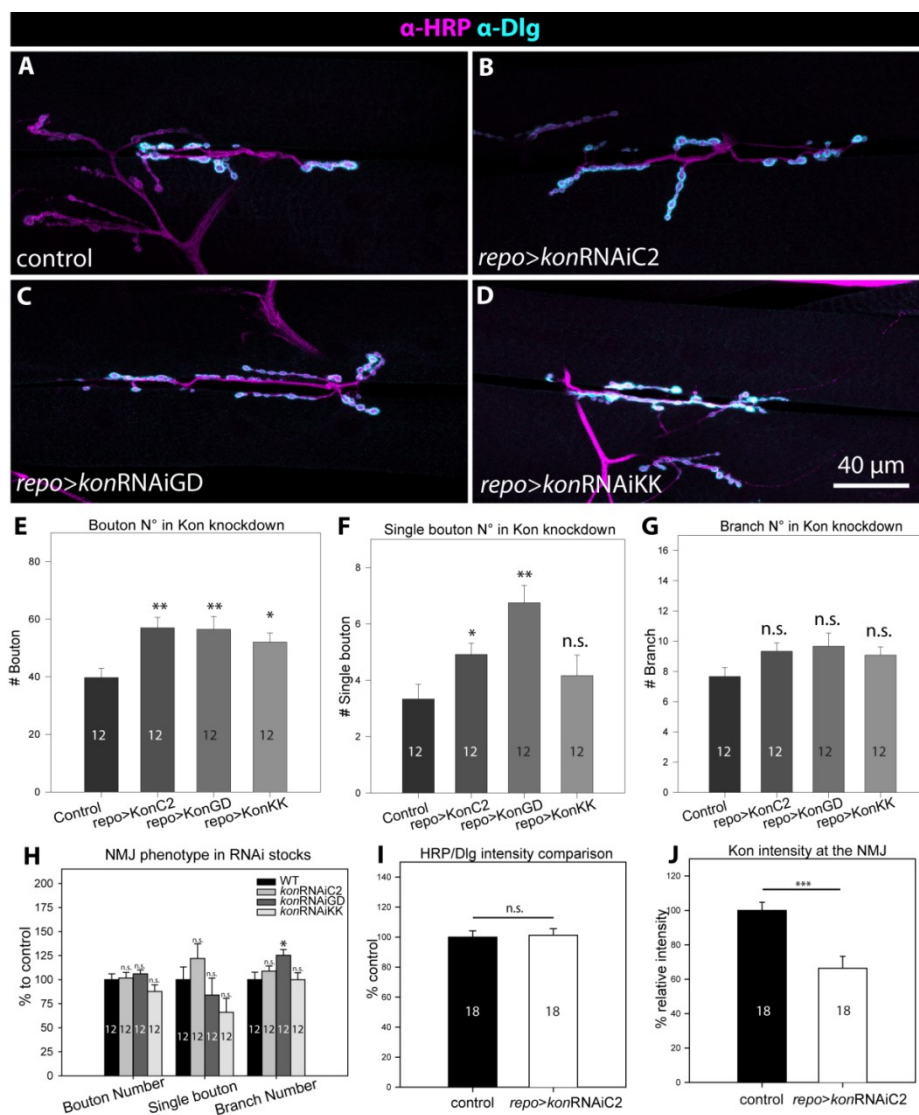


**Figure 3.10. Larva NMJ phenotypes observed in *kon* knockdown in glia.**

(A – D) m6/7 NMJ from L3 larva stained with  $\alpha$ -HRP and  $\alpha$ -Dlg. (A) control *UAS-dicer2;repo-GAL4/+* larva. (B) *kon* knockdown in glia (*UAS-dicer2/UAS-konRNAiC2;repo-GAL4/+*) (C) *UAS-dicer2/UAS-konRNAiGD;repo-GAL4/+* and (D) *UAS-dicer2/UAS-konRNAiKK;repo-GAL4/+*. (Next page)

**Figure 3.10. Larva NMJ phenotypes observed in kon knockdown in glia**

(From previous page) Statistical analysis of **(E)** bouton number **(F)** single bouton and **(G)** branch number in control and *kon* glial knockdown. Same genotypes as in A - D. **(H)** Statistical analysis of bouton, single bouton and branch number between wildtype and *konRNAi* stocks. Wildtype scores are set to 100% and the values for *konRNAi* C2, GD and KK have been changed accordingly. **(I)** Statistical analysis of the ( $\alpha$ -HRP/ $\alpha$ -Dlg) staining intensity quotient between control (*UAS-dicer2;repo-GAL4/+*) and *kon* knockdown in glia (*UAS-dicer2/UAS-konRNAiC2;repo-GAL4/+*). **(J)**  $\alpha$ -Kon<sup>ecto</sup> staining intensity statistical comparison. Mean and SEM are plotted as bar and error bar respectively in each graph. Number of animals analyzed is written in each bar. p values are represented by (\*) $p > 0,05$ ; (\*\*) $p < 0,01$ ; (\*\*\*) $p < 0,001$  and (n.s.) $p > 0,05$ .

### 3.3.4 Identifying the PNS glial layer(s) involved in Kon dependent NMJ phenotype

In the PNS, glial cells ensheath axons in order to protect and support them. It has been shown that glial cells form three distinct layers around axons and each of those glial layers can be uniquely identified and addressed by specific GAL4 drivers. The availability of those GAL4 drivers makes it possible to answer questions regarding the function of each of the glial layers in the PNS (von Hilchen et al., 2013), for instance which layer contributes to glia-Kon derived NMJ phenotype?

First, to separately visualize the morphology of each PNS glial layer around the NMJ, specific GAL4 drivers were crossed to a reporter line bearing in the second and in the third chromosome a copy of a membrane bound GFP (UAS-CD4::GFP), allowing to perform highly detailed imaging at the NMJ. Wrapping glia, the inner most glia layer, in intimate contact with axons, can be addressed by *nrv2*-GAL4. In *nrv2*-GAL4>CD4::GFP L3 larvae (Figure 3.11 A), there is continuous and homogeneous GFP coverage of axons, extended until a few micrometers distal from the appearance of the first presynaptic HRP positive bouton, surrounded by postsynaptic Dlg (arrowheads Figure 3.11 B,B'). The intermediate glial sheath, subperineurial glial layer, also forms the Blood-Brain-Barrier (BBB) and can be addressed by *Gli*-GAL4. The sheath extended by subperineurial glia enters in closer contact with the NMJ than wrapping glia (Figure 3.11 C), and matches with the appearance of the first bouton in each branch in m6/7 NMJ (arrowhead Figure 3.11 D,D'). Subperineurial glia was also shown to play a role in modulating NMJ growth and maintenance by engulfing detached ghost boutons, where they extend protrusions and gliobulbs intended to phagocyte neuronal debris (Fuentes-Medel et al., 2009) (bend arrow Figure 3.11 D,D'). The outermost glial layer can be addressed with *46F*-GAL4. This glial layer is called perineurial glia, and from all three layers this is the one that shows the least continuous and less complete axonal coverage, covering in some areas only a portion of the axons (Figure 3.11 E). *46F*-GAL4>CD4::GFP shows perineurial glia extending large filopodia, or gliopodia in this case, that reach within the NMJ even the last bouton in some branches, far beyond the first proximal bouton, where subperineurial glia stops (Arrow and arrowhead respectively Figure 3.11 F,F').



---

The above mentioned GAL4 drivers were used to knockdown *kon* in each of the glial layers in the PNS, and thus elucidate which layer (or layers) contributes to the Kon dependent m6/7 NMJ phenotype. As control group I used UAS-*kon*RNAiC2/+, which was then also used to knockdown *kon*. NMJ bouton and branch number were significantly increased in *kon* knockdown in subperineurial glia, whereas *kon* knockdown in perineurial glia caused a significantly increase in branch number (Figure 3.11 G,I). Interestingly, single bouton number was not affected by the knockdown of *kon* in either of the PNS glia layers (Figure 3.11 H), although pan-glial *kon* knockdown does result in a significant increase in single bouton number.

Using Flybow to identify and follow the development of each ePG until L3 (von Hilchen et al., 2013), it was possible to address in a single-cell level the identity of the glial cells contributing to m6/7 NMJ. Wrapping glia (ePG5), subperineurial glia (ePG4 and 7) and perineurial glia (ePG6 and 8), have shown in at least one case to ensheath this portion of the segmental nerve b (SNb), that forms m6/7 NMJ (Figure 3.11 J)

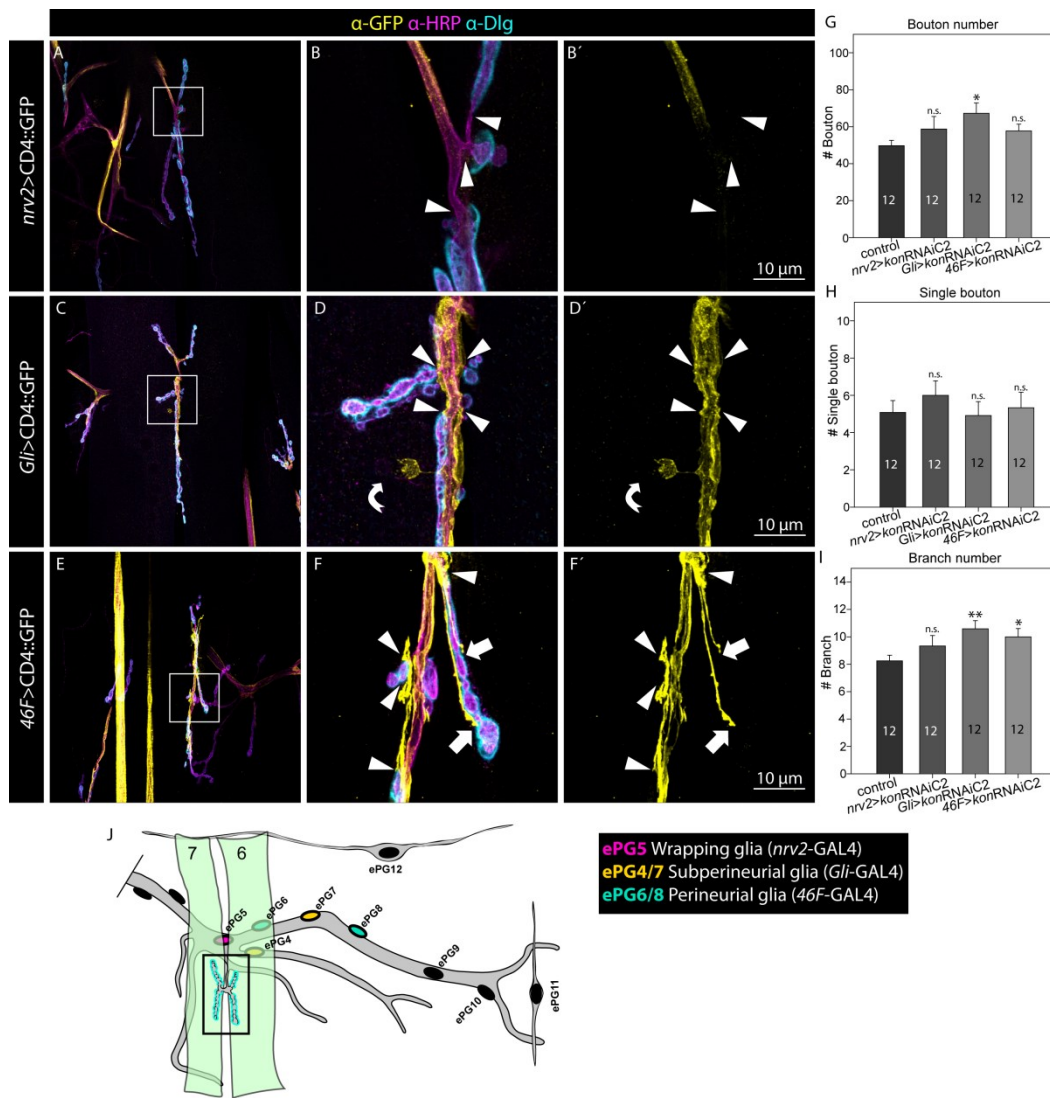


**Figure 3.11. m6/7 NMJ interaction with PNS glia in a single glia layer resolution and Kon dependent glial layer contribution to the NMJ phenotype**

(A – F') NMJ from m6/7 of L3 stained with  $\alpha$ -GFP,  $\alpha$ -HRP and  $\alpha$ -DlG (A) Wrapping glia (*nrv2-GAL4*>*CD4::GFP*). (B – B') Higher magnification of the region highlighted in (A). (C) Subperineurial glia (*Gli-GAL4*>*CD4::GFP*). (D - D') Enlargement of the region highlighted in (C). (E) Perineurial glia (*46F-GAL4*>*CD4::GFP*). (F - F') Enlargement of the region highlighted in (E). Arrowheads indicate the beginning of the first bouton in each NMJ branch and arrows the extension of gliopodia. Bend arrow indicates gliobulb. (G – I) Statistical analysis comparing *kon* knockdown in each glia layer to control (*konRNAiC2/+*). (G) Bouton number. (H) Single bouton number. (I) Branch number. (G – I) Mean and SEM are represented by bar and error bar respectively. Significance from *t*-test p-values are shown in each graph (\*) $p < 0,05$ ; (\*\*) $p < 0,01$  and (n.s.) $p > 0,05$ . (J) Illustration of the MFA (Modified from (von Hilchen et al., 2013)), with color code to highlight the relative position of the identified glia reaching m6/7 NMJ.

### 3.3.5 Effect of glial *kon* knockdown in pre-and postsynapse

Using pre-and postsynaptic markers to visualize the overall integrity of the NMJ after knockdown of *kon* in glia, I observed in *kon* knockdown animals (*repo>konRNAiC2*) a reduction in  $\alpha$ -Glutamate receptor IIA (GluRIIA) antibody staining intensity, thus meaning a reduction in GluRIIA accumulated at the postsynapse (arrowhead in Figure 3.12 B,B') as compared to control larvae (*repo-Gal4/+*) (arrowhead in Figure 3.12 A,A'). On the presynapse,  $\alpha$ -Bruchpilot (Brp) and  $\alpha$ -Futsch were used as markers;  $\alpha$ -Brp antibody labels functional and intact Active Zone (AZ), whereas  $\alpha$ -Futsch labels the cytoskeletal network in neurons. *kon* knockdown in glia does not affect AZ distribution an number, as compared to control animals, revealed by  $\alpha$ -Brp staining (Figure 3.12 C – D'). In control animals,  $\alpha$ -Futsch antibody staining appears as a fine but solid fiber running along all NMJ branches, ending in a bulb like structure in each last bouton in every branch (arrowhead in Figure 3.12 E,E'). In *kon* knockdown in glia,  $\alpha$ -Futsch fibers were less solid, ending abruptly before the last bouton in most branches and not forming the bulb like structure at the end of those branches (Arrow and arrowhead Figure 3.12 F,F')

Besides NMJ and pre-and postsynaptic marker differences observed in *kon* knockdown in glia, I also observed that posterior abdominal segments displayed what appears as NMJ degeneration signs. Those signs were mostly observed in the knockdown of *kon* using *konRNAiKK*. Several  $\alpha$ -HRP/ $\alpha$ -Dlg and  $\alpha$ -Dlg-only boutons like spheres were observed in the region where m6/7 NMJ is usually formed. They are organized and oriented same as in a normal NMJ, but completely fragmented (Figure 3.12 G-G'). A striking feature of this phenotype is the appearance of anti-Dlg positive boutons that lack any anti-HRP signal (Arrowhead Figure 3.12 G-G'), denoting a very fast branch retraction, even faster than the ability from muscle to disintegrate the postsynaptic machinery (For references in NMJ degeneration, see (Graf et al., 2011)).

Outside the NMJ, along the NER, the knockdown of *kon* in glia cells (*konRNAiKK*) leads to the formation of aberrant  $\alpha$ -HRP positive neuronal protrusions. These structures appeared randomly and were increased in the NER of posterior segments (Arrows Figure 3.12 H).

Higher magnifications of these structures revealed fine neuronal protrusions projecting in all directions (Arrows Figure 3.12 I). Single focal planes allowed to identify large vacuoles and single neuronal fibers (Arrows Figure 3.12 I',I'').

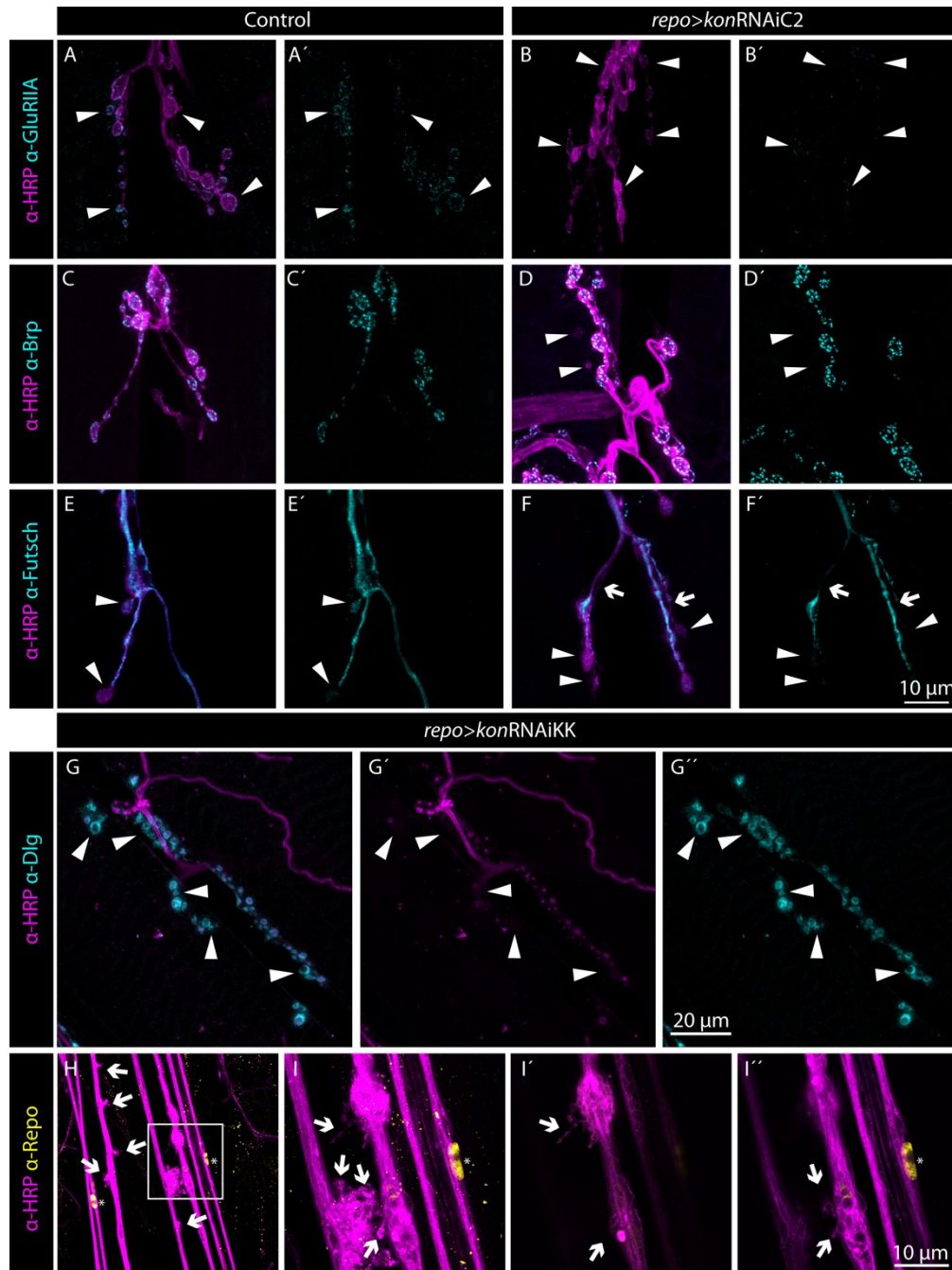


**Figure 3.12. Pre- and postsynaptic defects in *kon* knockdown in glia.**

Confocal images from m6/7 NMJ from L3 Larva stained with  $\alpha$ -HRP and  $\alpha$ -GluRIIA (A – B'),  $\alpha$ -Brp (C – D'),  $\alpha$ -Futsch (E – F') and  $\alpha$ -Dlg (G – G'). (Continues in next page)

### Figure 3.12. Pre-and postsynaptic defects in *kon* knockdown in glia

(From previous page)(A, A', C, C', E and E') Control larvae UAS-*dicer2*/+;*repo*-GAL4. (B, B', D, D', F and F') *kon* knockdown in glia using *konRNAiC2*. (G – I'') *kon* knockdown in glia using *konRNAiKK*. **(A)**  $\alpha$ -HRP boutons surrounded by  $\alpha$ -GluRIIA staining indicated by arrowheads. **(A')** Postsynaptic  $\alpha$ -GluRIIA staining. **(B)**  $\alpha$ -GluRIIA staining is reduced in the postsynapse. **(B')** Arrowheads indicate boutons surrounded by weak  $\alpha$ -GluRIIA staining. **(C - C')** Stereotypical  $\alpha$ -Brp pattern in the presynapse. **(D - D')** Not affected  $\alpha$ -Brp pattern in *kon* knockdown. Arrowheads indicate detached ghost boutons. **(E - E')** Arrowheads indicate the last bouton in each branch forming a  $\alpha$ -Futsch bulb-like structure, followed by continuous  $\alpha$ -Futsch thread. **(F – F')** Arrowheads indicate the last bouton in each branch, in this case not all of them are  $\alpha$ -Futsch positive. Arrows indicate the point in which the  $\alpha$ -Futsch thread is broken. **(G)** m6/7 NMJ from hemisegment A6. Loss of  $\alpha$ -HRP in some  $\alpha$ -Dlg boutons, labeled with arrowheads. In separate images **(G')** presynaptic  $\alpha$ -HRP and **(G'')** postsynaptic  $\alpha$ -Dlg with respective arrowheads. **(H)** NER from L3 larvae stained with  $\alpha$ -HRP and  $\alpha$ -Repo. Abnormal  $\alpha$ -HRP protrusions and filopodia (arrows), and glia nuclei along the nerves (asterisks) are labeled. **(I)** Enlargement of the region highlighted in (H), showing in detail HRP protrusions and filopodia formed along the NER. **(I')** Single focal plane from (I) showing single HRP protrusions. **(I'')** Single focal plane showing vacuoles formed within the nerves in the NER.

### 3.3.6 *kon* knockdown leads to impaired axonal transport and glia proliferation

Another phenotype observed in *kon* knockdown in glia (*konRNAiKK*) was the accumulation of  $\alpha$ -Brp positive vesicles along the NER. We observed that in wildtype animals,  $\alpha$ -Brp is present in a very low rate along the NER (Figure 3.13 A,B), and only accumulates at the presynapse (Figure 3.12 C – D and Figure 3.13 B). In *kon* knockdown in glia,  $\alpha$ -Brp vesicles accumulation along the NER is dramatically increased (Figure 3.13 D,E).  $\alpha$ -Brp vesicles are also found in  $\alpha$ -HRP sprouts and knots found along the NER in *kon* knockdown in glia (arrows in Figure 3.13 D, E). For more detail, see inlets in Figure 3.13 B and E.

*kon* knockdown in glia also results in a reduction in glia nuclei along the NER. In wildtype larvae,  $\alpha$ -Repo+ nuclei are evenly distributed along the axon, where the longer the axon the more glia nuclei are to be found. In Figure 3.13 C and F, both regions with relative identical size and containing the same number of axonal fibers (7 each), wildtype larva (Figure 3.13 C) displays 3 times more glia nuclei (16) than the *kon* knockdown in glia larva (5) (Figure 3.13 F). The reduction in glia nuclei number was also observed in the brain and VNC, whereas the MFA was not affected (Data not shown).

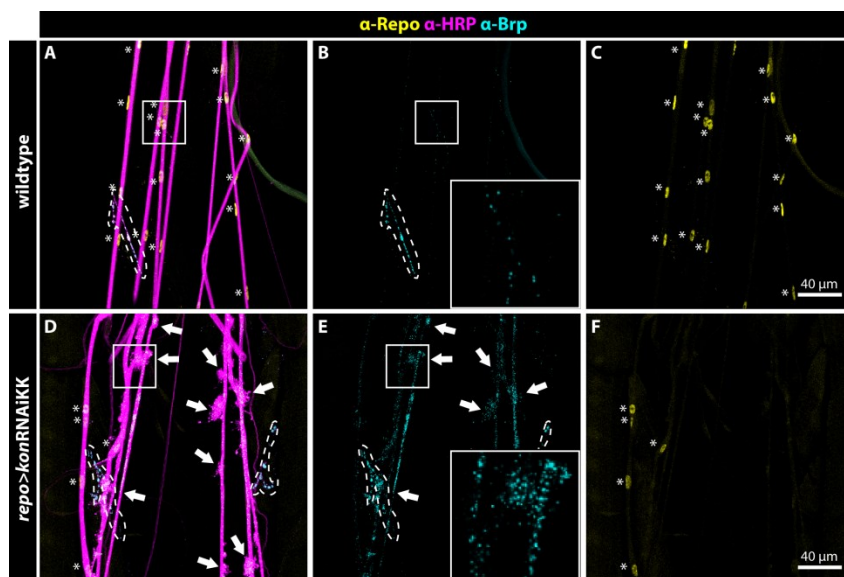


**Figure 3.13. Bruchpilot stalling along the NER in *kon* knockdown**

NER from L3 larva stained against Repo, HRP and Brp. Asterisks label all glia nuclei. Dashed line encircles m15/16 NMJ (Ventral Oblique 4/5). (B and E) Inlet from the selected region. (Continue in next page)

**Figure 3.13. Bruchpilot stalling along the NER in *kon* knockdown**

(From previous page) **(A)** Wildtype larva. Neither protrusions nor filopodia observed along the NER **(B)** From (A), Brp staining only. No Brp accumulation along the NER. **(C)** From (A), Repo staining only. **(D)** NER from *kon* knockdown in glia using *konRNAiKK*. Arrows indicate  $\alpha$ -HRP protrusions and filopodia formed along the NER. **(E)** From (D),  $\alpha$ -Brp vesicles accumulation along the NER. **(F)** From (D), anti-Repo staining only. The staining shows a significant reduction in the number of glia nuclei along the NER. In the confocal images, 16 glia nuclei in wildtype and only 5 in *kon* knockdown. Same magnification and region of the larva scanned in A-C as in D-F.

### 3.3.7 Muscle derived Kon also participates in NMJ formation

The NMJ is a rather complex structure, where jointly three types of cells (glia, neuron and muscle) act together to traduce synaptic impulses into a coordinated muscle movement. I have shown that a knockdown of *kon* in glia leads to a reduction in the intensity of  $\alpha$ -Kon antibody staining at the NMJ, but not a complete loss, raising two questions; first, whether muscle and/or neurons also contribute by segregating Kon to the NMJ, and second, whether the knockdown in either of them would also cause a NMJ phenotype.

In *kon* knockdown in neurons (*elav>konRNAiC2*), antibody staining against HRP did not show any major difference to controls (*elav-GAL4/+*) (Figure 3.14 A,B). In *elav>konRNAiC2* animals, the overall nervous system and muscle network were not affected, as there was no phenotype that could be observed. Statistical analysis of bouton, single bouton and branch number in *kon* knockdown in neurons revealed no significant differences to the control group (Figure 3.14 H).

In m6/7 NMJ,  $\alpha$ -HRP staining in *kon* knockdown in muscle larvae (*mef2>konRNAiC2*), as compared to control group (*mef2-GAL4/+*) (Figure 3.14 C,D) shows no major difference, except for an increased number of small satellite boutons being displayed (arrowhead in Figure 3.14 E,F). Statistical analysis comparing the number of those satellite boutons reveals a two fold increase as compared to control. There is a statistically significant difference in the number of satellite boutons displayed ( $p < 0,01$ ) (Figure 3.14 G). Despite the increase in satellite bouton number, no other NMJ phenotype was observed. Bouton, branch and single bouton number are statistically similar between *kon* knockdown in muscle and control larvae (Figure 3.14 I). Satellite bouton number differences have been so far only observed in *kon* knockdown in muscle.



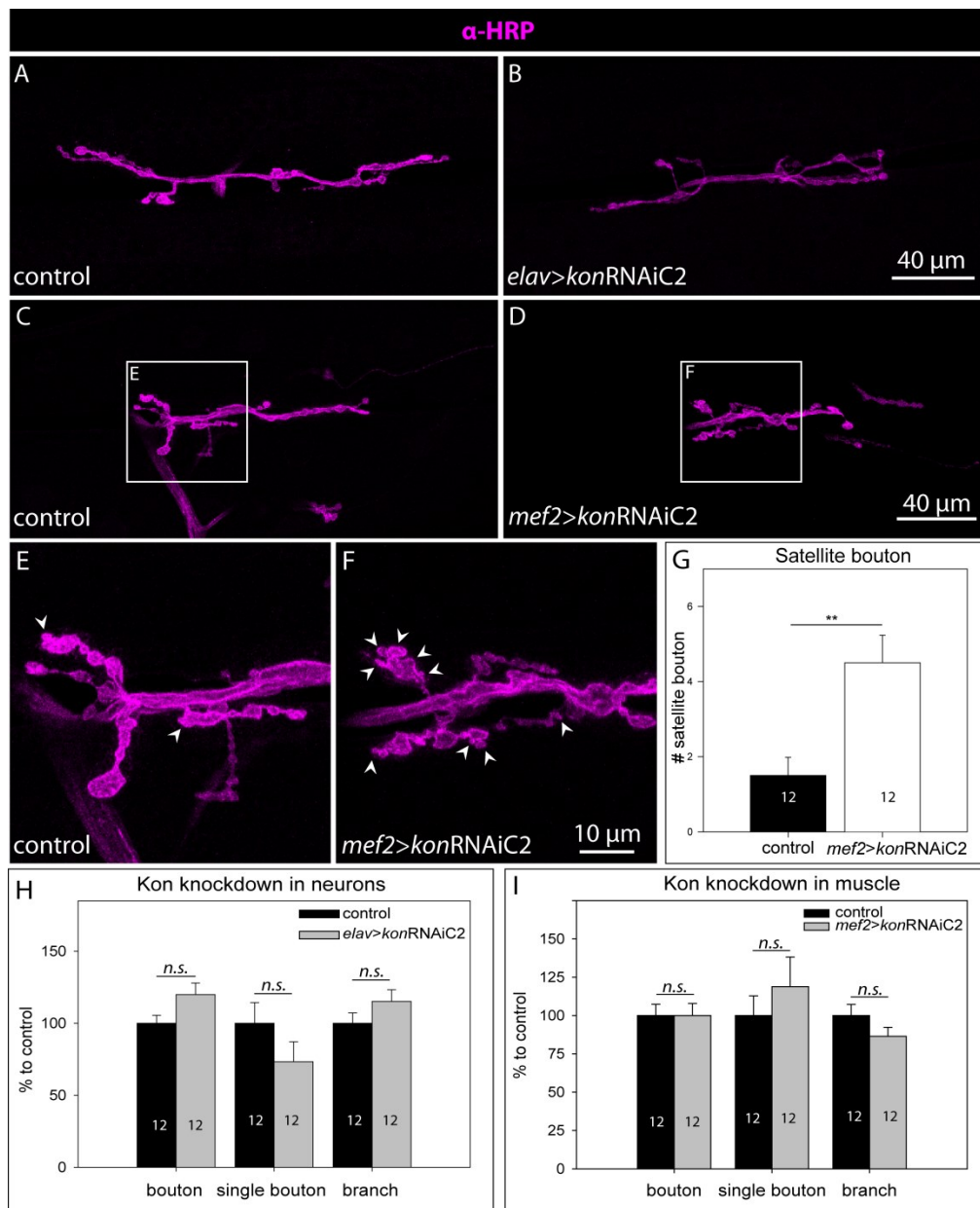


**Figure 3.14. NMJ scores in *kon* knockdown in neurons and muscle.**

(A – F) Confocal images of m6/7 NMJ stained against HRP. (A) Control larva for *kon* knockdown in neurons (*elav-GAL4/+*) (B) *kon* knockdown in neurons larva (*elav-GAL4;UAS-konRNAiC2*). (C) Control larva for *kon* knockdown in muscle (*mef2-GAL4/+*). (D) *kon* knockdown in muscle larva (*mef2-GAL4/UAS-konRNAiC2*). (E) Enlargement of the region highlighted in (C). (F) Enlargement of the region highlighted in (D). (E-F) Satellite boutons are marked with arrowhead. (G) Graph representing comparison of satellite bouton number in *kon* knockdown in muscle and control larva. (H) Statistical comparison of Bouton, single bouton and branch number between control and *kon* knockdown in neurons and (I) *kon* knockdown in muscle. In G, H and I, bar and error bar represents mean and SEM respectively. N=12 for all groups. *t*-test (\*\*) $p < 0,01$  and (n.s.) $p > 0,05$ .

### 3.3.8 The rescue of *kon* in muscle rescues muscle-tendon network impairment but induces an aberrant NMJ

The knockdown of *kon* in either glia or muscle leads to NMJ phenotypes. To test whether a systemic *kon* mutant would show similar or stronger phenotypes, I isolated *kon* transheterozygous mutant embryos (*kon*<sup>A04</sup>/*kon*<sup>c452</sup>) and allowed them to develop. Those animals reach late larval stages, although displaying severe problems, especially crawling difficulties, and often died during development. Some of the larvae reaching L3 were stained and used to visualize the overall muscle-tendon network. In *Kon* transheterozygous L3 larva, the muscle-tendon network is extremely affected, making it impossible to identify corresponding muscles or NMJs due to massive arrangement impairment (Figure 3.15 A - B'). It is impressive that although the severity of the muscle and NMJ phenotypes, *kon* transheterozygous larva can still crawl and feed.

An approach to circumvent the muscle-tendon network phenotype was to rescue *Kon* in muscles from *kon* transheterozygous (*kon*<sup>c25</sup>,*mef2*-GAL4/*kon*<sup>c1139</sup>,UAS-*kon*::HA). Antibody staining in L3 larvae reveals an overall muscle-tendon network reestablishment (Figure 3.15 C). There is a strong overlap at the NMJ of  $\alpha$ -*Kon*<sup>ecto</sup> and  $\alpha$ -HA antibody staining, although weak throughout the rest of the muscle field area (MFA) (Figure 3.15 D-D'). Antibody staining with  $\alpha$ -HRP and  $\alpha$ -Dlg in *Kon* muscle rescue larvae also revealed differences at the NMJ. In rescue animals, two different types of NMJ branches were observed; regular  $\alpha$ -HRP and  $\alpha$ -Dlg staining in long branches (arrows in Figure 3.15 E,E') and irregular non-bouton like shaped branches lacking  $\alpha$ -Dlg staining and with very diffuse  $\alpha$ -HRP staining (arrowhead in Figure 3.15 E,E'). In control animals (*kon*<sup>c25</sup>,*mef2*-GAL4/+) and also in previous experiments, this last irregular NMJ branch was never observed (Figure 3.15 F,F').

Statistical analysis of NMJ phenotypes revealed no statistical differences in bouton, single bouton or satellite bouton number, whereas the overall number of NMJ branches was significantly reduced in *kon* rescue in muscle as compared to control animals (Figure 3.15 H). There is also a four-fold statistically significant increase of ghost boutons,  $\alpha$ -HRP+ detached boutons, in *Kon* rescue in muscle larvae ( $p < 0,001$ ) (Figure 3.15 I).

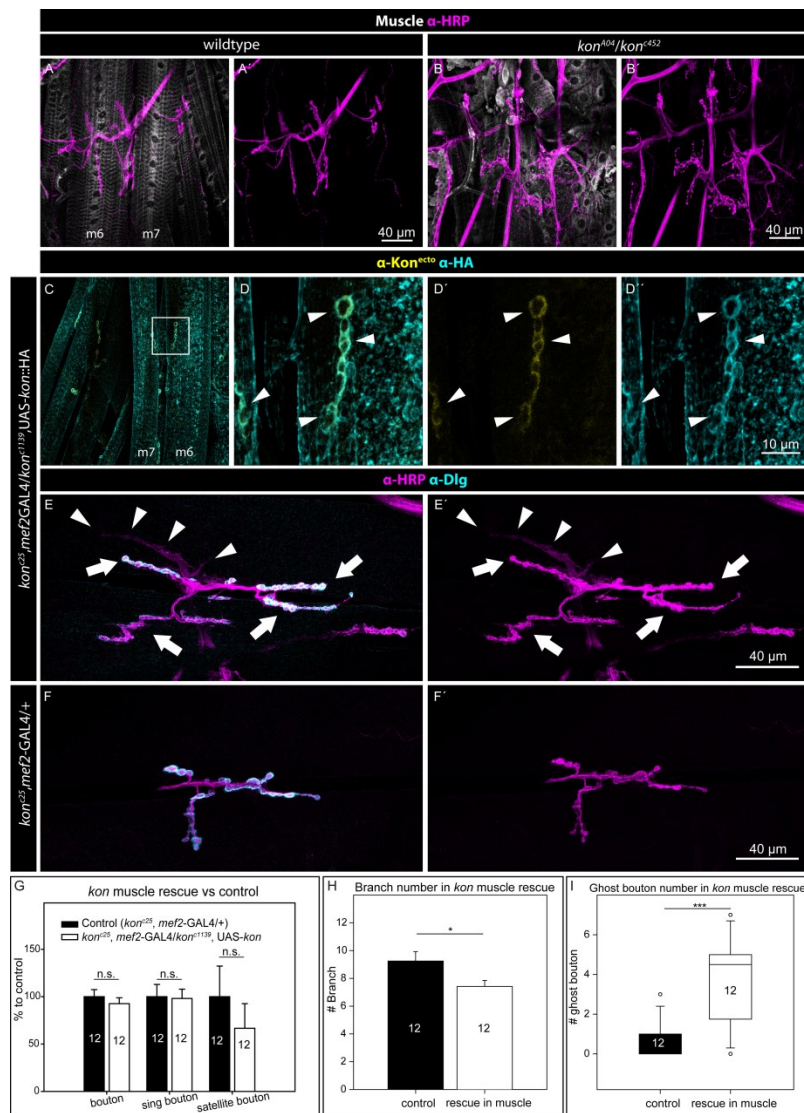


**Figure 3.15. NMJ phenotypes in Kon rescue in muscle.**

(A – F') Confocal image from L3 larva showing m6/7 NMJ. (A – A') Wildtype stained with  $\alpha$ -HRP. Muscles visible due to background staining. (B – B') Kon transheterozygous (*kon<sup>A04</sup>/kon<sup>c452</sup>*) stained with  $\alpha$ -HRP. Confocal shows the region where m6/7 NMJ is normally found, (C) Kon rescue in muscle larva (*kon<sup>c0025</sup>,mef2-GAL4/kon<sup>c1139</sup>,UAS-kon::HA*), stained with  $\alpha$ -Kon<sup>ecto</sup> and  $\alpha$ -HA. (D) Enlargement of the region highlighted in (C). (D')  $\alpha$ -Kon<sup>ecto</sup> only and (D'')  $\alpha$ -HA only show overlap at the NMJ. (E – F') Kon rescue in muscle and control stained with  $\alpha$ -HRP and  $\alpha$ -Dlg. (E - E') Kon rescue in muscle. Arrows indicate normal NMJ branches and arrowheads indicate NMJ branches with abnormal shape lacking postsynaptic  $\alpha$ -Dlg staining. (F – F') Control larva for Kon rescue in muscle (*kon<sup>c0025</sup>,mef2-GAL4/+*). (G) Statistical comparison of bouton, single bouton and satellite bouton number between control and Kon rescue in muscle. (H) Branch and (I) Ghost bouton number comparison are shown separately. Bar and error bar represents mean and SEM respectively. Group N is displayed within each bar. *t*-test performed, (\*)*p*<0,05; (\*\*\*)*p*<0,001 and (n.s.)*p*>0,05.

### 3.3.9 Kon overexpression in glia also leads to a NMJ phenotype

After rescuing Kon in muscle and observing the reestablishment of the muscle-tendon network and the resulting NMJ phenotypes, I decided to test whether the overexpression of Kon in glial cells would also affect the NMJ and result in phenotypes. L3 larvae overexpressing Kon in glia, using the pan glial driver *repo*-GAL4, were stained with  $\alpha$ -HRP,  $\alpha$ -Kon<sup>ecto</sup> and  $\alpha$ -Dlg. The overall NMJ shape was not affected by the overexpression of Kon in glia (Figure 3.16 A).  $\alpha$ -Kon<sup>ecto</sup> staining accumulated at the synapse, as previously observed in wildtype (Figure 3.8 G – H and Figure 3.16 A'), and also in glia along the PNS (Arrowheads Figure 3.16 A'). NMJ phenotypes scores, comparing control group (*repo*-GAL4/+) and Kon overexpression in glia (*UAS-kon::HA/+; repo*-GAL4/+) show a statistically significant increase in branch number, about 50% increase (Figure 3.16 B), same as a highly significant increase in bouton number, about 75% increase (Figure 3.16 C). Single bouton number remained unaffected, since both groups displayed on average  $\approx$ 4 single boutons, not representing a statistically significant difference (Figure 3.16 D).

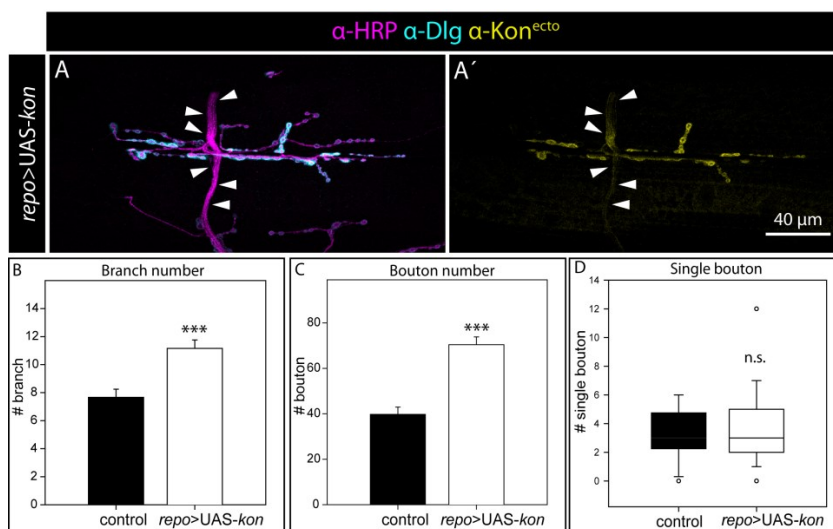


**Figure 3.16. m6/7 NMJ phenotype in Kon overexpression in glia using *repo*-GAL4.**

(A) m6/7 NMJ from L3 (*repo*>UAS-Kon) stained with  $\alpha$ -HRP,  $\alpha$ -Dlg and (A')  $\alpha$ -Kon<sup>ecto</sup>. Arrowheads indicate  $\alpha$ -Kon<sup>ecto</sup>, staining in glia covering axons. (B) Branch, (C) bouton and (D) single bouton number statistical comparison between Kon overexpression in glia (*repo*> UAS-*kon*) and control (*repo*-GAL4/+). (B, C) Bar and error bar represents mean and SEM respectively. (D) Data distribution are in box plot. N=12 for all groups. Rank sum (D) or *t*-test (B,C) was performed accordingly, (\*\*\*)  $p < 0,001$  and (n.s.)  $p > 0,05$ .

### 3.3.10 Kon overexpression in glia results in an extremely elongated VNC

The overexpression of Kon in glia not only results in an increased number of boutons and branches in m6/7 NMJ, it also results in a massive VNC elongation. I performed 4D recordings in embryos to observe the initial steps in the VNC elongated phenotype. Control (*repo>CD4::GFP*) and *kon* in glia overexpression (*repo>CD4::GFP>UAS-kon*) stage 13 embryos were selected and used for 4D imaging (see material and methods 2.3.4). During stage 14, no major difference in VNC length can be observed (Figure 3.17 A). In stage 15 there is a slight VNC retraction in both animals (Figure 3.17 A') and in stage 16, VNC condensation starts taking place, where the control embryo shows a clear reduction in VNC length as compared to *kon* overexpression (Figure 3.17 A''). In stage 17, the VNC in control embryo condensates further whereas the VNC in *kon* overexpression remains the same size as in stage 15 (Figure 3.17 A'''). This phenotype was observed with 100% penetrance in animals overexpressing *kon* in glia, and resulted in high rates of larval lethality, which also displayed severe crawling and feeding impairment, and complete lethality in pupal stages. Fine dissection of L3 larvae overexpressing Kon in glia shows an unusual adhesion of the VNC to the body wall, observed while dissecting the VNC from the whole animal. It was also possible to observe the contractile waves bending the VNC along with the body wall during larval crawling.

To elucidate which Kon domain plays a role in triggering the elongation of the VNC, four different versions of Kon were overexpressed in glia: Kon full length, PDZ-BD mutated ( $\text{Kon}^{\text{VB}}$ ), Kon lacking LamG ( $\text{Kon}^{\text{Del-LamG}}$ ) and Kon lacking CSPG ( $\text{Kon}^{\text{Del-CSPG}}$ ). As previously mentioned, Kon full-length overexpression resulted in a massive VNC elongation (arrowhead marks the VNC Figure 3.17 B,B'). Overexpressing  $\text{Kon}^{\text{VB}}$ , where the last amino acid has been changed from Valine to Glycine, no elongated VNC was observed, and the relative VNC length and brain size are identical to wildtype (Figure 3.17 C,C'). Interestingly, overexpression of  $\text{Kon}^{\text{Del-LamG}}$  (Figure 3.17 D,D') and  $\text{Kon}^{\text{Del-CSPG}}$  (Figure 3.17 E,E') also resulted in no VNC elongation, meaning that the observed phenotype requires all Kon domains and the lack of any of the them (PDZ-BD, LamG and CSPG repeats) was enough to abolish the elongation of the VNC.

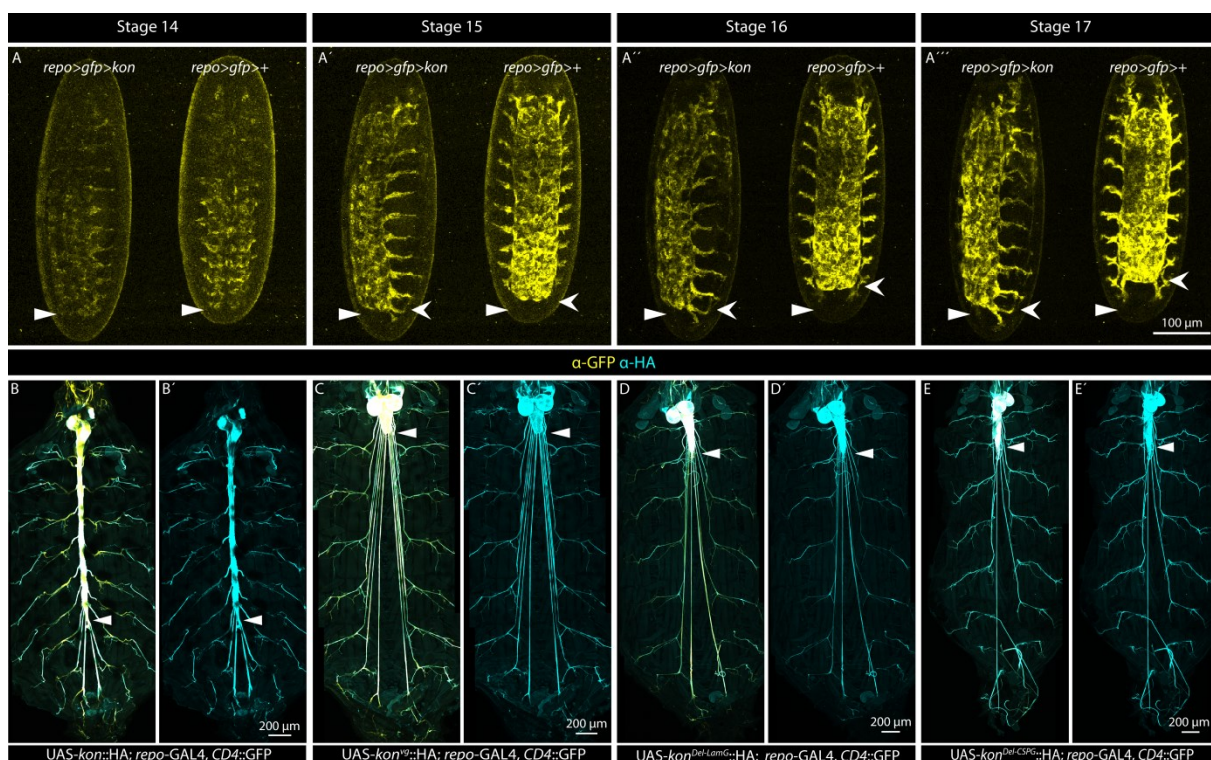


**Figure 3.17. Overexpression of Kon full-length only results in elongated VNC**

(A-A'') 4D recording of control (right, *repo>gfp*) and Kon overexpression in glia (left, *repo>gfp>kon*) embryos. Arrowhead indicates VNC length in stage 14 and open arrowhead indicates VNC retraction. (A) Stage 14, (A') stage 15, (A'') stage 16 and (A''') stage 17. (B – E') Fine dissected L3 larvae overexpressing different Kon versions in glia, stained with  $\alpha$ -GFP and  $\alpha$ -HA. (B - B') Kon full-length overexpression (*UAS-kon::HA*). (C – C') Kon<sup>VG</sup> (PDZ-BD mutated) overexpression (*UAS-kon<sup>VG</sup>::HA;repo-GAL4,UAS-CD4::GFP*). (D) Kon<sup>Del-LamG</sup> overexpression, lacking both LamG domains (*UAS-kon<sup>Del-LamG</sup>::HA;repo-GAL4,UAS-CD4::GFP*). (E) Overexpression of Kon<sup>Del-CSPG</sup>, Lack of CSPG domains (*UAS-kon<sup>Del-CSPG</sup>::HA;repo-GAL4,UAS-CD4::GFP*). Arrowhead indicates the length of the VNC.

The elongated VNC is a novel and attractive phenotype, which could allow studying Kon interacting partners in glia, but first is necessary to know how and when the VNC elongation starts, and second, whether this is a reversible phenotype. The following experiments were performed with help from a Bachelor student (Christina Heiser) under my supervision. We used the GAL4/GAL80<sup>ts</sup> system to accurately control the expression of Kon under the control of the *repo*-GAL4, by temperature switch (see material and methods). The results of those experiments are summarized in Figure 3.18. In short, Kon overexpression in glia in the embryo and until L1 is sufficient to produce the elongated VNC phenotype observable in L3.

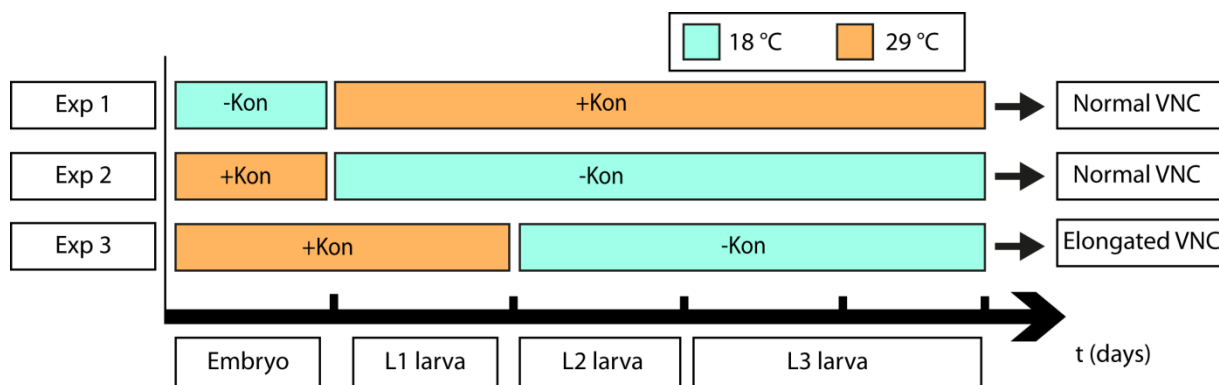


**Figure 3.18. Kon expression in GAL4/GAL80<sup>ts</sup> temperature shift experiments.**

Three different experiments were performed to determine when Kon has to be expressed in glia to induce the elongated VNC phenotype (*repo4.3>CD8::GFP/UAS-kon::HA;repo-GAL4,tubGAL80TS/+*). Embryos were kept at either permissive (29 °C) or restrictive temperature (18 °C). Experiment 1, embryos were kept at 18 °C and in L1 shifted to 29 °C, resulting in no elongated VNC. Experiment 2, embryos were kept at 29 °C and in L1 shifted to 18 °C, resulting in no elongated VNC. Experiment 3, embryos and L1 were kept at 29 °C and in L2 shifted to 18 °C, resulting in an elongation of the VNC.

### 3.3.11 Suppressor screen to identify Kon PDZ-BD interacting partners in glia

The elongated VNC is a suitable phenotype to perform a classical suppressor screen in which to look for proteins interacting with Kon in glial cells. Since Kon intracellular PDZ-BD was shown to play a role in promoting the elongated VNC phenotype, we will focus on putative interacting proteins bearing PDZ or PDZ-like domains. In this screen, we overexpressed *kon* in glial cells and simultaneously knockdown single candidate genes by simply crossing both parental lines (**Figure 3.19**, in red is shown the target genotype).

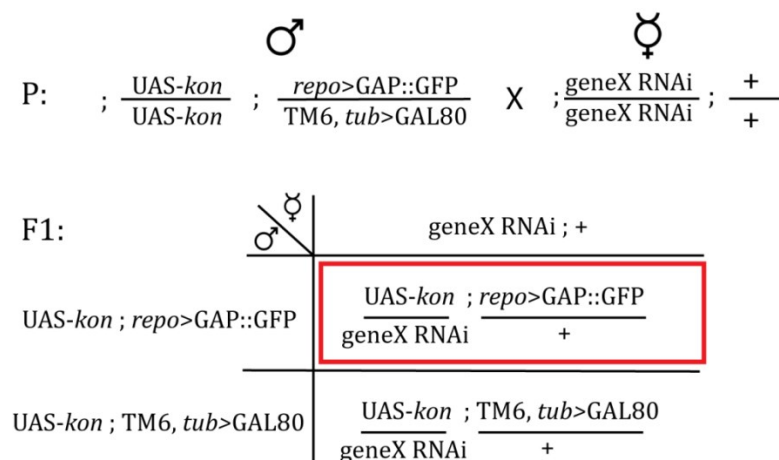


**Figure 3.19. Crossing scheme for the suppressor screen.**

Candidate genes to be screened were chosen based in known NG2/Kon PDZ-BD interacting proteins in vertebrates and in *Drosophila*. The first group was composed of *Drosophila* homologues or genes closely related in sequence to Mupp1 (Patj, InaD, Dlg and CG15803) and Syntenin (X11L $\beta$  and CG31342), determined by protein sequence BLAST in annotated *Drosophila* proteins. The second group was composed of proteins bearing sequence homology with the 7<sup>th</sup> PDZ domain of DGrip (Scribbled and Polychaetoid), shown to exclusively interact with Kon PDZ-BD in *Drosophila*. The details of the suppressor screen and results for every candidate gene can be seen in the Bachelor thesis work from Christina Heiser from March 2013 with the title “RNAi screen for Kon-tiki PDZ-binding domain



---

interactions partners in *Drosophila*". From the candidate genes mentioned above, the one that resulted in a conclusive VNC length reduction and thus suppression of the phenotype caused by the overexpression of Kon in glia was the knockdown of DGrip.

The VNC measurements were done based on the endogenous expression of GFP in all glia, which allowed the visualization of the length of the VNC without the need to open or fine dissect the larva. The results are expressed as the percentage of the total length of the larva represented by the VNC. In our experiments we observed that in average, when overexpressing Kon in glia, the VNC represents about 40% of the total length of the larva, whereas in wildtype it is only about 15% in average. Statistical analysis comparing both groups reveals highly significant differences (*t*-test,  $p < 0,001$ ) (Figure 3.20). To test our suppressor screen, we simultaneously overexpressed Kon and *kon*RNAiGD, the resulting VNC length was comparable to wildtype larvae VNC and statistically significant smaller than the VNC resulting from the overexpression of Kon in glia only (*t*-test,  $p < 0,001$ ) (Figure 3.20). When overexpressing simultaneously Kon and *dgrip*RNAi we observed that the length of the VNC was on average 20% the length of the larva, representing just half the length of Kon overexpression only, and slightly higher than in wildtype. Statistical analysis also revealed that *dgrip*RNAi significantly suppressed the elongated VNC phenotype as compared to Kon overexpression only (*t*-test,  $p < 0,001$ ) (Figure 3.20).

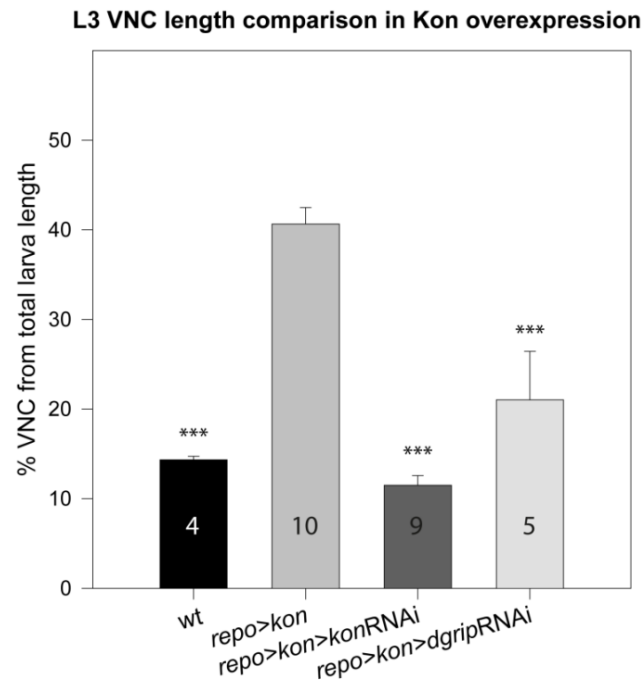


**Figure 3.20. VNC length measurements in glia suppressor screen**

Statistical analysis of the VNC length measurements performed in the suppressor screen. All groups were compared to *repo>kon* (*UAS-kon/+;repo-GAL4,UAS-GAP::GFP/+*), which gives the phenotype to be suppressed. The genotypes of each group are: *wt* (*repo-GAL4,UAS-GAP::GFP/+*), *repo>kon>konRNAi* (*UAS-kon/konRNAiGD;repo-GAL4,UAS-GAP::GFP/+*) and *repo>kon>dgripRNAi* (*UAS-kon/dgripRNAiGD;repo-GAL4,UAS-GAP::GFP/+*). Students *t*-test,  $p < 0,001$  (\*\*\*). Mean and SEM are represented in bar and error bar respectively. The number of animals measured per group is given in each bar.

### 3.3.12 Kon is also processed in *Drosophila* glial cells

Exploratory experiments showed that the overexpression of Kon<sup>VG</sup> in glia results in no NMJ phenotype (data not shown), whereas the overexpression of Kon in glia results in an increase in bouton and branch number (Figure 3.16), indicating that the PDZ-BD indeed plays a role in Kon mediated NMJ changes. In order to understand the mechanism by which glial derived Kon reaches the NMJ and also to understand the role that Kon's PDZ-BD plays in modulating the NMJ, I decided to perform Kon<sup>VG</sup> (UAS-*kon*<sup>VG</sup>::HA) and Kon (UAS-*kon*::HA) misexpression in glia (*repo*-GAL4), neurons (*elav*-GAL4) and muscles (*mef2*-GAL4), and to perform western blot in tissue lysates.

Via non detergent tissue disruption, we separated soluble (S1) from membrane bound non-soluble (T1) proteins. Both fractions were used to perform western blot analysis and to visualize possible tissue dependent differences occurring in Kon and Kon<sup>VG</sup>. Soluble and non-soluble fractions were loaded onto a gradient SDS-PAGE and blot visualization was performed using  $\alpha$ -HA antibody. As control we used wildtype larvae, lacking the HA tag. S1 and T1 were loaded together for each group and side by side Kon and Kon<sup>VG</sup> for each cell type; glia, neurons and muscles. We first observed in the soluble fraction, for all tissues, several bands at similar molecular weights, resembling a common shedding pattern. We further observed a relatively massive band at about 290 kD, resembling the full length protein anchored to the membrane in the T1 fraction. It is reported that in vertebrates NG2 can be cleaved by the action of Matrix Metalloproteinase-9 (MMP-9) (Schultz et al., 2014),  $\gamma$ -secretase and ADAM10 (Sakry et al., 2014). Our results raise the possibility that Kon can be also cleaved by homologous proteins in *Drosophila*, thus explaining the appearance of the multiple bands observed in each S1 lane (Figure 3.21).

At last, and most importantly, we observed a clear difference between the overexpression of Kon and Kon<sup>VG</sup>. In Kon full-length overexpression, in glia and neurons, a clear and prominent band in the membrane bound fraction T1 is present, whereas the overexpression of Kon<sup>VG</sup> results in a very weak band, right above the detection limit (Figure 3.21). Whether a mutation in the PDZ-BD could affect the transport of a protein to the membrane and thus

explain this observation, will be later included in the discussion. Unfortunately, for Kon overexpression in muscle, the quality of the staining in this area of the blot is not good enough to add conclusive observations, although we do observe the  $\approx 70$  kD band in all lanes.

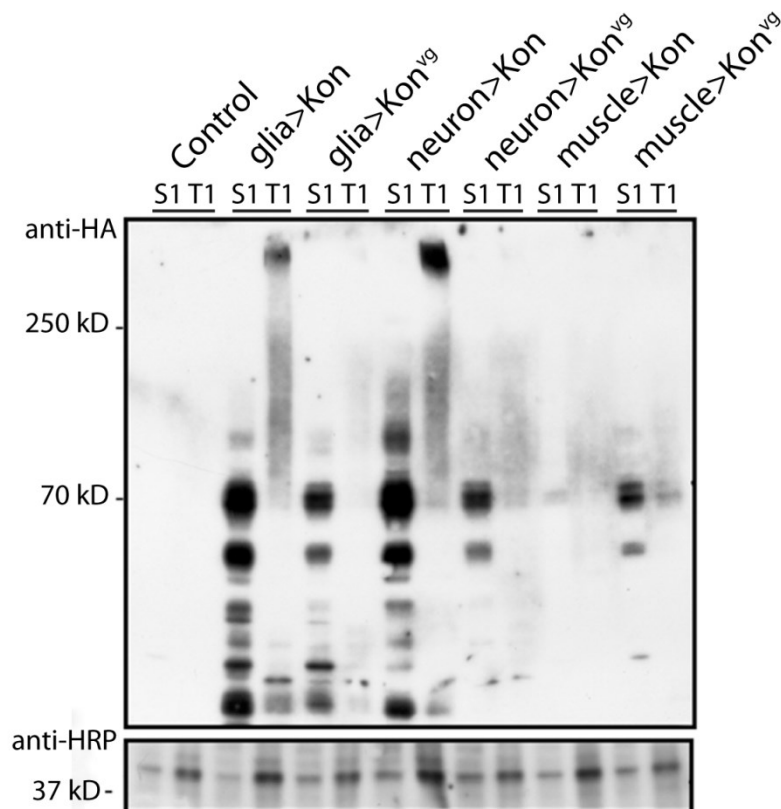


**Figure 3.21. Western blot showing Kon and Kon<sup>VG</sup> processing in *Drosophila***

Immunoblot using  $\alpha$ -HA antibody in whole L3 larvae tissue lysates. Kon or Kon<sup>VG</sup> were misexpressed in glia, muscles or neurons (*repo*-, *elav*- and *mef2*-GAL4 respectively). Control larvae (wildtype) do not express HA. S1 corresponds soluble and T1 corresponds to non-soluble fraction (see materials and methods). In all S1 fractions, several bands can be observed at similar molecular weights, being the most prominent the one found at  $\approx 70$  kD. As loading control  $\alpha$ -HRP was used. All S1 fractions, same as all T1 fractions, were obtained in identical conditions and the same amount of protein was loaded per lane/fraction.

### 3.3.13 DGrip and Kuzbanian are involved in glial Kon processing and NMJ dynamics

It was previously shown that glial Kon<sup>ecto</sup> accumulates in muscles and at the NMJ, and that the knockdown of Kon in glia leads to a reduction of  $\alpha$ -Kon<sup>ecto</sup> staining intensity in m6/7 NMJ. It was also shown that Kon is processed in glia, which is probably the key step that allows glial Kon<sup>ecto</sup> to shuttle to the synapse to mediate the formation or retraction of NMJ boutons and branches. To answer this, I decided to evaluate the effects in Kon localization and NMJ phenotypes in *dgrip* knockdown in glia and also knockdown and overexpression in glia of Kuzbanian (Kuz), ADAM10 homologue in *Drosophila*.

Control larvae (*repo-GAL4/+*), *dgrip* knockdown in glia (*UAS-dgripRNAi/UAS-dicer2;repo-GAL4*), *kuz* knockdown in glia (*UAS-kuzRNAi/UAS-dicer2;repo-GAL4*) and Kuz overexpression in glia (*UAS-kuz;repo-GAL4*) were stained with  $\alpha$ -Kon<sup>ecto</sup>,  $\alpha$ -HRP and  $\alpha$ -Dlg to visualize Kon<sup>ecto</sup> distribution and NMJ morphology. Control animals show the typical NMJ morphology and Kon<sup>ecto</sup> distribution, forming groups of speckles in muscles 6/7 in a random but even distribution and a continuous staining around the NMJ (Figure 3.22 A). In *dgrip* knockdown in glia, less  $\alpha$ -Kon<sup>ecto</sup> speckles in m6/7 were observed, together with an increase in the intensity of  $\alpha$ -Kon<sup>ecto</sup> at the NMJ (Figure 3.22 B). Knockdown of *kuz* in glia results in a reduction in the amount of  $\alpha$ -Kon<sup>ecto</sup> speckles found in m6/7, as compared to control animals, whereas the  $\alpha$ -Kon<sup>ecto</sup> staining at the NMJ is not affected (Figure 3.22 C). In Kuz overexpression in glia, considerably more  $\alpha$ -Kon<sup>ecto</sup> speckles in muscles can be found, as well as an increase of  $\alpha$ -Kon<sup>ecto</sup> staining at the NMJ (Figure 3.22 D). Together, these results showed a direct correlation between the knockdown in glia of *dgrip* or *kuz* with a reduction in the amount of  $\alpha$ -Kon<sup>ecto</sup> speckles found in muscles, where both proteins may play a role in Kon<sup>ecto</sup> shedding in glia. An opposite effect was observed in the overexpression of Kuz in glia, which resulted in an increase in Kon<sup>ecto</sup> shedding to the muscle and thus more  $\alpha$ -Kon<sup>ecto</sup> speckles in m6/7.

Statistical analysis of NMJ phenotypes also revealed a correlation between  $\alpha$ -Kon<sup>ecto</sup> intensity at the NMJ and bouton number. In *dgrip* knockdown and in Kuz overexpression, the intensity of  $\alpha$ -Kon<sup>ecto</sup> at the NMJ is increased as compared to control group, same as the number of boutons, which are significantly increased ( $p < 0,001$ ). In *kuz* knockdown in glia no differences

were observed in the intensity of  $\alpha$ -Kon<sup>ecto</sup> at the NMJ, as well as in the number of boutons (Figure 3.22 E). Statistical analysis of NMJ branch number reveals that only *dgrip* knockdown results in a significant increase in branches, as compared to control animals, although it is not significantly higher than in *kon* knockdown (Figure 3.22 F). At last, single bouton number was significantly higher only in the knockdown of *kuz* in glia, displaying on average 2 more single boutons than control group (Figure 3.22 G).

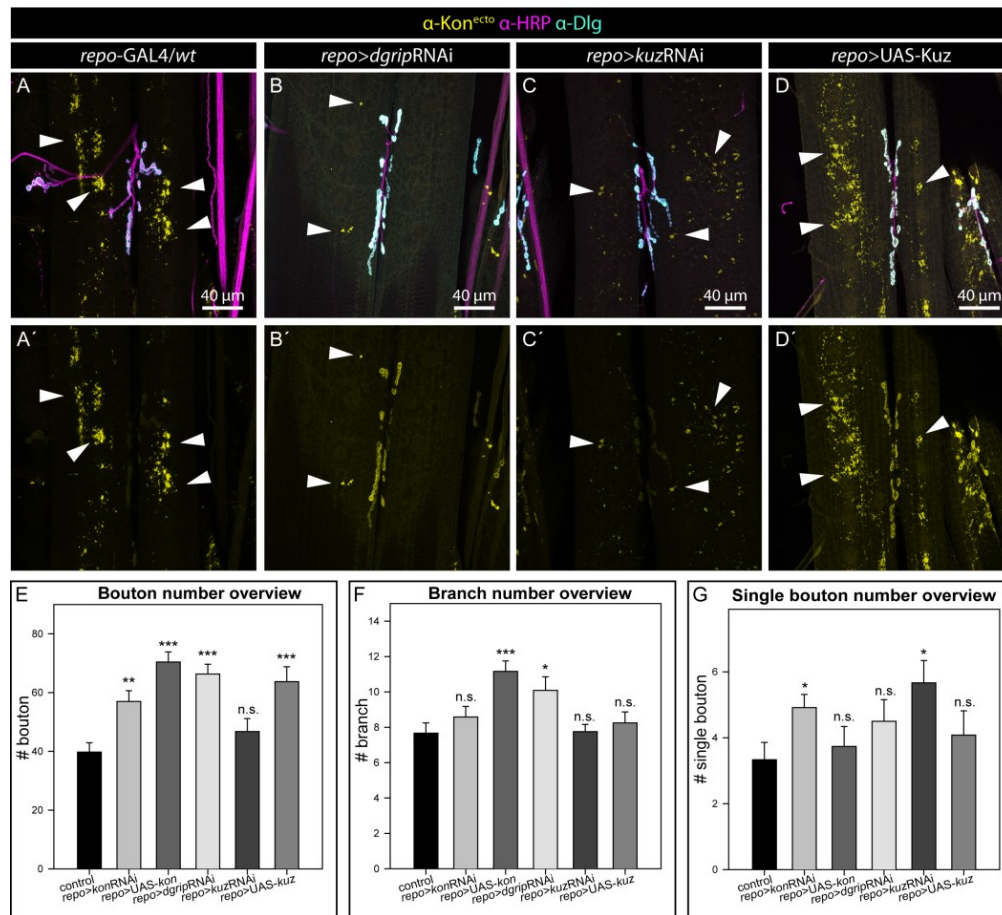


**Figure 3.22. NMJ phenotypes in glia knockdown of *dgrip* and *kuz*, and Kuz overexpression in glia.**

(A – D') m6/7 NMJ from L3 larva all stained with  $\alpha$ -Kon<sup>ecto</sup>,  $\alpha$ -HRP and  $\alpha$ -Dlg. Arrowheads indicate  $\alpha$ -Kon<sup>ecto</sup> speckles found in muscles 6 and 7. (A – A') Control larva (*repo*-GAL4/+), (B – B') *dgrip* knockdown in glia, (C – C') *kuz* knockdown in glia (D – D') Kuz overexpression in glia. (E) Bouton (F) branch and (G) single bouton number statistical analysis in control larva (*repo*-GAL4/+), knockdown of *kon*, *dgrip* and *kuz*, and overexpression of Kon and Kuz in glia. Students *t*-test between each group and control group. (\*) $p \leq 0,05$ ; (\*\*)  $p < 0,01$ ; (\*\*\*)  $p < 0,001$  and (n.s.)  $p > 0,05$ . 12 larvae were analyzed for each group.

The results here presented show that in *Drosophila*, Kon is expressed and processed in glia. Glial Kon<sup>ecto</sup> in larvae was shown to shuttle to muscles and the synapse, where it mediates NMJ bouton and branches expansion and retraction. It was also shown that *kon* knockdown in glia leads to pre-and postsynaptic alterations, together with signs of transport defects along the NER. Taken together, these results may lead to open a new field in NG2 research in vertebrates, regarding the role of NG2 at the NMJ and for transport along the nerves.

## 4 Discussion

“*Drosophila* has and will continue to contribute to many aspects of neuroscience. Current and future research in many areas of fly neurobiology will pave the way to new genes, new pathways and new approaches that will pioneer numerous fields of neurobiology, including vertebrate neurobiology” (extract from the review from (Bellen et al., 2010)). The comparative functional analysis in *Drosophila* of factors controlling mouse glia differentiation, performed and presented in this thesis, aimed to find evidence of similar pathways and/or homologous functions of the studied candidate genes, and thus help understand better their role during development.

### 4.1 **Src kinases and Glorund are not involved in glial differentiation and neuron-glia cross-talk in *Drosophila***

After a thorough analysis of Src kinases (Src42A and Src64B) and Glorund expression via antibody staining, even though in this work the focus of the analysis performed was focused on the glial expression, no major differences were observed with the information available in the literature. Src42A is ubiquitously expressed as already reported by (Takahashi et al., 2005), whereas Src64B is restricted to the tracheal pits in early development and to commissural and longitudinal axons in late embryo, also previously reported by (Wouda et al., 2008). Glorund is ubiquitously expressed and restricted to the nucleus, as shown by (Kalifa et al., 2006) and antibody staining in embryos and larvae. Mutants of either Src kinases or Glo did not display any major glial phenotype. The nervous system phenotypes observed in *Src42A* mutant embryos were observed in longitudinal axons in the VNC and were also previously described by (Wouda et al., 2008) in a pathway that involves Wnt5 and Derailed. The phenotypes described in the literature for *glo* mutants include defects in early embryo axis patterning and impaired neuronal dendritic arborization in larva. Nevertheless in our experiments, and also in the literature, no embryonic glial phenotypes were observed (Kalifa et al., 2006; Brechbiel and Gavis, 2008). The importance of these candidate genes in vertebrates lies in their role during myelination, in which they participate in the site-specific translation control of MBP mRNA, a protein which is not expressed in *Drosophila*.



## 4.2 Kon-tiki is also expressed in glia during embryonic development

According to the literature, embryonic Kon expression is restricted to the tip of extending myoblast during the formation of the muscle-tendon network, as revealed by double antibody staining ( $\alpha$ -Mhc and  $\alpha$ -Kon shown in (Schnorrer et al., 2007)). According to the same publication, *kon* mRNA is expressed in the according muscles, although the evidence shown in the publication is less convincing. From whole mount *in situ* hybridization, *kon* mRNA has been described to be expressed in stages 10 in longitudinal visceral muscle precursor and in later stages in body wall muscles, but most prominently in the ventral longitudinal group: muscles 6, 7, 12 and 13 (Estrada et al., 2007; Schnorrer et al., 2007). In my results, using *in situ* hybridization combined with antibody staining (*kon* mRNA and  $\alpha$ -Repo), revealed that peripheral, VNC and brain glia also expresses *kon* mRNA. This difference in the observations is due to the sensitivity of the detection techniques used. Whereas in the publication from Schnorrer, they used an enzymatic reaction to develop a visible signal, less sensitive, we used double labeling with fluorescent dyes and microscopy with higher resolution, adding sensitivity and accuracy to the observations.

## 4.3 Glia derived Kon may interact with Laminins and Integrins at the NMJ

In vertebrates, besides oligodendrocyte progenitor cells (OPC), NG2 is also found in several other cells, such as pericytes, aortic smooth muscle, melanoma forming cells and skeletal muscle, all adult dividing cells (reviewed in (Levine and Nishiyama, 1996)). There are major similarities between OPCs and skeletal muscle-derived progenitor cells, they have been even tested to be used as additional source for OPCs in the brain as therapy to reverse neural degeneration and repair lesions (Birbrair et al., 2013). In humans, NG2 can be also found in skeletal muscles in the sarcolemma and accumulated at the NMJ. In *Drosophila*, although Kon does play a role during embryonic muscle-tendon network formation, there was to date no information about the role of Kon at the NMJ, neither about Kon expression/accumulation at the NMJ in embryonic, larval or adult stages. Alterations in the level of NG2 accumulated at the NMJ and sarcolemma in humans have been associated with various muscle dystrophies, such as Merosin-negative congenital muscle dystrophy, Duchene muscular dystrophy,

gamma-sarcoglycanopathy and Ullrich scleroatonic muscular dystrophy, a collagen 6 associated pathology ((Petrini et al., 2003; Petrini et al., 2005), all of which at this stage may indicate a path to follow in order to better understand the multiple roles of Kon/NG2.

The results here presented have shown Kon accumulating at the NMJ and muscle in larval stages. The origin of Kon accumulated at the NMJ was demonstrated to be not only muscle but also glia derived, as shown by antibody staining intensity measurements ( $\alpha$ -Kon<sup>ecto</sup>) at the NMJ in *kon* knockdown in glia (Figure 3.10 J). Furthermore, the knockdown of *kon* in glia also leads to a significant increase in NMJ bouton number. In vertebrates, Merosin-negative congenital muscle dystrophy is also associated with reduced NG2 accumulation at the NMJ (Petrini et al., 2003). This pathology is related with a loss of Merosin (Laminin-211), a protein found in the basement membrane of muscles that interacts with Integrin  $\alpha$ 7 $\beta$ 1 and with the sugar chains of  $\alpha$ -Dystroglycan, among others (reviewed by (Gawlik and Durbeej, 2011)). In *Drosophila*, several studies highlight the importance of cell adhesion molecules, Integrins and basement membrane proteins in NMJ formation, function and maintenance (Rohrbough et al., 2000; Rushton et al., 2009; Koper et al., 2012), thus likely establishing a link between NG2/Kon and these proteins in NMJ physiology.

#### **4.4 Peri-and Subperineurial glia layers contribute distinctively to Kon dependent NMJ phenotype**

Glial cells actively interact and modulate the NMJ; they clear the synapse not only from excessive neurotransmitters, but also from debris and detached ghost boutons, which in turn will promote the expansion of the NMJ (Fuentes-Medel et al., 2009). In the PNS, glial cells form three distinct layers (Stork et al., 2008; von Hilchen et al., 2013), each of them interacting in different degrees with the NMJ. Subperineurial glial layer was reported to participate more actively with the NMJ than wrapping and perineurial glia (Fuentes-Medel et al., 2009; Brink et al., 2012). Selective expression of membrane bound GFP in each of the three glial layers allowed to observe in detail the differences in glia membrane dynamics around the NMJ. While wrapping glia layer do not reach as far as NMJ boutons, subperineurial and perineurial glia do contact and interact with the NMJ. In a selective

knockdown of *kon* in each glial layer, I observed that the knockdown in subperineurial glia was sufficient to promote the increase in bouton number observed in *kon* knockdown using a pan-glial driver, and the knockdown of *kon* in perineurial and subperineurial glia resulted in a significant increase in branch number. These results suggest that bouton and branch formation are controlled by independent pathways and glial layers, and the evidence shown indicates that Kon plays a role in both pathways, and independently in both glial layers.

#### **4.5 Pre-and postsynaptic changes upon *kon* knockdown in glia result in NMJ degeneration**

A closer look at the NMJ using several synaptic structure markers in *kon* knockdown in glia, revealed a loss of  $\alpha$ -GluRIIA antibody staining in the postsynapse (Figure 3.12 A-B'). A recent publication shows that in *Drosophila*, glial secreted wingless (*wg*) shuttles to the muscle and NMJ, where it controls GluRIIA clustering at the postsynapse. They observed that a knockdown of *wg* in subperineurial glia results in an increase in the intensity and volume occupied by GluRIIA clusters in the postsynapse, while bouton number remained unchanged (Kerr et al., 2014). In vertebrates, it was recently shown that the activity-dependent cleaved NG2 ectodomain (NG2<sup>ecto</sup>) plays an important role in GluR-dependent long-term potentiation (LTP) in brain, in which the lack of NG2<sup>ecto</sup> results in impaired GluR-dependent LTP and decreased neuronal glutamate excitability (Sakry et al., 2014). Taken together, glial secreted molecules influence directly the postsynapse by affecting synaptic responsiveness and neurotransmitter receptor clustering, a process in which Kon may also be involved. The knockdown of *wg* in glia also resulted in electrophysiological changes, as for instance a marked increase in the frequency of miniature excitatory junctional potentials in muscle 6 (Kerr et al., 2014), encouraging future electrophysiological studies in *kon* knockdown in glia.

As presynaptic markers I used  $\alpha$ -Futsch and  $\alpha$ -Bruchpilot (Brp), together with  $\alpha$ -HRP, which allows an integral look at the state and functionality of the presynapse. In *kon* knockdown in glia,  $\alpha$ -Futsch staining pattern is altered, as shown by interrupted  $\alpha$ -Futsch thread and lack of the solid  $\alpha$ -Futsch bulb in the last bouton. These phenotypes have been previously observed in *ankyrin 2* (*ank2*) mutants, which affects microtubule arrangement at the presynapse.

Furthermore, Ank2 is downstream of the *wg*-*frizzled2* (*fz2*)-G $\alpha$  signal transduction pathway that leads to Futsch anchoring to the microtubule during NMJ formation (Figure 4.1). This pathway was also confirmed in mammalian Neuro-2a (N2a) cells, implying a high degree of conservation (Luchtenborg et al., 2014). Although with the evidence here shown it would be premature to add Kon in the *wg*-Fz2-G $\alpha$  signal transduction, yet again we observe a *wg* dependent signaling pathway correlated with a phenotype addressed to the knockdown of *kon* in glia. In the glia-neuron direct signaling, it has been also shown that a released glial prodegenerative signal (TNF $\alpha$ ) acts upon TNFR in neurons to promote NMJ retraction, also resulting in a similar  $\alpha$ -Futsch phenotype in the presynapse (Keller et al., 2011). In vertebrates, NG2 has shown protective properties against TNF $\alpha$  dependent prodegenerative signal (Chekenya et al., 2008), which opens the question whether the lack of Kon at the NMJ, due to the knockdown in glia, leaves motoneurons more sensitive to glial derived TNF $\alpha$  and thus resulting in the NMJ degeneration observed.  $\alpha$ -Brp $^{+}$  vesicles distribution and number in the presynapse does not seem to be affected by *kon* knockdown in glia.

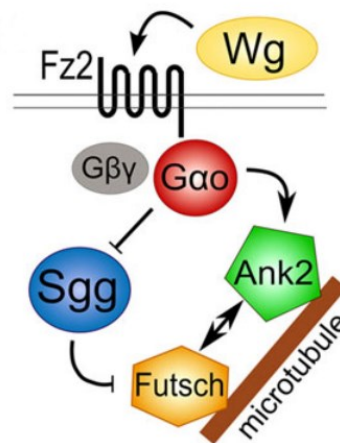


**Figure 4.1 Model of *wg* induced microtubule cytoskeleton regulation**

*Wg*-dependent activated Fz2 binds to heterotrimeric Go protein, blocking Shaggy (Sgg)-mediated Futsch phosphorylation, allowing Ank2-Futsch interaction and promoting NMJ remodeling and growth. (Figure copied from (Luchtenborg et al., 2014))

Chain like arranged presynaptic boutons innervate muscles, opposed by postsynaptic structures that can be labeled with  $\alpha$ -Discs large (Dlg). In *kon* knockdown in glia, L3 larvae showed in posterior hemisegments postsynaptic  $\alpha$ -Dlg staining lacking presynaptic  $\alpha$ -HRP staining. They also showed presynaptic membrane disruption and fragmentation of the NMJ branch (Figure 3.12 G-G'). Both observations combined are the most common features of NMJ retraction (Massaro et al., 2009). Graf and colleagues (Graf et al., 2011) divided NMJ retraction into 3 stages: Pre-retraction (involving reduction of  $\alpha$ -Futsch staining and microtubules), early retraction (identified by the withdrawal of  $\alpha$ -Brp and  $\alpha$ -DVGLUT staining) and late retraction (characterized by breakdown of  $\alpha$ -FasII and  $\alpha$ -HRP staining, as consequence of axon membrane disintegration). From this characterization, the phenotype observed in anterior hemisegments represents early NMJ retraction, which gradually increases in severity towards posterior hemisegments..

#### 4.6 *kon* knockdown in glia affects neuronal transport along the NER

The first evidence involving transport impairment in *kon* knockdown in glia comes from the  $\alpha$ -Futsch staining phenotype observed:  $\alpha$ -Futsch thread disruption in the presynapse and no bulb like structure in the last NMJ bouton (Figure 3.12 E-F'). In an Amyotrophic lateral sclerosis (ALS)-like paradigm in *Drosophila*, overexpressing TDP-43<sup>WT</sup> or TDP-43<sup>G298S</sup> (Estes et al., 2013), it was observed a severe *futsch* mRNA transport impairment, caused by the cytosolic aggregation of TDP-43. In turn, TDP-43 was described as carrier for *futsch* mRNA and therefore resulting in the observed reduced transport along the axon. This *futsch* mRNA transport impairment in neurons resulted in similar phenotypes at the NMJ (Coyne et al., 2014) as observed in *kon* knockdown in glia (Figure 3.12 E-F'). The second evidence for a transport impairment mediated by *kon* knockdown in glia is the fact that NMJ retraction severity increases in more posterior hemisegments, correlating the severity of the phenotype with the distance between the NMJ and the VNC, and thus the distance needed to be covered by the cargo being transported towards the NMJ. Further evidence about the neuronal transport impairment is the accumulation of  $\alpha$ -Brp+ vesicles along the nerve extension region (NER) (Figure 3.13). This is considered one of the most typical hallmarks of impaired axonal transport (Hurd and Saxton, 1996), and has been also observed in *ank2*

mutants (Keller et al., 2011), *stathmin* mutants (Graf et al., 2011), overexpression in *Drosophila* of an APP familial Alzheimer's disease mutation or overexpression of expanded amounts of glutamine repeats (polyQ77), related with Huntington's disease (Kang et al., 2014), all of them resulting in severely compromised presynaptic microtubule integrity and axonal accumulation of presynaptic proteins. The knockdown of *kon* in glia also resulted in the formation of aberrant protrusions and knots along the NER (Figure 3.13). So far, I have not found identical phenotypes in the literature with the same degree of aberrant structures or swollen axons, although it seems to be a common phenotype observed in larvae displaying transport impairment along the axon, since the term "swollen axons" is repeatedly mentioned in several related publications (Hurd and Saxton, 1996) (Torroja et al., 1999a; Fuger et al., 2012). In a recent publication from Vanessa Auld, they have shown evidence that the knockdown of  $\beta$ PS integrin in glia, as well as overexpression of MMP2, results in impaired wrapping of glia around the axon (Xie and Auld, 2011). Some of their images are so far the closest comparable phenotype to the resulting in *kon* knockdown in glia and may provide hints for a link between Kon and Integrins in yet another context, which should be studied further.

#### **4.7 *kon* knockdown results in less glia along the NER**

Surprising was the observation that the number of glial cells along the NER in *kon* knockdown was reduced. To discuss this observation I will take the comments in the publications from von Hilchen (von Hilchen et al., 2013) and Pandey (Pandey et al., 2011). The first publication nicely shows that in wildtype, the only glial cell that proliferates and contributes mostly to NER glia is the perineurial ePG2, and also that this glia is programmed to produce a given number of cells, regardless the length of the axon. Only blocking mitosis, either by *Cyclin A* (*CycA*) knockdown or *Retinoblastoma-family* protein (*Rbf*) overexpression, the number of glial cells along the NER can be reduced (von Hilchen et al., 2013). The second publication argues that the spacing between glia nuclei is determinant in the number of cells to be found along the NER, which means that the length of the axon at last will determine the number of glia nuclei to be found and not a pre-programmed mitotically active cell (Pandey et al., 2011). In *kon* knockdown in glia, against the observations from von Hilchen and Pandey, neither the

overall number of glia nor the spacing between glial cells along the NER is comparable to wildtype. There is indeed a notorious reduction in the number of glial cells and an increased spacing between glia nuclei as compared to wildtype (Figure 3.13). This might tell a role for Kon in the proliferation of perineurial glia along the NER, and thus also raise the question of whether the reduction in perineurial glia number is causal or consequence of the neuronal transport impairment along the NER, previously described. It needs to be investigated, together with a more detailed statistical analysis, the role of Kon in glial proliferation. In vertebrates, NG2 cells are identified as a highly proliferative cell population, and direct links between NG2 and growth factors (FGF2 and PDGF-AA) have suggested a NG2 dependent sensitization and thus control of proliferation (reviewed by (Stallcup and Huang, 2008)). There are indications in the literature that *kon* knockdown in Neuroblasts, using *inscutable*-GAL4, results in smaller lineages (Neumuller et al., 2011); therefore it is extremely interesting to observe a similar effect in the proliferation of glial cells along the NER, although it should be further studied.

#### 4.8 Postsynaptic Kon allows sprout consolidation

To test whether the pre-or postsynapse also contributes to Kon dependent NMJ phenotypes, the same *kon*RNAi fly stock was crossed to a muscle-specific (*mef2*) or neuron-specific (*elav*) GAL4 driver, and the NMJ was scored for phenotypes. The knockdown of *kon* in neurons did not lead to any NMJ phenotype. It is somehow not surprising, since neither Kon protein nor *kon* mRNA were observed in neurons (Figure 3.8). Muscles were already shown to express Kon in the embryo and in the larvae (Figure 3.8) and the knockdown of *kon* in muscles results in an increase in satellite bouton number. During NMJ expansion there is a critical step called sprout consolidation, which refers to the process that promotes presynaptic sprouts to consolidate themselves as either a newly born bouton or a nascent NMJ branch. In this process of maturation, the *Drosophila*  $\beta$ -amyloid precursor protein (APPL) has been shown to play a key role. APPL accumulates in the presynaptic membrane of motoneurons, where it promotes sprout formation, and upon binding to an unknown ligand, both are internalized (APPL+ligand) resulting in microtubule rearrangement and the consolidation of the sprout, very likely through the G $\alpha$ -Ank2-Futsch pathway (Torroja et al., 1999b). These immature

sprouts, also called satellite boutons, are significantly increased in *kon* knockdown in muscle, meaning that the lack of Kon at the postsynapse results in satellite bouton consolidation impairment. Interestingly, in a *Drosophila* hyperexcitable mutant (Ether-à-go-go (*eag*) and Shaker (*Sh*) double mutant) the number of satellite boutons upon APPL overexpression was reduced (Torroja et al., 1999b), meaning that synaptic activity promotes the consolidation of satellite boutons (Budnik et al., 1990), probably by a higher release of the unknown ligand that promotes APPL internalization. In vertebrates, there has been shown a certain affinity of NG2+ cells for A $\beta$ , including A $\beta$  plaques being endocytosed by NG2+ cells, but unfortunately there is not enough evidence of a direct interaction between NG2 and A $\beta$  (Li et al., 2013). The increase of satellite bouton caused by the knockdown of *kon* in muscle may be then the result of either Kon being the unknown ligand that promotes APPL internalization or Kon being a carrier for the ligand, which in either case, upon knockdown, truncates the consolidation of satellite boutons (See **Figure 4.2**).

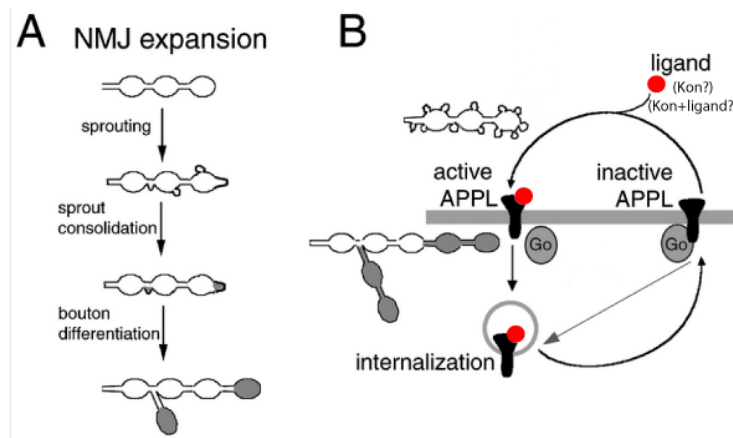


**Figure 4.2 Role of APPL in satellite bouton consolidation may include Kon interaction**

**(A)** Process of NMJ expansion. Sprout formation and consolidation are followed by bouton differentiation. **(B)** APPL signal transduction pathway in the consolidation of sprouts or satellite boutons. Ligand dependent internalization and microtubules rearrangement mediated by Go. Modified from (Torroja et al., 1999b).



#### 4.9 Kon rescue in muscle and aberrant NMJ branches

Muscle-tendon network phenotypes observed in embryo and larvae were rescued by bringing back Kon in muscles (*kon*<sup>c25</sup>,*mef2*-GAL4/*kon*<sup>c1139</sup>,UAS-*kon*::HA) (Figure 3.15). Bouton, single bouton and satellite bouton number were normal, whereas the number of NMJ branches was reduced and the number of ghost boutons increased (Figure 3.15 H,I respectively). The rescue of Kon in muscle using *mef2*-GAL4 results in a significant increase in the level of Kon in muscles, therefore increased availability of Kon in the postsynapse as compared to control or wildtype level. From the previous section, I discussed the role of Kon in the consolidation of newly born boutons, and how the knockdown of Kon in muscles results in an increase in satellite boutons. The opposite scenario in this case, the overexpression of Kon in muscle, might lead to a faster consolidation of newly born boutons, favoring the process of adding boutons to a branch rather than extending new branches. Regarding the increase in ghost boutons number, similar phenotypes have been observed in Draper and Ced6 knockdown in muscle, both members of the phagocytic pathway described to be responsible for ghost boutons clearance at the *Drosophila* NMJ (Fuentes-Medel et al., 2009). In rats, it has been shown that NG2 induced expression in microglia reduces drastically the phagocytic activity in these cells (Zhu et al., 2012), similar to what is seen in Kon rescue in muscles, since an increase in ghost bouton number at the NMJ is a feature of impaired phagocytic activity in muscles. Nevertheless, the pathway by which NG2 interferes with phagocytosis is still under debate, to which *Drosophila* now offers to contribute to.

#### 4.10 Kon overexpression in glial promotes NMJ branches formation

In several muscle dystrophies, Petrini and colleagues observed that the levels of NG2 at the NMJ and muscles were altered, being in some cases upregulated and in others downregulated (Petrini et al., 2003, Petrini, 2005 #383). Kon overexpression in glia resulted in an upregulation of  $\alpha$ -Kon<sup>ecto</sup> staining at the NMJ, together with significantly higher numbers of boutons and branches (Figure 3.16). A higher availability of glial derived Kon at the NMJ may positively influences the consolidation of satellite boutons and therefore results in a general higher number of branches and boutons. In vertebrates, NG2 has been

extensively studied in vasculature lumen formation during development and tumorous progression (Ozerdem and Stallcup, 2003) (Chekenya and Pilkington, 2002), acting at the ECM to promote basement membrane remodeling. The similarities between vascular and perisynaptic basement membrane (Yurchenco, 2011) might be used by NG2/Kon to in both cases promote the remodeling of the lumen and thus the extension of the vasculature or the NMJ. Furthermore, the positive role of sulfate proteoglycans in synapse formation (reviewed by (Bernfield et al., 1999), (Van Vactor et al., 2006)) also argues for a positive correlation between higher availability of Kon at the NMJ and an increased number of branches and boutons, which is indeed the phenotype observed in Kon overexpression in glia.

#### **4.11 Kon also interacts with DGrip in glial cells**

The overexpression of Kon in glia also resulted in an unexpected phenotype, an oversized VNC that could be visible from embryonic stage 16 onwards (Figure 3.17), and reaching almost 3 times the size of wildtype VNC in L3 larvae. To trigger this phenotype it is necessary to overexpress Kon full-length in glia during embryonic development and until L1 stages, where VNC elongation is not reversible (Figure 3.17 and Figure 3.18). Only the overexpression of Kon full-length resulted in the elongated VNC phenotype, whereas the overexpression of Kon versions either lacking extracellular domains or with a mutation in the PDZ-Binding domain (BD) did not affect the length of the VNC. I used this phenotype in a suppressor screen to search for Kon PDZ-BD interacting proteins in glia. From the screened candidates, only DGrip showed a significant reduction in the length of the VNC (Figure 3.20), thus giving some evidence about a conserved Kon-DGrip interaction not only in the context of muscle-tendon network establishment (Estrada et al., 2007; Schnorrer et al., 2007), but also in glia.

#### **4.12 Kon processing in *Drosophila***

Shedding off the ectodomain of membrane bound proteoglycans is a well-studied posttranslational mechanism, often regulated by cell activity, inflammatory response or as a pathophysiological process (reviewed in (Bernfield et al., 1999) and (Nam and Park, 2012)). For instance, upon brain injury, NG2+ cells are activated promoting NG2 expression and

ectodomain shedding (Wennstrom et al., 2014). Synaptic activity on NG2+ cells also promotes NG2 shedding, which then in turn regulates normal neuronal synaptic communication (Sakry et al., 2014). In *Drosophila*, a western blot detecting misexpressed Kon in glia, muscles and neurons also revealed a stereotypical Kon<sup>ecto</sup> processing pattern, repeated in all tissues (Figure 3.21). It also revealed that the misexpression of a Kon PDZ-BD mutated version (Kon<sup>vg</sup>) resulted in a lower amount of Kon present in the membrane bound fraction, which may argue for a link between the PDZ-BD and Kon transport and anchor to the plasma membrane. Similar observations have been made for cystic fibrosis transmembrane conductance regulator (CFTR), where the PDZ-BD plays a role in the proper transport and anchor of the protein to the plasma membrane (Moyer et al., 1999; Milewski et al., 2001). It is nevertheless necessary to perform quantitative western blot analysis in order to conclusively attribute to the PDZ-BD of Kon a role in protein transport to the membrane.

#### **4.13 DGrip and Kuzbanian pave the road for glial Kon to reach muscles and the NMJ**

Glial derived Kon accumulates at larval muscle and at the NMJ, where it positively influences the integrity of the pre-and postsynapse. The mechanism used by glial Kon to reach the NMJ and muscles is unknown, but appears to be based on a conserved property of Kon/NG2, which is the shedding of the ectodomain. In vertebrates, several matrix metalloproteinases (MMP-9: (Liu and Shubayev, 2011; Schultz et al., 2014); MMP-13: (Joo et al., 2014) and MMP-14: (Nishihara et al., 2014)) and ADAM10 ((Sakry et al., 2014) have been shown to shed soluble NG2. In *Drosophila*, there is so far no evidence for a role of MMPs or ADAMs in Kon<sup>ecto</sup> shedding in the literature. In mouse and *Drosophila*, Notch extracellular portion is cleaved upon binding to Delta by homologous proteins, ADAM10 and its fly homologue Kuzbanian (Kuz) respectively, which implies a high degree of conservation in the mechanisms and substrates they process (Tian et al., 2008) (Delwig and Rand, 2008). It is then also possible that the ADAM10 dependent processing of NG2 maybe also conserved and thus in *Drosophila* there is a Kuz dependent Kon processing. Interestingly, in Kuz overexpression in glia, the amount and intensity of Kon<sup>ecto</sup> speckles in muscles, as well as the intensity of Kon<sup>ecto</sup> staining at the NMJ, are both increased significantly. In *kuz* knockdown in glia, an

opposite effect is observed, a mild reduction in Kon<sup>ecto</sup> speckles in muscles and staining intensity at the NMJ. At this point it is not possible to rule out other proteases also being responsible for glial Kon<sup>ecto</sup> shedding and therefore is suggested as a matter of further study.

A second candidate in glial Kon processing was DGrip. I observed in *dgrip* knockdown in glia an increase in the accumulation of  $\alpha$ -Kon<sup>ecto</sup> staining at the NMJ, whereas a clear reduction in  $\alpha$ -Kon<sup>ecto</sup> speckles in muscles. This might be the key evidence showing two independent pathways, one shuttling Kon to the perisynaptic mesh and the other releasing Kon to the muscles. Glial Kon release to the muscles in this case would be mediated by DGrip, hence knockdown of *dgrip* in glia results in a reduction of Kon<sup>ecto</sup> in muscles, whereas Kuz plays a role in both pathways. Several publications describe active glial release of growth related molecules, for instance Wg (Kerr et al., 2014), TGF- $\beta$  ligand (Maverick) (Fuentes-Medel et al., 2012) and TNF- $\alpha$  (Eiger) (Keller et al., 2011), although in none of the publications above there is a distinction between a targeted release to the NMJ or muscle, and the step involving the shuttle of growth related molecules to the postsynaptic tissue is merely a given step. Another question is whether glial Kon shuttles to the muscle alone, in a multimer complex or in vesicles. By immunohistochemistry, Kon<sup>ecto</sup> staining in muscles shows rather microdomain/vesicle-like staining, which I have consistently called speckles (Figure 3.8). There is some evidence in the literature for a PDZ-BD mediated NG2 multimer formation with Sintenin-1 (Chatterjee et al., 2008), Mupp1 and GRIP (Trotter et al., 2010), which in this case could be used to favor the targeted interaction of Kon with other molecules prior release to the muscles. Furthermore, proteoglycans have been shown to serve as carriers for growth related molecules in neural development and regeneration (reviewed by (Carulli et al., 2005)), open the possibilities for a novel glia-muscle-neuron communication pathway, mediated by Kon.

Bouton, single bouton and NMJ branch phenotypes were also observed. *dgrip* knockdown and Kuz overexpression, both also characterized by a significant increase in Kon<sup>ecto</sup> accumulation at the NMJ, resulted in a significant increase in bouton number. *kuz* knockdown in turn did not affect bouton number. Branch number was significantly increased in *dgrip* knockdown and single bouton number was significantly increased in *kuz* knockdown.

It is worth noting the variety of phenotypes observed with DGrip and Kuz regarding bouton, single bouton and NMJ branch, and to stress the point that the direct effect attributable to their interaction with Kon is the resulting  $\alpha$ -Kon<sup>ecto</sup> staining pattern, and that the NMJ phenotypes observed also has the component of their endogenous interaction with other proteins in glia.

#### 4.14 Kon, a pleiotropic factor in glial development

In the table below (Table 4.1), I attempt to briefly summarize all the phenotypes observed and some candidates as interacting partners for Kon during development, in the context of the phenotypes observed:

**Table 4.1 Summary of phenotypes observed**

| Tissue                              | Phenotype  | Candidate interacting partners                            |
|-------------------------------------|--|---|
| Glia (Kon knockdown)                | Increased bouton and single bouton number  | Integrins   |
|                                     | Reduced postsynaptic GluRIIA clustering  | GluRIIA   |
|                                     | NMJ degeneration. Presynaptic microtubule disintegration   | Futsch – Ankirin – Eiger (TNF- $\alpha$ ) – Wengen (TNFR) |
|                                     | Axonal transport impairment  | Futsch - Ankirin  |
|                                     | Glia proliferation along NER   | FGF2 – PDGF-AA  |
| Perineurial glia (Kon knockdown)    | Increased branch number  | Integrins   |
| Subperineurial glia (Kon knockdown) | Increased bouton and branch number   | Integrins   |
| Glia (Kon overexpression)           | Increased number of boutons and branches   | Integrins   |
|                                     | VNC elongation   | Integrins – DGrip - ECM                                   |
| Glia (Kuz overexpression)           | Increased $\alpha$ -Kon <sup>ecto</sup> staining in muscle and NMJ. Increased bouton number                    | Kon   |
| Glia ( <i>kuz</i> knockdown)        | Reduced $\alpha$ -Kon <sup>ecto</sup> staining in muscle and NMJ. Increased single bouton number               | Kon   |
| Glia ( <i>dgrip</i> knockdown)      | $\alpha$ -Kon <sup>ecto</sup> staining is reduced in muscles and increased at the NMJ. Increased bouton number | Kon   |

|                             |   |                      |
|-----------------------------|---|----------------------|
| Muscle (Kon knockdown)      | Satellite bouton increase                                   | APPL - Wg            |
| Muscle (Kon overexpression) | Reduced number of branches                                  | APPL - Wg            |
|                             | Increased number of ghost boutons<br>– reduced phagocytosis | Draper – Ced6 – APPL |

In short, Kon is a pleiotropic gene with multiple roles not only in glial differentiation but also in function. Glial Kon seems to play a pivotal role in glia-muscle and glia-muscle-neuron multipartite interaction, and also seems to interact with numerous other proteins. The seminal work here presented pretends to improve the understanding of the processes in which Kon is involved and encourages the further study of the presented phenotypes and pathways not only in *Drosophila*, but also in mouse and higher organisms. There is a number of questions that still remain unsolved.

## 5 Summary

The present study offers a comparative functional analysis of factors controlling glial differentiation in *Drosophila* and mouse. Three candidate genes (Fyn Src kinase, hnRNPF/H and NG2), were selected from mouse and their homologues (Src42A and 64B, Glorund and Kon-tiki (Kon)) studied in *Drosophila*. Mutations in any of these genes are not associated with major embryonic nervous system development phenotypes. Src kinases and Glorund were shown to be ubiquitously expressed, whereas *kon* mRNA showed selective expression in muscle, CNS and PNS glia. Kon was also shown to be expressed in L3 larvae, accumulated at the NMJ and in muscles in the form of speckles. Knockdown of *kon* in glia resulted in NMJ phenotypes, mainly characterized by a significant increase in bouton number and a reduction in  $\alpha$ -Kon<sup>ecto</sup> staining intensity at the NMJ. From the three glial layers ensheathing the peripheral nervous system, subperineurial glial showed to be the one contributing the most to *kon* knockdown dependent NMJ phenotypes, while perineurial glia had a minor and wrapping glia no role. The knockdown of *kon* in glia also showed to affect GluRIIA clustering in the postsynapse, same as microtubule arrangement in the presynapse, as seen by  $\alpha$ -Futsch pattern interruptions and alterations. *kon* knockdown in glia also resulted in impaired axonal transport, as seen by the accumulation of  $\alpha$ -Brp vesicles along the nerves, abnormal formation of neuronal derived protrusions and swellings, filled with vacuole-like structures. Glia number along the peripheral nerves is also reduced as consequence of *kon* knockdown. Muscle derived Kon was shown to accumulate at the NMJ and play a role in bouton consolidation and to interfere with ghost bouton phagocytosis. NMJ bouton and branch number was also significantly increased in Kon overexpression in glia, arguing that the level of Kon at the NMJ and muscle plays a role in NMJ formation and maintenance, rather than an On/Off switch, similar to the role of NG2 in several human myopathies. The overexpression of Kon in glia also resulted in a massive elongation of the VNC, which served in a suppressor screen to identify DGrip as a PDZ-BD interaction partner of Kon in glia. It was shown that Kon is processed in glia and preliminary results indicate that Kuz may play a role in the shedding of Kon<sup>ecto</sup>. Kon is a pleiotropic gene with various roles in glia-neuron and glia-neuron-muscle interaction, some of which still need to be uncovered.

## 6 References

Bellen, H. J., Tong, C. and Tsuda, H. (2010) '100 years of Drosophila research and its impact on vertebrate neuroscience: a history lesson for the future', *Nat Rev Neurosci* 11(7): 514-22.

Bernfield, M., Gotte, M., Park, P. W., Reizes, O., Fitzgerald, M. L., Lincecum, J. and Zako, M. (1999) 'Functions of cell surface heparan sulfate proteoglycans', *Annu Rev Biochem* 68: 729-77.

Birbrair, A., Zhang, T., Wang, Z. M., Messi, M. L., Enikolopov, G. N., Mintz, A. and Delbono, O. (2013) 'Skeletal muscle neural progenitor cells exhibit properties of NG2-glia', *Exp Cell Res* 319(1): 45-63.

Birbrair, A., Zhang, T., Wang, Z. M., Messi, M. L., Olson, J. D., Mintz, A. and Delbono, O. (2014) 'Type-2 pericytes participate in normal and tumoral angiogenesis', *Am J Physiol Cell Physiol* 307(1): C25-38.

Brechbiel, J. L. and Gavis, E. R. (2008) 'Spatial regulation of nanos is required for its function in dendrite morphogenesis', *Curr Biol* 18(10): 745-50.

Brink, D., Gilbert, M. and Auld, V. (2009) 'Visualizing the live Drosophila glial-neuromuscular junction with fluorescent dyes', *J Vis Exp*(27).

Brink, D. L., Gilbert, M., Xie, X., Petley-Ragan, L. and Auld, V. J. (2012) 'Glial processes at the Drosophila larval neuromuscular junction match synaptic growth', *PLoS One* 7(5): e37876.

Broadie, K. S. and Bate, M. (1993) 'Development of the embryonic neuromuscular synapse of Drosophila melanogaster', *J Neurosci* 13(1): 144-66.

Budnik, V., Zhong, Y. and Wu, C. F. (1990) 'Morphological plasticity of motor axons in Drosophila mutants with altered excitability', *J Neurosci* 10(11): 3754-68.

Carulli, D., Laabs, T., Geller, H. M. and Fawcett, J. W. (2005) 'Chondroitin sulfate proteoglycans in neural development and regeneration', *Curr Opin Neurobiol* 15(1): 116-20.



Chatterjee, N., Stegmuller, J., Schatzle, P., Karram, K., Koroll, M., Werner, H. B., Nave, K. A. and Trotter, J. (2008) 'Interaction of syntenin-1 and the NG2 proteoglycan in migratory oligodendrocyte precursor cells', *J Biol Chem* 283(13): 8310-7.

Chekenya, M., Enger, P. O., Thorsen, F., Tysnes, B. B., Al-Sarraj, S., Read, T. A., Furmanek, T., Mahesparan, R., Levine, J. M., Butt, A. M. et al. (2002) 'The glial precursor proteoglycan, NG2, is expressed on tumour neovasculature by vascular pericytes in human malignant brain tumours', *Neuropathol Appl Neurobiol* 28(5): 367-80.

Chekenya, M., Krakstad, C., Svendsen, A., Netland, I. A., Staalesen, V., Tysnes, B. B., Selheim, F., Wang, J., Sakariassen, P. O., Sandal, T. et al. (2008) 'The progenitor cell marker NG2/MPG promotes chemoresistance by activation of integrin-dependent PI3K/Akt signaling', *Oncogene* 27(39): 5182-94.

Chekenya, M. and Pilkington, G. J. (2002) 'NG2 precursor cells in neoplasia: functional, histogenesis and therapeutic implications for malignant brain tumours', *J Neurocytol* 31(6-7): 507-21.

Coyne, A. N., Siddegowda, B. B., Estes, P. S., Johannesmeyer, J., Kovalik, T., Daniel, S. G., Pearson, A., Bowser, R. and Zarnescu, D. C. (2014) 'Futsch/MAP1B mRNA Is a Translational Target of TDP-43 and Is Neuroprotective in a Drosophila Model of Amyotrophic Lateral Sclerosis', *J Neurosci* 34(48): 15962-74.

Delwig, A. and Rand, M. D. (2008) 'Kuz and TACE can activate Notch independent of ligand', *Cell Mol Life Sci* 65(14): 2232-43.

Doherty, J., Logan, M. A., Tasdemir, O. E. and Freeman, M. R. (2009) 'Ensheathing glia function as phagocytes in the adult Drosophila brain', *J Neurosci* 29(15): 4768-81.

Duffy, J. B. (2002) 'GAL4 system in Drosophila: a fly geneticist's Swiss army knife', *Genesis* 34(1-2): 1-15.

Estes, P. S., Daniel, S. G., McCallum, A. P., Boehringer, A. V., Sukhina, A. S., Zwick, R. A. and Zarnescu, D. C. (2013) 'Motor neurons and glia exhibit specific individualized responses to

TDP-43 expression in a *Drosophila* model of amyotrophic lateral sclerosis', *Dis Model Mech* 6(3): 721-33.

Estrada, B., Gisselbrecht, S. S. and Michelson, A. M. (2007) 'The transmembrane protein Perdido interacts with Grip and integrins to mediate myotube projection and attachment in the *Drosophila* embryo', *Development* 134(24): 4469-78.

Feng, Z. and Ko, C. P. (2008) 'Schwann cells promote synaptogenesis at the neuromuscular junction via transforming growth factor-beta1', *J Neurosci* 28(39): 9599-609.

Fuentes-Medel, Y., Ashley, J., Barria, R., Maloney, R., Freeman, M. and Budnik, V. (2012) 'Integration of a retrograde signal during synapse formation by glia-secreted TGF-beta ligand', *Curr Biol* 22(19): 1831-8.

Fuentes-Medel, Y., Logan, M. A., Ashley, J., Ataman, B., Budnik, V. and Freeman, M. R. (2009) 'Glia and muscle sculpt neuromuscular arbors by engulfing destabilized synaptic boutons and shed presynaptic debris', *PLoS Biol* 7(8): e1000184.

Fuger, P., Sreekumar, V., Schule, R., Kern, J. V., Stanchev, D. T., Schneider, C. D., Karle, K. N., Daub, K. J., Siegert, V. K., Flotenmeyer, M. et al. (2012) 'Spastic paraplegia mutation N256S in the neuronal microtubule motor KIF5A disrupts axonal transport in a *Drosophila* HSP model', *PLoS Genet* 8(11): e1003066.

Fukushi, J., Makagiansar, I. T. and Stallcup, W. B. (2004) 'NG2 proteoglycan promotes endothelial cell motility and angiogenesis via engagement of galectin-3 and alpha3beta1 integrin', *Mol Biol Cell* 15(8): 3580-90.

Gawlik, K. I. and Durbeej, M. (2011) 'Skeletal muscle laminin and MDC1A: pathogenesis and treatment strategies', *Skelet Muscle* 1(1): 9.

Graf, E. R., Heerssen, H. M., Wright, C. M., Davis, G. W. and DiAntonio, A. (2011) 'Stathmin is required for stability of the *Drosophila* neuromuscular junction', *J Neurosci* 31(42): 15026-34.

- Hurd, D. D. and Saxton, W. M. (1996) 'Kinesin mutations cause motor neuron disease phenotypes by disrupting fast axonal transport in *Drosophila*', *Genetics* 144(3): 1075-85.
- Jahn, O., Tenzer, S. and Werner, H. B. (2009) 'Myelin proteomics: molecular anatomy of an insulating sheath', *Mol Neurobiol* 40(1): 55-72.
- Joo, N. E., Miao, D., Bermudez, M., Stallcup, W. B. and Kapila, Y. L. (2014) 'Shedding of NG2 by MMP-13 Attenuates Anoikis', *DNA Cell Biol* 33(12): 854-62.
- Kalifa, Y., Armenti, S. T. and Gavis, E. R. (2009) 'Glorund interactions in the regulation of *gurken* and *oskar* mRNAs', *Dev Biol* 326(1): 68-74.
- Kalifa, Y., Huang, T., Rosen, L. N., Chatterjee, S. and Gavis, E. R. (2006) 'Glorund, a *Drosophila* hnRNP F/H homolog, is an ovarian repressor of *nanos* translation', *Dev Cell* 10(3): 291-301.
- Kang, M. J., Hansen, T. J., Mickiewicz, M., Kaczynski, T. J., Fye, S. and Gunawardena, S. (2014) 'Disruption of axonal transport perturbs bone morphogenetic protein (BMP)--signaling and contributes to synaptic abnormalities in two neurodegenerative diseases', *PLoS One* 9(8): e104617.
- Karram, K., Chatterjee, N. and Trotter, J. (2005) 'NG2-expressing cells in the nervous system: role of the proteoglycan in migration and glial-neuron interaction', *J Anat* 207(6): 735-44.
- Keller, L. C., Cheng, L., Locke, C. J., Muller, M., Fetter, R. D. and Davis, G. W. (2011) 'Glial-derived prodegenerative signaling in the *Drosophila* neuromuscular system', *Neuron* 72(5): 760-75.
- Kerr, K. S., Fuentes-Medel, Y., Brewer, C., Barria, R., Ashley, J., Abruzzi, K. C., Sheehan, A., Tasdemir-Yilmaz, O. E., Freeman, M. R. and Budnik, V. (2014) 'Glial wingless/Wnt regulates glutamate receptor clustering and synaptic physiology at the *Drosophila* neuromuscular junction', *J Neurosci* 34(8): 2910-20.

- Koper, A., Schenck, A. and Prokop, A. (2012) 'Analysis of adhesion molecules and basement membrane contributions to synaptic adhesion at the *Drosophila* embryonic NMJ', *PLoS One* 7(4): e36339.
- Levine, J. M. and Nishiyama, A. (1996) 'The NG2 chondroitin sulfate proteoglycan: a multifunctional proteoglycan associated with immature cells', *Perspect Dev Neurobiol* 3(4): 245-59.
- Li, W., Tang, Y., Fan, Z., Meng, Y., Yang, G., Luo, J. and Ke, Z. J. (2013) 'Autophagy is involved in oligodendroglial precursor-mediated clearance of amyloid peptide', *Mol Neurodegener* 8: 27.
- Lin, S. C. and Bergles, D. E. (2002) 'Physiological characteristics of NG2-expressing glial cells', *J Neurocytol* 31(6-7): 537-49.
- Liu, H. and Shubayev, V. I. (2011) 'Matrix metalloproteinase-9 controls proliferation of NG2+ progenitor cells immediately after spinal cord injury', *Exp Neurol* 231(2): 236-46.
- Luchtenborg, A. M., Solis, G. P., Egger-Adam, D., Koval, A., Lin, C., Blanchard, M. G., Kellenberger, S. and Katanaev, V. L. (2014) 'Heterotrimeric Go protein links Wnt-Frizzled signaling with ankyrins to regulate the neuronal microtubule cytoskeleton', *Development* 141(17): 3399-409.
- Lue, N. F., Chasman, D. I., Buchman, A. R. and Kornberg, R. D. (1987) 'Interaction of GAL4 and GAL80 gene regulatory proteins in vitro', *Mol Cell Biol* 7(10): 3446-51.
- Massaro, C. M., Pielage, J. and Davis, G. W. (2009) 'Molecular mechanisms that enhance synapse stability despite persistent disruption of the spectrin/ankyrin/microtubule cytoskeleton', *J Cell Biol* 187(1): 101-17.
- McGuire, S. E., Le, P. T., Osborn, A. J., Matsumoto, K. and Davis, R. L. (2003) 'Spatiotemporal rescue of memory dysfunction in *Drosophila*', *Science* 302(5651): 1765-8.

- Milewski, M. I., Mickle, J. E., Forrest, J. K., Stafford, D. M., Moyer, B. D., Cheng, J., Guggino, W. B., Stanton, B. A. and Cutting, G. R. (2001) 'A PDZ-binding motif is essential but not sufficient to localize the C terminus of CFTR to the apical membrane', *J Cell Sci* 114(Pt 4): 719-26.
- Moyer, B. D., Denton, J., Karlson, K. H., Reynolds, D., Wang, S., Mickle, J. E., Milewski, M., Cutting, G. R., Guggino, W. B., Li, M. et al. (1999) 'A PDZ-interacting domain in CFTR is an apical membrane polarization signal', *J Clin Invest* 104(10): 1353-61.
- Nam, E. J. and Park, P. W. (2012) 'Shedding of cell membrane-bound proteoglycans', *Methods Mol Biol* 836: 291-305.
- Neumuller, R. A., Richter, C., Fischer, A., Novatchkova, M., Neumuller, K. G. and Knoblich, J. A. (2011) 'Genome-wide analysis of self-renewal in Drosophila neural stem cells by transgenic RNAi', *Cell Stem Cell* 8(5): 580-93.
- Nishihara, T., Remacle, A. G., Angert, M., Shubayev, I., Shiryaev, S. A., Liu, H., Dolkas, J., Chernov, A. V., Strongin, A. Y. and Shubayev, V. I. (2014) 'Matrix metalloproteinase-14 both sheds cell surface NG2 proteoglycan on macrophages and governs the response to peripheral nerve injury', *J Biol Chem*.
- Nishiyama, A., Komitova, M., Suzuki, R. and Zhu, X. (2009) 'Polydendrocytes (NG2 cells): multifunctional cells with lineage plasticity', *Nat Rev Neurosci* 10(1): 9-22.
- O'Reilly, A. M., Ballew, A. C., Miyazawa, B., Stocker, H., Hafen, E. and Simon, M. A. (2006) 'Csk differentially regulates Src64 during distinct morphological events in Drosophila germ cells', *Development* 133(14): 2627-38.
- Ozerdem, U. and Stallcup, W. B. (2003) 'Early contribution of pericytes to angiogenic sprouting and tube formation', *Angiogenesis* 6(3): 241-9.
- Pandey, R., Blanco, J. and Udolph, G. (2011) 'The glucuronyltransferase GlcAT-P is required for stretch growth of peripheral nerves in Drosophila', *PLoS One* 6(11): e28106.

- Passlick, S., Trotter, J., Seifert, G., Steinhauser, C. and Jabs, R. (2014) 'The NG2 Protein Is Not Required for Glutamatergic Neuron-NG2 Cell Synaptic Signaling', *Cereb Cortex*.
- Perez-Moreno, J. J., Bischoff, M., Martin-Bermudo, M. D. and Estrada, B. (2014) 'The conserved transmembrane proteoglycan Perdido/Kon-tiki is essential for myofibrillogenesis and sarcomeric structure in *Drosophila*', *J Cell Sci*.
- Petrini, S., Tessa, A., Carrozzo, R., Verardo, M., Pierini, R., Rizza, T. and Bertini, E. (2003) 'Human melanoma/NG2 chondroitin sulfate proteoglycan is expressed in the sarcolemma of postnatal human skeletal myofibers. Abnormal expression in merosin-negative and Duchenne muscular dystrophies', *Mol Cell Neurosci* 23(2): 219-31.
- Petrini, S., Tessa, A., Stallcup, W. B., Sabatelli, P., Pescatori, M., Giusti, B., Carrozzo, R., Verardo, M., Bergamin, N., Columbaro, M. et al. (2005) 'Altered expression of the MCSP/NG2 chondroitin sulfate proteoglycan in collagen VI deficiency', *Mol Cell Neurosci* 30(3): 408-17.
- Richardson, W. D., Young, K. M., Tripathi, R. B. and McKenzie, I. (2011) 'NG2-glia as multipotent neural stem cells: fact or fantasy?', *Neuron* 70(4): 661-73.
- Rival, T., Soustelle, L., Cattaert, D., Strambi, C., Iche, M. and Birman, S. (2006) 'Physiological requirement for the glutamate transporter dEAAT1 at the adult *Drosophila* neuromuscular junction', *J Neurobiol* 66(10): 1061-74.
- Robins, S. C., Trudel, E., Rotondi, O., Liu, X., Djogo, T., Kryzskaya, D., Bourque, C. W. and Kokoeva, M. V. (2013) 'Evidence for NG2-glia derived, adult-born functional neurons in the hypothalamus', *PLoS One* 8(10): e78236.
- Rohrbough, J., Grotewiel, M. S., Davis, R. L. and Broadie, K. (2000) 'Integrin-mediated regulation of synaptic morphology, transmission, and plasticity', *J Neurosci* 20(18): 6868-78.
- Rushton, E., Rohrbough, J. and Broadie, K. (2009) 'Presynaptic secretion of mind-the-gap organizes the synaptic extracellular matrix-integrin interface and postsynaptic environments', *Dev Dyn* 238(3): 554-71.

- Sakry, D., Neitz, A., Singh, J., Frischknecht, R., Marongiu, D., Biname, F., Perera, S. S., Endres, K., Lutz, B., Radyushkin, K. et al. (2014) 'Oligodendrocyte Precursor Cells Modulate the Neuronal Network by Activity-Dependent Ectodomain Cleavage of Glial NG2', *PLoS Biol* 12(11): e1001993.
- Schneider, S., Bosse, F., D'Urso, D., Muller, H., Sereda, M. W., Nave, K., Niehaus, A., Kempf, T., Schnolzer, M. and Trotter, J. (2001) 'The AN2 protein is a novel marker for the Schwann cell lineage expressed by immature and nonmyelinating Schwann cells', *J Neurosci* 21(3): 920-33.
- Schnorrer, F., Kalchauer, I. and Dickson, B. J. (2007) 'The transmembrane protein Kon-tiki couples to Dgrip to mediate myotube targeting in *Drosophila*', *Dev Cell* 12(5): 751-66.
- Schultz, N., Nielsen, H. M., Minthon, L. and Wennstrom, M. (2014) 'Involvement of matrix metalloproteinase-9 in amyloid-beta 1-42-induced shedding of the pericyte proteoglycan NG2', *J Neuropathol Exp Neurol* 73(7): 684-92.
- Sepp, K. J. and Auld, V. J. (1999) 'Conversion of lacZ enhancer trap lines to GAL4 lines using targeted transposition in *Drosophila melanogaster*', *Genetics* 151(3): 1093-101.
- Shindo, M., Wada, H., Kaido, M., Tateno, M., Aigaki, T., Tsuda, L. and Hayashi, S. (2008) 'Dual function of Src in the maintenance of adherens junctions during tracheal epithelial morphogenesis', *Development* 135(7): 1355-64.
- Snaidero, N., Mobius, W., Czopka, T., Hekking, L. H., Mathisen, C., Verkleij, D., Goebbels, S., Edgar, J., Merkler, D., Lyons, D. A. et al. (2014) 'Myelin membrane wrapping of CNS axons by PI(3,4,5)P3-dependent polarized growth at the inner tongue', *Cell* 156(1-2): 277-90.
- Stallcup, W. B. (2002) 'The NG2 proteoglycan: past insights and future prospects', *J Neurocytol* 31(6-7): 423-35.
- Stallcup, W. B. and Huang, F. J. (2008) 'A role for the NG2 proteoglycan in glioma progression', *Cell Adh Migr* 2(3): 192-201.

- Stork, T., Engelen, D., Krudewig, A., Silies, M., Bainton, R. J. and Klambt, C. (2008) 'Organization and function of the blood-brain barrier in *Drosophila*', *J Neurosci* 28(3): 587-97.
- Sun, B., Xu, P. and Salvaterra, P. M. (1999) 'Dynamic visualization of nervous system in live *Drosophila*', *Proc Natl Acad Sci U S A* 96(18): 10438-43.
- Takahashi, M., Takahashi, F., Ui-Tei, K., Kojima, T. and Saigo, K. (2005) 'Requirements of genetic interactions between *Src42A*, *armadillo* and *shotgun*, a gene encoding E-cadherin, for normal development in *Drosophila*', *Development* 132(11): 2547-59.
- Tian, L., Wu, X., Chi, C., Han, M., Xu, T. and Zhuang, Y. (2008) 'ADAM10 is essential for proteolytic activation of Notch during thymocyte development', *Int Immunol* 20(9): 1181-7.
- Torroja, L., Chu, H., Kotovsky, I. and White, K. (1999a) 'Neuronal overexpression of APPL, the *Drosophila* homologue of the amyloid precursor protein (APP), disrupts axonal transport', *Curr Biol* 9(9): 489-92.
- Torroja, L., Packard, M., Gorczyca, M., White, K. and Budnik, V. (1999b) 'The *Drosophila* beta-amyloid precursor protein homolog promotes synapse differentiation at the neuromuscular junction', *J Neurosci* 19(18): 7793-803.
- Trotter, J., Karram, K. and Nishiyama, A. (2010) 'NG2 cells: Properties, progeny and origin', *Brain Res Rev* 63(1-2): 72-82.
- Van Vactor, D., Wall, D. P. and Johnson, K. G. (2006) 'Heparan sulfate proteoglycans and the emergence of neuronal connectivity', *Curr Opin Neurobiol* 16(1): 40-51.
- von Hilchen, C. and Altenhein, B. (2014) 'Tracing cells throughout development: insights into single glial cell differentiation', *Fly (Austin)* 8(2).
- von Hilchen, C. M., Bustos, A. E., Giangrande, A., Technau, G. M. and Altenhein, B. (2013) 'Predetermined embryonic glial cells form the distinct glial sheaths of the *Drosophila* peripheral nervous system', *Development* 140(17): 3657-68.



- von Hilchen, C. M., Hein, I., Technau, G. M. and Altenhein, B. (2010) 'Netrins guide migration of distinct glial cells in the *Drosophila* embryo', *Development* 137(8): 1251-62.
- Wang, E. and Cambi, F. (2009) 'Heterogeneous nuclear ribonucleoproteins H and F regulate the proteolipid protein/DM20 ratio by recruiting U1 small nuclear ribonucleoprotein through a complex array of G runs', *J Biol Chem* 284(17): 11194-204.
- Wang, E., Dimova, N. and Cambi, F. (2007) 'PLP/DM20 ratio is regulated by hnRNPH and F and a novel G-rich enhancer in oligodendrocytes', *Nucleic Acids Res* 35(12): 4164-78.
- Wennstrom, M., Janelidze, S., Bay-Richter, C., Minthon, L. and Brundin, L. (2014) 'Pro-inflammatory cytokines reduce the proliferation of NG2 cells and increase shedding of NG2 in vivo and in vitro', *PLoS One* 9(10): e109387.
- White, R., Gonsior, C., Kramer-Albers, E. M., Stohr, N., Huttelmaier, S. and Trotter, J. (2008) 'Activation of oligodendroglial Fyn kinase enhances translation of mRNAs transported in hnRNP A2-dependent RNA granules', *J Cell Biol* 181(4): 579-86.
- Wolfstetter, G. and Holz, A. (2012) 'The role of LamininB2 (LanB2) during mesoderm differentiation in *Drosophila*', *Cell Mol Life Sci* 69(2): 267-82.
- Wouda, R. R., Bansraj, M. R., de Jong, A. W., Noordermeer, J. N. and Fradkin, L. G. (2008) 'Src family kinases are required for WNT5 signaling through the Derailed/RYK receptor in the *Drosophila* embryonic central nervous system', *Development* 135(13): 2277-87.
- Xie, X. and Auld, V. J. (2011) 'Integrins are necessary for the development and maintenance of the glial layers in the *Drosophila* peripheral nerve', *Development* 138(17): 3813-22.
- Yano, T., Lopez de Quinto, S., Matsui, Y., Shevchenko, A., Shevchenko, A. and Ephrussi, A. (2004) 'Hrp48, a *Drosophila* hnRNPA/B homolog, binds and regulates translation of oskar mRNA', *Dev Cell* 6(5): 637-48.
- Yurchenco, P. D. (2011) 'Basement membranes: cell scaffoldings and signaling platforms', *Cold Spring Harb Perspect Biol* 3(2).

Zhu, L., Xiang, P., Guo, K., Wang, A., Lu, J., Tay, S. S., Jiang, H. and He, B. P. (2012) 'Microglia/monocytes with NG2 expression have no phagocytic function in the cortex after LPS focal injection into the rat brain', *Glia* 60(9): 1417-26.

Ziegenfuss, J. S., Biswas, R., Avery, M. A., Hong, K., Sheehan, A. E., Yeung, Y. G., Stanley, E. R. and Freeman, M. R. (2008) 'Draper-dependent glial phagocytic activity is mediated by Src and Syk family kinase signalling', *Nature* 453(7197): 935-9.

Zuo, H. and Nishiyama, A. (2013) 'Polydendrocytes in development and myelin repair', *Neurosci Bull* 29(2): 165-76.

## 7 Appendix

### $\alpha$ -Kon<sup>ecto</sup> antibody generation, nucleotide and peptide sequence

The following is the nucleotide sequence resulting after cloning the fragments of exon 6 and exon 7 of *kon* into pQE32:

```

Query 1   ATGAGAGGATCTCACCATCACCATCACCATGGGATCCTGGTCAACGATCTTCCACTGGGA 60
          |
Sbjct 2   ATGAGAGGATCTCACCATCACCATCACCATGGGATCCTGGTCAACGATCTTCCACTGGGA 61

Query 61  TTCGCCGAGATGACTATCTCCCGCAGCCTGGCCCTCAACTGCCTGTGGAAGTATCCATGC 120
          |
Sbjct 62  TTCGCCGAGATGACTATCTCCCGCAGCCTGGCCCTCAACTGCCTGTGGAAGTATCCATGC 121

Query 121  GTGGAGTACAATCCCTGCCTTAAGAGCGGAATCTGCAGTCAGCACGGAGTGGACGGCTTC 180
          |
Sbjct 122  GTGGAGTACAATCCCTGCCTTAAGAGCGGAATCTGCAGCAGCACGGAGTGGACGGCTTC 181

Query 181  ATCTGCTACTGCGATCAGTCCTACTGCATCAAGGCCGATTTTCAGGGACCTTTTGAGCTC 240
          |
Sbjct 182  ATCTGCTACTGCGATCAGTCCTACTGCATCAAGGCCGATTTTCAGGGACCTTTTGAGCTC 241

Query 241  TTCACAGAAACCAGTCCAGAGCTAGAGCTGCTCTATGTCTCACCCATGCAGCTTTTAGAA 300
          |
Sbjct 242  TTCACAGAAACCAGTCCAGAGCTAGAGCTGCTCTATGTCTCACCCATGCAGCTTTTAGAA 301

Query 301  GGTGGAAGTGCCTTTCTATCGCCCCACTTCATAGACATTATACTCGATCTGCGACGTTAT 360
          |
Sbjct 302  GGTGGAAGTGCCTTTCTATCGCCCCACTTCATAGACATTATACTCGATCTGCGACGTTAT 361

Query 361  CCAAGTCTGAACGAGCAATCCATTATTTCCATGTGGTACATCAGCCGAAATATGGACAA 420
          |
Sbjct 362  CCAAGTCTGAACGAGCAATCCATTATTTCCATGTGGTACATCAGCCGAAATATGGACAA 421

Query 421  CTCTTGCACTACTCAGCTGAAAAAGCCATATTTGTGCCTTGCCGCACATTTAACCTCGTT 480
          |
Sbjct 422  CTCTTGCACTACTCAGCTGAAAAAGCCATATTTGTGCCTTGCCGCACATTTAACCTCGTT 481

Query 481  GATTTGGCCACAGATAAATTGAAGTATGTGCACAATGGCCAAGAGAACTTCAATGATCAT 540
          |
Sbjct 482  GATTTGGCCACAGATAAATTGAAGTATGTGCACAATGGCCAAGAGAACTTCAATGATCAT 541

Query 541  GCCACACTGGATATGCAGATCTTTGGGGATGTGCACAAGATAACCGGAGAATATATTGGGC 600
          |
Sbjct 542  GCCACACTGGATATGCAGATCTTTGGGGATGTGCACAAGATAACCGGAGAATATATTGGGC 601

Query 601  AAGCATAGGTTTCCTTTTACATGCCAATATAACACCCATAAATGATCCACCGCAATTAAGA 660
          |
Sbjct 602  AAGCATAGGTTTCCTTTTACATGCCAATATAACACCCATAAATGATCCACCGCAATTAAGA 661

Query 661  CTGCAGCCAAGCTTAATTAGCTGA 684
          |
Sbjct 662  CTGCAGCCAAGCTTAATTAGCTGA 685

```

As query was used the annotated sequence expected to be obtained after cloning. The subject is the resulting sequence after cloning, sequenced using especially designed primers for the pQE plasmid. In the sequence is highlighted in red two single nucleotide changes detected. Since these are nucleotide substitutions, there is no frame shift observed neither a stop codon insertion, nor aminoacid substitution. Below, in capital letters is the corresponding peptide sequence and in bold letters the 6xHis tag.

```
atgagaggatctcaccatcaccatcaccatgggatcctgggtcaacgatcttccactggga
M R G S H H H H H H G I L V N D L P L G
ttcgccgagatgactatctcccgcagcctggccctcaactgctgtggaagtatccatgc
F A E M T I S R S L A L N C L W K Y P C
gtggagtacaatccctgccttaagagcgggaatctgcagcccagcacggagtggacgggttc
V E Y N P C L K S G I C S Q H G V D G F
atctgctactgcgatcagtcctactgcatcaaggccgattttcagggaccttttgagctc
I C Y C D Q S Y C I K A D F Q G P F E L
ttcacagaaaccagtcagagctagagctgctctatgtctcaccatgcagcttttagaa
F T E T S P E L E L L Y V S P M Q L L E
ggggaactgcctttctatcgccccacttcatagacattatactcgatctgcgacgttat
G G T A F L S P H F I D I I L D L R R Y
ccaagtctgaacgagcaatccattattttccatgtggtacatcagccgaaatattggacaa
P S L N E Q S I I F H V V H Q P K Y G Q
ctcttgacgtactcagctgaaaaagccatatttgtgccttgccgcacatttaacctcgtt
L L Q Y S A E K A I F V P C R T F N L V
gatttgccacagataaattgaagtatgtgcacaatggccaagagaa
D L A T D K L K Y V H N G Q E
```

---

**Abbreviation index**

|      |  |
|------|--|
| AD   | Alzheimer's disease                      |
| ALS  | Amyotrophic lateral sclerosis            |
| BBB  | Blood brain barrier                      |
| BSC  | Bloomington stock center                 |
| CNS  | Central nervous system                   |
| CSPG | Chondroitin sulfate proteoglycan         |
| DS   | Downstream                               |
| EC   | Endothelial cell                         |
| ecto | Ectodomain                               |
| ePG  | embryonic peripheral glia                |
| FISH | Fluorescent <i>in situ</i> hybridization |
| GAL  | Galactosidase                            |
| GFP  | Green fluorescent protein                |
| GMC  | Ganglion mother cell                     |
| HRP  | Horseradish peroxidase                   |
| IF   | Intermediate fascicle                    |
| ISN  | Intersegmental nerve                     |
| LF   | Lateral fascicle                         |
| LG   | Longitudinal glia                        |
| LTP  | Long term potentiation                   |
| m6/7 | Muscle 6 and 7                           |
| MF   | Medial fascicle                          |
| MFA  | Muscle field area                        |

---

|      |                                      |
|------|--------------------------------------|
| MS   | Multiple sclerosis                   |
| n.s. | Not significant                      |
| NB   | Neuroblast                           |
| NER  | Nerve extension region               |
| NMJ  | Neuromuscular junction               |
| PCR  | Polymerase chain reaction            |
| PG   | Perineurial glia                     |
| PNS  | Peripheral nervous system            |
| SEM  | Standard error of the mean           |
| SN   | Segmental nerve                      |
| SNb  | Segmental nerve b                    |
| SPG  | Subperineurial glia                  |
| UAS  | Upstream activating sequence         |
| US   | Upstream                             |
| VDRC | Vienna <i>Drosophila</i> RNAi center |
| VNC  | Ventral nerve cord                   |

---

**Figures index**

|  |    |
|--|----|
| Figure 1.1 Model of the myelin sheath wrapping in vertebrates nervous system .....   | 3  |
| Figure 1.2 Illustration of MBP mRNA silenced transport and site specific translation .....                                       | 4  |
| Figure 1.3. NG2 structure and domains. ....  | 6  |
| Figure 1.4 Debris and ghost boutons clearance carried out by glia and muscle at the NMJ....                                      | 12 |
| Figure 1.5 Illustration of glia-muscle-neuron signaling cascade to promote NMJ growth .....                                      | 13 |
| Figure 2.1 GAL4/UAS system in <i>Drosophila</i> .....  | 17 |
| Figure 2.2. Epitope for $\alpha$ -Kon <sup>ecto</sup> generation.....  | 20 |
| Figure 3.1. Src42A is ubiquitously expressed during <i>Drosophila</i> embryonic development. ....                                | 32 |
| Figure 3.2. Src64B is expressed in the tracheal pits and longitudinal and commissural axons in the <i>Drosophila</i> embryo..... | 33 |
| Figure 3.3. BP102 staining in wildtype and Src kinase mutant embryos. ....   | 34 |
| Figure 3.4. Src42A homozygous and heterozygous mutant embryos stained against the microtubule marker Futsch. ....                | 36 |
| Figure 3.5. Src42A mutant and Src42A glial knockdown do not affect ePG migration.....  | 38 |
| Figure 3.6. Glo is downregulated in LG during embryonic development .....  | 40 |
| Figure 3.7. Nervous system development in Glo mutant background .....  | 42 |
| Figure 3.8. Kon and <i>kon</i> expression in embryo and larva. ....  | 44 |
| Figure 3.9. $\alpha$ -Repo and $\alpha$ -Futsch staining in Kon mutant and <i>kon</i> knockdown in glia.....                     | 45 |
| Figure 3.10. Larva NMJ phenotypes observed in <i>kon</i> knockdown in glia. ....   | 47 |

---

|   |    |
|---|----|
| Figure 3.11. m6/7 NMJ interaction with PNS glia in a single glia layer resolution and Kon dependent glial layer contribution to the NMJ phenotype ..... | 51 |
| Figure 3.12. Pre-and postsynaptic defects in <i>kon</i> knockdown in glia. ....   | 53 |
| Figure 3.13. Bruchpilot stalling along the NER in <i>kon</i> knockdown.....   | 55 |
| Figure 3.14. NMJ scores in <i>kon</i> knockdown in neurons and muscle.....  | 58 |
| Figure 3.15. NMJ phenotypes in Kon rescue in muscle.....  | 60 |
| Figure 3.16. m6/7 NMJ phenotype in Kon overexpression in glia using <i>repo</i> -GAL4.....  | 61 |
| Figure 3.17. Overexpression of Kon full-length only results in elongated VNC .....  | 63 |
| Figure 3.18. Kon expression in GAL4/GAL80 <sup>ts</sup> temperature shift experiments. ....   | 64 |
| Figure 3.19. Crossing scheme for the suppressor screen.....   | 65 |
| Figure 3.20. VNC length measurements in glia suppressor screen.....   | 67 |
| Figure 3.21. Western blot showing Kon and Kon <sup>VG</sup> processing in <i>Drosophila</i> .....   | 69 |
| Figure 3.22. NMJ phenotypes in glia knockdown of <i>dgrip</i> and <i>kuz</i> , and Kuz overexpression in glia.....                                      | 71 |
| Figure 4.1 Model of wg induced microtubule cytoskeleton regulation.....   | 77 |
| Figure 4.2 Role of APPL in satellite bouton consolidation may include Kon interaction .....   | 81 |



---

**Tables index**

|   |    |
|---|----|
| Table 2.1 Fly strains used during the course of this investigation .....                  | 15 |
| Table 2.2. List of antibodies.....  | 18 |
| Table 2.3. List of primers used for the generation of $\alpha$ -Kon <sup>ecto</sup> ..... | 20 |
| Table 4.1 Summary of phenotypes observed.....   | 86 |

---

## Curriculum vitae

### Personal information

---

Name: Álvaro Enrique Bustos Bustos  
 Date of birth: April 24<sup>th</sup>, 1984  
 City of birth: Concepción, Chile  
 Citizenship: Chilean  
 Address: Lotharstr. 4, 55116 Mainz  
 Email: alvaro.bustos@gmail.com

### Education

---

- 04/2009 – 02/2015 Dr. *rer nat* candidate. Mainz Neuro Graduate School Program. Joint project between the Institute of Genetics and Dept. of Molecular Cell Biology, Johannes Gutenberg-Universität Mainz
- Thesis title: “Comparative functional analysis of factors controlling glial differentiation in *Drosophila* and mouse”
- 03/2002 – 02/2009 Successful completion of Biotechnology & Management Engineering studies at Universidad San Sebastián, Concepción – Chile.
- Final mark: 6,5 (With honours). Scale 1,0 – 7,0. Top mark within promotion
  - Thesis work title: “Effect of neuroprotective drugs in pro- and antiapoptotic proteins in rodent brains”. 6 months research (Jun – Nov 2008) performed at the Neuroscience discovery research dept., Abbott - Ludwigshafen (currently AbbVie)
  - Degree recognized in Germany as “Diplom Ingenieur in Biotechnologie”
- December 2001 High school studies completion. Colegio San Ignacio, Concepción. Chile.

### Publications

---

Predetermined embryonic glial cells form the distinct glial sheaths of the *Drosophila* peripheral nervous system. Christian M. von Hilchen, **Álvaro E. Bustos**, Angela Giangrande, Gerhard M. Technau and Benjamin Altenhein. (2013) *Development* 140, 3657-3668

## Eidesstattliche Erklärung

Versicherung gemäß §11, Abs.3d der Promotionsordnung

1. Ich habe die als Dissertation vorgelegte Arbeit selbst angefertigt und alle benutzten Hilfsmittel (Literatur, Apparaturen, Material) in der Arbeit angegeben.
2. Ich habe und hatte die als vorgelegte Dissertation vorgelegte Arbeit nicht als Prüfungsarbeit für eine staatliche oder andere wissenschaftliche Prüfung eingereicht.
3. Ich hatte weder die als Dissertation vorgelegte Arbeit noch Teile einer Ab-handlung davon bei einer anderen Fakultät bzw. einem anderen Fachbereich als Dissertation eingereicht.

Mainz, den

---

Álvaro E. Bustos

## Acknowledgements